VRIJE UNIVERSITEIT

Effects of instanton interactions on the phases of quark matter

ACADEMISCH PROEFSCHRIFT

ter verkrijging van de graad Doctor aan
de Vrije Universiteit Amsterdam,
op gezag van de rector magnificus
prof.dr. L.M. Bouter,
in het openbaar te verdedigen
ten overstaan van de promotiecommissie
van de faculteit der Exacte Wetenschappen
op donderdag 17 juni 2010 om 15.45 uur
in het auditorium van de universiteit,
De Boelelaan 1105

door

Jorn Kerst Boomsma

geboren te Venhuizen

promotor: prof.dr. P.J.G. Mulders
copromotor: dr. D. Boer

Voor oma

This thesis is partly based on the following publications:

- *Spontaneous CP violation in the strong interaction at $\theta = \pi$.*
  D. Boer, J.K. Boomsma,
  Phys. Rev. D **78**, 054027 (2008).

- *Spontaneous CP violation in the NJL model at $\theta = \pi$.*
  D. Boer, J.K. Boomsma,
  Proceedings of the International Conference on Strong and Electroweak Matter (SEWM 2008), Amsterdam, the Netherlands, 26-29 Aug 2008.
  Nucl. Phys. A **820**, 251C-254C (2009).

- *Spontaneous CP violation in the NJL model at $\theta = \pi$.*
  J.K. Boomsma, D. Boer,
  Proceedings of the 8th Conference on Quark Confinement and the Hadron Spectrum (Confinement8), Mainz, Germany, 1-6 Sep 2008.
  PoS Confinement8, 134 (2008).

- *High temperature CP-restoring phase transition at $\theta = \pi$.*
  J.K. Boomsma, D. Boer,
  Phys. Rev. D **80**, 034019 (2009).

- *Influence of strong magnetic fields and instantons on the phase structure of the two-flavor Nambu–Jona-Lasinio model.*
  J.K. Boomsma, D. Boer,
  Phys. Rev. D **81**, 074005 (2010).

Contents

Chapter 1

Introduction

It is generally assumed that during the Big Bang equal amounts of matter and antimatter were produced, but the amount of matter in the visible Universe is presently much larger than that of antimatter. Sakharov (1967) argued that one of the three conditions to explain this discrepancy is that at some point in the history of the Universe CP invariance should have been violated[1]. CP is the combined transformation of charge conjugation (C) and a parity transformation (P). Apparently, as there is more matter than antimatter, CP was (at least at some point) not a symmetry of Nature.

In 1964 it was discovered by Christenson, Cronin, Fitch, and Turlay that the weak interaction violates CP invariance. They observed CP-violating decays of neutral kaons. These experimental results were explained later by Kobayashi and Maskawa (1973). Because the weak interaction violates CP invariance, CP is also not a symmetry of the Standard Model. However, the amount of violation from this interaction is not enough to explain the observed abundance of matter (Dine and Kusenko, 2004).

What about the strong interaction? In the strong interaction there is also a theoretical possibility of CP violation, which is connected to the existence of topologically nontrivial solutions to the classical equations of motion of Quantum Chromodynamics (QCD) called instantons. The Lagrangian of QCD naturally incorporates a term that can lead to the violation of CP invariance, the θ-term. The amount of CP invariance from this term is set by the dimensionless parameter θ, known as the vacuum angle of QCD, which has a periodicity of 2π. The θ-term can be written as a total derivative (cf. next section), and one would naively expect that this term cannot have physical implications. This reasoning is indeed true for Quantum Electrodynamics, but because of the existence of instantons, in QCD the θ-term can influence the physics.

Naturalness arguments would imply a value of θ of approximately 1, but from measurements of the electric dipole moment of the neutron it is known that the amount of strong CP violation is very small, the present upper bound on θ is 10^{-10}. The reason for this smallness is currently unknown and is referred to as the strong CP problem. In

[1]The other conditions of Sakharov are that the interactions that cause the asymmetry violate both charge-conjugation invariance and baryon number. In addition, these interactions should take place out-of-equilibrium.

this thesis we will not address the strong CP problem, but investigate, among others, the possibility of spontaneous CP violation in the strong interaction.

At $\theta = 0$, the Lagrangian of QCD is invariant under CP. In addition, the Vafa-Witten theorem states that parity cannot be spontaneously violated at $\theta = 0$ (Vafa and Witten, 1984). For C-even terms their conclusions also hold for CP. This means that spontaneous CP violation is not possible in the vacuum at $\theta = 0$. However, Kharzeev, Pisarski, and Tytgat conjectured that it might be possible that parity and CP-violating bubbles can be created in heavy-ion collisions with nonzero density and temperature. Earlier suggestions for such states were made by Lee (1973) and also by Morley and Schmidt (1985). Other work on such CP-odd bubbles, especially on their dynamics, was done by Buckley, Fugleberg, and Zhitnitsky (2000). Such a CP-violating bubble would correspond to a state with an effective θ. If these states exist, they might also be relevant for the early Universe. However, they can probably not account for the asymmetry of matter and antimatter as nonzero θ is a C-even effect. Possible experimental signatures for such bubbles in heavy-ion collisions were discussed by Voloshin (2004, 2009), Selyuzhenkov (2006, 2009), and Abelev et al. (2009a,b). Nonzero θ, effective or not, corresponds to explicit CP violation, except for the cases $\theta = n\pi$, with integer n.

A special case for the parameter θ is the value π. Also in this case the Lagrangian is invariant under CP, but now there is a possibility of a CP-violating ground state, i.e. spontaneous CP violation, which was already discovered by Dashen (1971) before the advent of QCD. The conditions for spontaneous CP violation have been investigated further by studying the θ-behavior of the strong interaction (see e.g. Witten, 1980; di Vecchia and Veneziano, 1980; Smilga, 1999; Tytgat, 2000; Akemann, Lenaghan, and Splittorff, 2002; Creutz, 2004; Metlitski and Zhitnitsky, 2005, 2006; Fujihara, Inagaki, and Kimura, 2007). These investigations may lead to a better understanding of the topological structure of the QCD vacuum.

Investigations of the θ-term and instantons are very difficult due to their nonperturbative nature. Even in lattice QCD it is impossible to study the full θ-dependence as the fermion determinant becomes complex at nonzero θ. Most knowledge about the θ-dependence of the strong interaction has been obtained using the low-energy effective theory called chiral perturbation theory. Another possibility is to use model calculations, which we will do in this work. In Chapter 4, based on Boer and Boomsma (2008), the influence of θ and instantons on the QCD phase diagram is studied using such a model, the two-flavor Nambu–Jona-Lasinio (NJL) model, which we will introduce in Chapter 3. In this work we especially investigate the conditions for spontaneous CP violation. We will see that the occurrence of spontaneous CP violation depends on the instanton interaction strength with respect to the quark masses. Another observation is that CP invariance is restored at high temperature in a second order phase transition.

Mizher and Fraga (2009) investigated the temperature dependence of spontaneous CP violation at $\theta = \pi$ in the linear sigma model coupled to quarks. They found at high temperature a first order CP-restoring phase transition, in disagreement with our findings in the NJL model. In Chapter 5 we will elaborate on the differences between the two models and discuss how they lead to a different order of the phase transition. A first-order transition and a crossover have rather different experimental signatures, as usually in a

first-order transition energy is released (or absorbed), which does not happen in a second order transition or a crossover. Mizher and Fraga (2009) also observed that the phase transition becomes stronger if one includes a strong magnetic field. Moreover, also at $\theta = 0$ the phase structure of quark matter is modified by a strong magnetic field.

The inclusion of a strong magnetic field was inspired by the investigations of Kharzeev, McLerran, and Warringa (2008), who observed that in non-central heavy-ion collisions very strong magnetic fields can be produced, of order 10^{19} G. Furthermore, they noted that variations of topological charge, which induce variations of net chirality, in a strong magnetic field give rise to an electrical current. This induced current is known as the chiral magnetic effect and could perhaps be observed in heavy-ion collisions. Instantons are a possible source for these variations of topological charge. The interplay between instantons and strong magnetic fields will be investigated in Chapter 6.

Apart from heavy-ion collisions, more situations in the Universe exist (or have existed) where very strong magnetic fields and quark matter plays a role, namely in a special class of neutron stars, called magnetars. Possibly also during the electroweak phase transition in the early Universe huge magnetic fields were produced (Vachaspati, 1991; Olesen, 1992). Much effort has been put into the study how strong magnetic fields change the behavior of nuclear matter, for a review see Lattimer and Prakash (2007) and references therein. As already noted in the previous paragraph, a magnetic field can affect the phase structure of a material considerably. This is because the orbital motion of charged particles is quantized inside a magnetic field, known as Landau quantization. But the up and down quark have of course different charges, so this quantization is different for them and this leads to different behavior for the two quarks. However, instanton effects induce mixing between the quarks, which has an equalizing effect. In Chapter 6 we will see that the competition between the effects of magnetic fields and instantons gives rise to interesting phenomena, such as spontaneous isospin violation, and also sets of nearly degenerate minima with very different amounts of chiral symmetry breaking arise.

A brief outline of this thesis is as follows: we will begin with a short review of instantons and the θ-term. The next chapter is a review of the QCD phase diagram, where we start with a general discussion of phase diagrams and phase transitions, after which we discuss the standard phase diagram as a function of temperature and baryon chemical potential. We also consider non-standard phase diagrams, e.g. as a function of θ or the quark masses. Furthermore, we briefly discuss how one obtains both theoretical and experimental information about the QCD phase diagram. In Chapter 3 the NJL model is introduced. We continue with a detailed study of the θ-dependence of the phase structure of this model in Chapter 4, which is an extended version of the work published in Boer and Boomsma (2008). Then we compare the high temperature results of the NJL model with the linear sigma model coupled to quarks (LSMq) in Chapter 5, based on Boomsma and Boer (2009). In the two related models a different order of the CP restoring phase transition is predicted; we discuss how this difference comes about. Finally in Chapter 6 the influence of magnetic field and instantons on quark matter is discussed, based on Boomsma and Boer (2010). The thesis ends with a summary and conclusions.

1.1 QCD, instantons and the θ-term

Quantum Chromodynamics (QCD) is the quantum field theory that describes the strong interaction. In this section only a glance at the theory will be presented, for more information see for instance the books of Muta (1998) and Smilga (2001). QCD is an $SU(3)$ Yang-Mills theory with quarks and gluons as the degrees of freedom. The Lagrangian is equal to

$$\mathscr{L}_{\text{QCD}} = \sum_f \bar{\psi}_f \left(i\not{D} - m_f \right) \psi_f - \frac{1}{4} F_a^{\mu\nu} F^a_{\mu\nu}, \tag{1.1}$$

where

$$\begin{aligned} D_\mu &= \partial_\mu - igt^a A^a_\mu, \\ F^a_{\mu\nu} &= \partial_\mu A^a_\nu - \partial_\nu A^a_\mu - g f^{abc} A^b_\mu A^c_\nu, \end{aligned} \tag{1.2}$$

the t^a's are the generators of $SU(3)$ in the fundamental representation, normalized as

$$\operatorname{Tr} t^a t^b = \delta^{ab}/2. \tag{1.3}$$

The gauge fields A^a_μ represent the gluons and the ψ_f-field denotes the quark field of flavor f. The strength of the interactions is set by the coupling constant $\alpha_s = g^2/4\pi$. Finally, f^{abc} are the structure constants of $SU(3)$.

The Lagrangian of QCD looks simple, but leads to a large variety of remarkable phenomena. Asymptotic freedom is one of the most famous ones, which is the fact that the coupling constant becomes small at energies higher than approximately 1 GeV. A small coupling constant means that perturbative methods can be used, i.e., quantities in the theory can be expanded in the coupling constant. Asymptotic freedom was one of the main reasons to consider QCD as the theory for the strong interaction.

In this thesis the vacuum structure of QCD is studied, this means energies smaller than 1 GeV, so unfortunately perturbation theory can not be used. For a large part, the vacuum structure is determined by the symmetries of the theory. Since we are interested in the low energy structure of QCD, only quarks that are much lighter than 1 GeV have to be considered, i.e. the up, down and strange quark. In most of this thesis, also the strange quark is neglected.

The Lagrangian of massless QCD is invariant under the global symmetry group

$$U(N_f)_L \otimes U(N_f)_R \cong SU(N_f)_L \otimes SU(N_f)_R \otimes U(1)_V \otimes U(1)_A. \tag{1.4}$$

This symmetry is assumed to be spontaneously broken by a nonzero $\langle\bar{\psi}\psi\rangle$-condensate, after which $SU(N_f)_V \otimes U(1)_V$ remains. However, this would imply the existence of N_f^2 Goldstone bosons. In the case of two flavors, one can interpret three particles as Goldstone bosons, the pions, connected to the broken $SU(2)$ symmetry. The pions are not entirely massless due to the small explicit symmetry breaking from the quark masses. This can be generalized to three flavors, although the remaining $SU(3)_V$-symmetry is broken considerably, as $m_s \gg m_{u,d}$. The kaons, together with the η, are then also interpreted as

Goldstone bosons, which are all connected to the broken $SU(3)$ symmetry. But now there is a problem, where is the ninth Goldstone boson? The η' has the right quantum numbers, but is in reality much heavier than the other bosons and can therefore not be interpreted as a Goldstone boson. The puzzle of the missing Goldstone boson was named the $U(1)_A$ problem in the 1970's and was solved by 't Hooft (1976, 1986).

The solution of 't Hooft is connected to instantons. The solution starts with the observation that $U(1)_A$ is not really a symmetry of the theory. Whereas the action of the massless theory is invariant under $U(1)_A$, the measure of the fermion fields is not. Under the $U(1)_A$ transformation

$$\psi \rightarrow e^{i\alpha\gamma_5}\psi, \tag{1.5}$$

the measure changes as (Fujikawa, 1979)

$$\mathcal{D}\psi\mathcal{D}\bar{\psi} \rightarrow \exp\left(\frac{-i\alpha g^2 N_f}{16\pi^2}\int \mathrm{d}^4x F^a_{\mu\nu}\tilde{F}^{\mu\nu}_a\right)\mathcal{D}\psi\mathcal{D}\bar{\psi}, \tag{1.6}$$

where we have introduce the dual field $\tilde{F}^{\mu\nu}_a = \frac{1}{2}\epsilon^{\mu\nu\rho\sigma}F^a_{\rho\sigma}$. Eq. (1.6) leads to the axial anomaly equation, in the chiral limit given by

$$\partial_\mu j^\mu_5 = -2N_f q(x), \tag{1.7}$$

where j^μ_5 is the singlet axial current,

$$j^\mu_5 = \sum_f \bar{\psi}_f\gamma^\mu\gamma_5\psi_f \tag{1.8}$$

and $q(x)$ is the topological charge density

$$q(x) = \frac{g^2}{32\pi^2}F^a_{\mu\nu}\tilde{F}^{\mu\nu}_a. \tag{1.9}$$

If the field $F^{\mu\nu}$ at infinity corresponds to a pure gauge field, the integral of $q(x)$ over space-time yields integer values. Eq. (1.7) indicates that the singlet axial current is not conserved on the quantum level, $U(1)_A$ is only a symmetry of the classical theory.

The extra term that is created by the transformation in Eq. (1.6) can be written as a total derivative,

$$\frac{g^2 N_f}{16\pi^2}F^a_{\mu\nu}\tilde{F}^{\mu\nu}_a = \partial_\mu K^\mu, \tag{1.10}$$

where the current K_μ equals

$$K^\mu = \frac{g^2 N_f}{8\pi^2}\epsilon^{\mu\nu\rho\sigma}\left(A^a_\nu\partial_\rho A^a_\sigma + \frac{1}{3}gf^{abc}A^a_\nu A^b_\rho A^c_\sigma\right). \tag{1.11}$$

One would naively expect that such a term vanishes when integrated over, which is indeed true in QED, but not in Yang-Mills theories like QCD. Belavin et al. (1975) pointed out that Yang-Mills theories allow for topologically nontrivial field configurations that give

a nonvanishing result for the integral of Eq. (1.6). 't Hooft (1976, 1986) called these configurations instantons. For a review of instantons and how they contribute to meson masses, see for example the texts of Cheng and Li (1984) and Weinberg (1996). The most important fact at this point is that $U(1)_A$ is not a symmetry of the quantum theory, it is anomalously broken and there is no missing Goldstone boson.

Thus the solution to the $U(1)_A$ problem is the existence of instantons, but this leads to a new problem, the strong CP problem. In an $SU(N)$ gauge theory like QCD the vacuum is topologically nontrivial. Multiple vacuum states with equal energies exist, each with a different topological quantum number, the winding number. These different quantum states cannot be continuously deformed into each other and are separated by finite energy barriers. Instantons represent tunneling solutions between these vacuum states, consequently the true vacuum of QCD is a superposition of vacua with different winding numbers. This true vacuum can be written as

$$|\theta\rangle = \sum_n e^{in\theta} |n\rangle \,, \tag{1.12}$$

where $|\theta\rangle$ is the true vacuum, characterized by the angle θ and $|n\rangle$ is a vacuum state with winding number n. The angle θ is a new parameter in the theory and has to be determined from experiment. Using naturalness arguments one would expect a value of order 1 as the parameter is dimensionless.

Standard perturbative QCD is an expansion around the vacuum with winding number 0, it does not include tunneling effects between the different winding number vacua. As a consequence, effects of nonzero θ can never be seen in perturbation theory.

The effect of nonzero θ can be calculated by incorporating an extra term in the Lagrangian,

$$\mathscr{L}_\theta = \frac{\theta g^2}{32\pi^2} F^a_{\mu\nu} \tilde{F}^{\mu\nu}_a \,. \tag{1.13}$$

When θ is not equal to 0 (mod π) this term violates P and CP. Note that this θ-term can only have physical consequences when all the quarks are massive, more on this in Sect. 1.5. In Sect. 1.3 we will argue, following the low-energy arguments of Crewther et al. (1979) and experimental results that θ is very small, smaller than 10^{-10}. The reason for this is unknown and commonly referred to as the strong CP problem, arguably the largest unresolved issue in QCD besides confinement.

1.2 The θ-dependence of low-energy effective theories

Effective theories have to be used to study the θ-dependence of QCD due to the nonperturbative nature of the θ-term. Using Chiral Perturbation Theory (χPT), the low-energy effective theory of the pseudo-Goldstone bosons of QCD, a condition for the ground state can be found, see Sect. 1.3. As previously mentioned, the pseudo-Goldstone bosons of QCD are the pions, kaons and the η meson. The masses of these particles are due the explicit symmetry breaking by the quark masses. For an introduction to χPT see for example Weinberg (1996). In the construction of χPT the philosophy of Weinberg (1979) is

followed, the theory contains all possible interactions consistent with the low-energy symmetries of the strong interaction and is a combined expansion in the masses and momenta of the mesons.

To second order in the masses and momenta, the most general Lagrangian for the pseudo-Goldstone bosons is quite simple, it has the following form

$$\mathscr{L} = \frac{f_\pi^2}{4}\mathrm{Tr}\left[\partial_\mu U \partial^\mu U^\dagger\right] + \Sigma \mathrm{Re}\left[\mathrm{Tr}\left(\mathrm{MU}\right)\right], \tag{1.14}$$

where U is an $SU(N_f)$ field representing the pseudo-Goldstone bosons, f_π is the pion decay constant, the constant Σ equals $|\langle\bar{\psi}\psi\rangle|$ and the matrix M denotes the quark mass matrix. In our numerical analyses in this chapter, we employ the parameters used by Tytgat (2000), $m_u = 4\,\mathrm{MeV}$, $m_d = 7\,\mathrm{MeV}$, $m_s = 150\,\mathrm{MeV}$ and $\Sigma = (250\,\mathrm{MeV})^3$, which reproduce the experimental values for the meson masses reasonably well. Furthermore, the chosen value for the chiral condensate is quite close to the result obtained using QCD sum rules (Dosch and Narison, 1998) and lattice calculations (Giusti et al., 1999).

Standard χPT does not include the η' meson, as it is not a pseudo-Goldstone boson. However, the effect of the anomaly disappears in the large-N_c limit, turning the pseudoscalar singlet η' into a pseudo-Goldstone boson. If one also expands in $1/N_c$, the η' can be incorporated in the framework. The effects of the anomaly have to be included in Eq. (1.14). Witten (1980) and di Vecchia and Veneziano (1980) have shown using large-N_c arguments that the effects of the anomaly and instantons can be included by promoting U to become an element of $U(N_f)$, i.e. also take the pseudo-scalar singlet into account, and adding an extra interaction term

$$\mathscr{L}_{\mathrm{anomaly}} = -\frac{\tau}{2}(i\log\det U + \theta)^2, \tag{1.15}$$

where τ is the topological susceptibility, defined in terms of the topological charge density as $\tau = \int \mathrm{d}^4x\,\langle q(x)q(0)\rangle$. This interaction term breaks the $U(1)_A$ symmetry and consequently gives a mass to the η' meson, even in the chiral limit. In the chiral limit the topological susceptibility is directly related to the mass of the η' meson (Witten, 1979; Veneziano, 1979)

$$\tau = \frac{f_\pi^2 m_{\eta'}^2}{2N_f}. \tag{1.16}$$

In the large-N_c limit, the topological susceptibility is of order $O(1)$, f_π^2 and Σ are of order $O(N_c)$ and the quark masses are of order $O(1)$. From these large-N_c counting rules we can conclude that when $N_c \to \infty$, the effects of the anomaly disappear ($\mathscr{L}_{\mathrm{anomaly}} \ll \mathscr{L}$) and the η' meson becomes a Goldstone boson.

In the following $\tau = (200\,\mathrm{MeV})^4$, also used by Tytgat (2000), which leads to a reasonable value for the mass of the η' meson. The topological susceptibility can also be calculated on the lattice; for a recent comparison of the various lattice results see Table 1 of Vicari and Panagopoulos (2009). The chosen value is consistent with these values.

Now we are ready to find the ground state of the theory, this means we have to minimize the potential that is contained in the Lagrangian $\mathscr{L}_{\mathrm{chiral}} = \mathscr{L} + \mathscr{L}_{\mathrm{anomaly}}$, which we

will refer to as the chiral Lagrangian. At $\theta = 0$, the field U that minimizes the potential is just the unit matrix. But at $\theta \neq 0$ this is not true anymore. Using $U(N_f)_L \otimes U(N_f)_R$ transformations, the field that minimizes the potential can always be put in diagonal form, but as a consequence the mass term may be affected, more on this in Sect. 1.5. Let us focus for now on the three flavor case. The minimum can always be brought to the following form

$$\langle U \rangle = \begin{pmatrix} e^{i\phi_u} & & \\ & e^{i\phi_d} & \\ & & e^{i\phi_s} \end{pmatrix}. \tag{1.17}$$

A CP transformation exchanges $U \leftrightarrow U^\dagger$, so whenever one or more of the ϕ_i are unequal to $0 \pmod{\pi}$, the ground state violates CP invariance.

The minimization of the potential boils down to solving the following coupled equations

$$m_i \sin\phi_i = \frac{\tau}{\Sigma}\left(\theta - \sum_{j=1}^{N_f} \phi_j\right), \tag{1.18}$$

with the considered choice of parameters, $\tau/\Sigma \cong 102\,\text{MeV}$. At $\theta = 0$ the solution for $\langle U \rangle$ with the lowest energy is always equal to the unit matrix, which means that CP is conserved, consistent with the Vafa-Witten theorem[2]. At $\theta \neq 0$, this is not true anymore. Due to the explicit CP violation, the ground state is then also CP-violating. At $\theta = \pi$, the situation is again different, the Lagrangian is then invariant under CP, but this does not hold automatically for the ground state. At this value for θ it may be possible that Eq. (1.18) has a nontrivial solution that minimizes the potential. Such a solution violates CP invariance, which will be discussed in more detail in the next section, after which we present the arguments for the claim that $\theta < 10^{-10}$ in Nature. We continue in Sect. 1.4 with the possibility of CP-violating local minima at $\theta = 0$.

1.3 The value of θ in Nature

At $\theta = \pi$ spontaneous CP violation can occur. At this value for θ the action is invariant under CP. However, this is not always the case for the ground state. Depending on the value of the quark masses, τ and Σ, there can be a two-fold degenerate CP-violating ground state. The two ground states are related by a CP transformation. This phenomenon is named after Dashen (1971), who discovered it before the introduction of QCD. At the time it was believed that a CP-violating condensate could be the source of the observed CP violation in experiments (Nuyts, 1971), but was later ruled out because it gives a too high value for the amplitude $\eta \to \pi\pi$ (Bég, 1971).

For realistic values of the parameters in Eq. (1.18) and $\theta = \pi$, the ground state is CP-conserving, so how can we differentiate between the cases $\theta = 0$ and $\theta = \pi$ without

[2] In this thesis we make two assumptions regarding the θ-dependence of the strong interaction. Firstly, we assume that also at $\theta \neq 0$, there is still confinement and chiral symmetry is also still broken. However, this may not be the case, see for example Schierholz (1995). Secondly, we assume that at $\theta = 0$ the free energy is smooth, see Asorey (2004) for a discussion about this property.

CP violation? Crewther et al. (1979) argued that this can be done by looking at ratios of meson masses. Their argument goes as follows, they start with the observation that the case $\theta = \pi$ with positive up-quark mass is equivalent to $\theta = 0$ and a negative up-quark mass, see Sect. 1.5. In that situation, with $|m_d| > |m_u|$, the potential is still minimized by the unit matrix, which means that the condensates all have equal sign. Using $\langle U \rangle = \mathbb{1}$ as the vacuum, the following ratio of meson masses can be derived at $\theta = 0$:

$$\left(m_{K^0}^2 - m_{K^+}^2 - m_{\pi^0}^2 + m_{\pi^+}^2\right)/m_{\pi^0}^2 = \frac{m_d - m_u}{m_d + m_u} \tag{1.19}$$

which is always smaller than one. According to Crewther et al. (1979), at $\theta = \pi$ the ratio equals

$$\left(m_{K^0}^2 - m_{K^+}^2 - m_{\pi^0}^2 + m_{\pi^+}^2\right)/m_{\pi^0}^2 = \frac{m_d + m_u}{m_d - m_u} \tag{1.20}$$

which is larger than one. If one inserts the physical values of these masses, the ratio equals approximately 0.3, implying that $\theta = 0$, or at least very close to zero. In Chapter 4 we will add an argument why in Nature $\theta \approx 0$, again by looking at meson masses.

We can go further in restricting θ by looking at the electric dipole moment (EDM) of the neutron. On dimensional grounds, for small θ the neutron EDM should be of order (Baluni, 1979; Crewther et al., 1979)

$$d_n \approx |\theta| e m_\pi^2/m_N^3 \approx 10^{-16}|\theta| e\,\mathrm{cm} \tag{1.21}$$

The experimental upper bound for the neutron EDM is $2.9\times10^{-26} e$ cm (Baker et al., 2006), leading to an upper limit for θ of order 10^{-10}. A less stringent bound of $|\theta| \lesssim (2-3)\times10^{-7}$ is obtained by looking at parity violation in nuclear reactions (Kawarabayashi and Ohta, 1981).

1.4 Metastable CP-violating states at $\theta = 0$

Kharzeev, Pisarski, and Tytgat (1998) pointed out that Eq. (1.18) allows for metastable CP-violating solutions at $\theta = 0$. This possibility arises when τ/Σ is smaller than the lightest quark mass. Then Eq. (1.18) has nontrivial solutions, where $\phi_{u,d,s} \neq 0$ and therefore violate CP invariance, effectively they correspond to states with a nonzero θ. Using our values of the parameters, the local minima arise when $\tau/\Sigma < 0.251 m_u$. In Nature τ/Σ is much larger than the lightest quark mass, so these metastable states do not normally occur. However, Kharzeev et al. argued that these states might be relevant at high-temperature in heavy-ion collisions.

The argument of Kharzeev, Pisarski, and Tytgat goes as follows, they considered the option that τ/Σ is temperature dependent. Using large N_c arguments, it can be argued that the topological susceptibility τ decreases with increasing temperature. This temperature dependence can be inferred from the fact that $\tau \sim O(1)$ at zero temperature and $\tau \sim e^{-aN_c}$ at high temperatures (Gross, Pisarski, and Yaffe, 1981). The parameter $a = 8\pi^2/g^2N_c$ is constant in the large-N_c limit, indicating that $\tau \approx 0$ at high temperatures and large N_c.

Furthermore, also Σ decreases when one increases the temperature. It is assumed that there is only one phase transition at high temperature, which is of second order. The temperature dependence of the parameters is taken to correspond to the mean field behavior, i.e. $\Sigma \sim (T_d - T)^{1/2}$ and $\tau \sim (T_d - T)^2$, hence $\tau/\Sigma \sim (T_d - T)^{3/2}$. Here T_d denotes the temperature of the phase transition. If we now insert the chosen values for the parameters, we can see that the temperature must be very close to the transition temperature in order for the local minima to occur. Such metastable states could in principle be seen in heavy-ion collisions. Kharzeev, Pisarski, and Tytgat (1998) discuss two possible experimental signatures. First of all, because the metastable state violates parity invariance, parity violating decays become possible, such as $\eta \to \pi^0\pi^0$. Furthermore, it is in principle possible to observe P- and CP-violating bubbles using pion correlations that are P and CP odd, but one needs large event samples and the estimated magnitude of the effect is uncertain (Kharzeev, 2006, and references therein). Another method suggested by Kharzeev is that a parity odd bubble would lead to charge separation. Voloshin (2004) proposed an observable that would measure this separation. For a discussion of the experimental results, see Voloshin (2009), Selyuzhenkov (2006, 2009) and Abelev et al. (2009a,b). These results indicate that CP odd effects may indeed be present in heavy-ion collisions, but alternative explanations for charge separation may exist. In Chapter 4 we will address the issue of local minima in the NJL model.

1.5 Chiral transformations and negative quark mass

As discussed in Sect. 1.3, a theory with $\theta = \pi$ can be related to a theory with a negative quark mass. Since this sometimes leads to confusion concerning the terminology used for the meson spectrum, we will elaborate on this relation in this section.

We start with the QCD partition function including the θ term:

$$Z = \int \mathcal{D}\psi\mathcal{D}\bar{\psi}\mathcal{D}A \; e^{i\int \mathrm{d}^4x\,[\mathscr{L}_{\mathrm{QCD}}+\mathscr{L}_\theta]}, \tag{1.22}$$

where

$$\begin{aligned}\mathscr{L}_{\mathrm{QCD}} &= \bar{\psi}\,(i\not{D} - m)\,\psi - \frac{1}{4}F_a^{\mu\nu}F^a_{\mu\nu},\\ \mathscr{L}_\theta &= \frac{\theta g^2}{32\pi^2}F^a_{\mu\nu}\tilde{F}_a^{\mu\nu}.\end{aligned} \tag{1.23}$$

Eq. (1.6) shows that the fermion measure of gauge theories is not invariant under chiral transformations, which can be used to remove $\mathscr{L}_\theta$. Since the mass term is not invariant under chiral transformations either, a θ dependence then appears in the mass term. One obtains

$$Z = \int \mathcal{D}\psi'\mathcal{D}\bar{\psi}'\mathcal{D}A \; e^{i\int \mathrm{d}^4x\,\mathscr{L}'_{\mathrm{QCD}}}. \tag{1.24}$$

Although the *physical* results one obtains using the transformed expression will be equivalent, one has to be careful when evaluating vacuum expectation values. We define vacuum

expectation values of an operator $O = O(\psi, \bar{\psi})$ in terms of the original fields (the one of the Lagrangian (1.23)) and in terms of the transformed or "primed" fields as follows:

$$\begin{aligned}\langle O\rangle_\theta &= \int \mathcal{D}\psi\mathcal{D}\bar{\psi}\mathcal{D}A\; O(\psi,\bar{\psi})\; e^{i\int \mathrm{d}^4x[\mathscr{L}_{\mathrm{QCD}}+\mathscr{L}_\theta]},\\ \langle O'\rangle_\theta &= \int \mathcal{D}\psi'\mathcal{D}\bar{\psi}'\mathcal{D}A\; O'(\psi',\bar{\psi}')\; e^{i\int \mathrm{d}^4x\mathscr{L}'_{\mathrm{QCD}}}.\end{aligned} \tag{1.25}$$

The condensates $\langle O\rangle_\theta$ and $\langle O'\rangle_\theta$ differ for $\theta \neq 0$ and are related by a θ-dependent transformation. For instance,

$$\langle\bar{\psi}\psi\rangle_\theta = \int \mathcal{D}\psi\mathcal{D}\bar{\psi}\mathcal{D}A\; \bar{\psi}\psi\; e^{i\int \mathrm{d}^4x[\mathscr{L}_{\mathrm{QCD}}+\mathscr{L}_\theta]} \neq \int \mathcal{D}\psi'\mathcal{D}\bar{\psi}'\mathcal{D}A\; \bar{\psi}'\psi'\; e^{i\int \mathrm{d}^4x\mathscr{L}'_{\mathrm{QCD}}} = \langle\bar{\psi}'\psi'\rangle_\theta\,. \tag{1.26}$$

When discussing a vacuum expectation value like $\langle\bar{\psi}\psi\rangle_\theta$ it has to be accompanied by a statement about which Lagrangian one is using.

In what follows we will select the chiral transformation that only affects the up quark:

$$\begin{aligned}u_L &= e^{-i\theta/2}u'_L,\\ u_R &= e^{i\theta/2}u'_R.\end{aligned} \tag{1.27}$$

This removes $\mathscr{L}_\theta$ from the Lagrangian and the up-quark mass term changes according to

$$\bar{u}m_u u = \bar{u}'\left[m_u\cos\theta + m_u i\gamma_5\sin\theta\right]u'. \tag{1.28}$$

For $\theta = \pi$ a negative up-quark mass results. In addition,

$$\langle\bar{u}u\rangle_\theta = \langle\bar{u}'u'\rangle_\theta\cos\theta + \langle\bar{u}'i\gamma_5u'\rangle_\theta\sin\theta. \tag{1.29}$$

Later in this thesis, we will use the following notation for the meson condensates:

$$\begin{aligned}\langle\sigma\rangle &= \langle\bar{\psi}\lambda_0\psi\rangle\,, & \langle\boldsymbol{a}_0\rangle &= \langle\bar{\psi}\boldsymbol{\lambda}\psi\rangle\\ \langle\eta\rangle &= \langle\bar{\psi}\lambda_0 i\gamma_5\psi\rangle\,, & \langle\boldsymbol{\pi}\rangle &= \langle\bar{\psi}\boldsymbol{\lambda}i\gamma_5\psi\rangle\,,\end{aligned} \tag{1.30}$$

where the $\lambda_a = (\lambda_0, \boldsymbol{\lambda})$ denote the generators of $U(2)$, normalized as $\mathrm{Tr}\,\lambda_a\lambda_b = 2\delta_{ab}$. These condensates transform according to:

$$\begin{aligned}\langle\sigma\rangle &= \frac{1}{2}(\cos\theta+1)\,\langle\sigma'\rangle + \frac{1}{2}(\cos\theta-1)\,\langle a_0^{0\prime}\rangle + \frac{1}{2}\sin\theta\,\langle\eta'\rangle + \frac{1}{2}\sin\theta\,\langle\pi^{0\prime}\rangle\,,\\ \langle a_0^{\pm}\rangle &= \cos\frac{\theta}{2}\,\langle a_0^{\pm\prime}\rangle + \sin\frac{\theta}{2}\,\langle\pi^{\pm\prime}\rangle\,,\\ \langle a_0^{0}\rangle &= \frac{1}{2}(\cos\theta-1)\,\langle\sigma'\rangle + \frac{1}{2}(\cos\theta+1)\,\langle a_0^{0\prime}\rangle + \frac{1}{2}\sin\theta\,\langle\eta'\rangle + \frac{1}{2}\sin\theta\,\langle\pi^{0\prime}\rangle\,,\\ \langle\eta\rangle &= \frac{1}{2}(\cos\theta+1)\,\langle\eta'\rangle + \frac{1}{2}(\cos\theta-1)\,\langle\pi^{0\prime}\rangle - \frac{1}{2}\sin\theta\,\langle\sigma'\rangle - \frac{1}{2}\sin\theta\,\langle a_0^{0\prime}\rangle\,,\\ \langle\pi^{\pm}\rangle &= \cos\frac{\theta}{2}\,\langle\pi^{\pm\prime}\rangle - \sin\frac{\theta}{2}\,\langle a_0^{\pm\prime}\rangle\,,\\ \langle\pi^{0}\rangle &= \frac{1}{2}(\cos\theta-1)\,\langle\eta'\rangle + \frac{1}{2}(\cos\theta+1)\,\langle\pi^{0\prime}\rangle - \frac{1}{2}\sin\theta\,\langle\sigma'\rangle - \frac{1}{2}\sin\theta\,\langle a_0^{0\prime}\rangle\,.\end{aligned} \tag{1.31}$$

Therefore, one has to be careful assigning the names π^0 and η to the condensates after doing a chiral transformation. For example, Fujihara, Inagaki, and Kimura (2007) discuss a $\langle\pi^0\rangle$-condensate using a Lagrangian without θ term, but with negative up or down quark mass. This corresponds to an $\langle\eta\rangle$-condensate using a Lagrangian with positive quark masses and a θ-term with $\theta = \pi$. We emphasize that these transformations are just a matter of consistently naming mesons and vacuum expectations values, but this is nevertheless important for the comparison of quantities from different calculations. For instance, $\langle\pi^0\rangle \neq 0$, while $\langle\pi^\pm\rangle = 0$ would suggest $SU(2)_V$-breaking, whereas $\langle\eta\rangle \neq 0$ indicates $U(1)_A$-breaking (for the $N_f = 2$-case), an important distinction.

1.6 Summary

In this chapter QCD and its low-energy symmetries were discussed. The QCD vacuum is topologically nontrivial, characterized by the QCD vacuum angle θ. Due to the existence of nonperturbative objects called instantons, nonzero θ can have observable effects. When $\theta \neq 0 \pmod{\pi}$, the theory is explicitly CP-violating.

We continued with reviewing the low-energy effective theory of the strong interaction, chiral perturbation theory (χPT). We discussed how instanton effects can be incorporated in this theory. This extension of χPT is widely used in the literature to study the θ-dependence of the QCD vacuum. The case $\theta = \pi$ is special, as it allows for spontaneous CP violation, known as Dashen's phenomenon, which we will study in detail using the NJL model in Chapter 4 and 5. Our investigations will also include finite temperature and density effects.

We presented the arguments that in Nature $\theta \approx 0$, which indicates that the ground state of the strong interaction is to very good approximation CP-conserving. However, conjectures about metastable CP-violating states at high temperatures have been put forward in connection with heavy-ion collisions. In these states θ is effectively nonzero, consequences of them may be probed in heavy-ion collisions.

Finally we discussed the relation between a theory with $\theta = \pi$ and positive quark masses and the case $\theta = 0$ with one of the quark masses negative. Observables are equal in both cases, but this does not apply to the meson condensates expressed in terms of the quark fields. This fact is often not explicitly addressed in the literature, but important in the discussion of symmetry breaking.

We continue our introduction in the next chapter with reviewing what is known about QCD matter in extreme conditions.

Chapter 2

The QCD phase diagram

In this chapter the phase diagram of the strong interaction will be discussed. First we introduce some general aspects of phase diagrams and phase transitions. Then we will summarize the "standard" phase diagram as function of temperature and baryon chemical potential, which is a measure of the baryon density, and discuss how one obtains both experimental and theoretical knowledge about the phase diagram. We continue with what is known about the phases of QCD as a function of some other parameters, like the number of flavors, masses, and θ. This chapter puts the rest of the thesis in a larger perspective. It is based on Braun-Munzinger and Wambach (2009), Meyer-Ortmanns and Reisz (2007), to which we refer for further details and also to the books of Shuryak (2004), Kapusta and Gale (2006), Kogut and Stephanov (2004).

2.1 Phase transitions

Usually a phase diagram consists of various different phases as a function of the external parameters. One can change the phase of the system by changing these external parameters, for example, water becomes ice when cooled under atmospheric pressure. In this example the change of phase is induced by temperature. Of course, also the other external parameters, like the magnetic field and chemical potential can induce such a phase transition.

Phase transitions are usually connected to changes in the symmetry of the system. Let us discuss as an example the chiral phase transition in QCD. As we already mentioned in Sect. 1.1, in massless QCD, chiral symmetry is broken at low temperatures due to a nonzero $\langle\bar{\psi}\psi\rangle$ condensate. However, at high temperatures it is assumed that chiral symmetry is restored, the condensate then is zero. Between the two phases there is a difference in chiral symmetry corresponding to a zero or nonzero value of $\langle\bar{\psi}\psi\rangle$ respectively. We will loosely call such a quantity that is zero in one phase and nonzero in the other an order parameter, albeit it is in some cases actually a disorder parameter.

Very often it happens that order parameters can only be found in some idealized form

of the theory, like $\langle\bar{\psi}\psi\rangle$ in the case of the chiral phase transition in massless QCD. In the case of massive QCD, $\langle\bar{\psi}\psi\rangle$ never becomes zero and the symmetry does not get fully restored due to explicit symmetry breaking from the quark masses. Usually it is nevertheless possible to use a quantity like $\langle\bar{\psi}\psi\rangle$ as an order parameter since it behaves qualitatively differently in the two phases. In the case of chiral symmetry breaking one speaks about the phase with broken chiral symmetry and the phase where chiral symmetry is approximately restored. For convenience, we will refer to the first phase as the chiral-broken phase and to the second one as the approximate chiral-restored phase.

Phase transitions are characterized by how derivatives of the thermodynamic potential behave across the phase transition. When one of the first derivatives of the potential is discontinuous, it is classified as a first order transition. When it is the second or higher derivative that is discontinuous, it is called a second order phase transition. The transition is called a crossover when the potential is analytic across the transition. In the case of the chiral phase transition, the order of the phase transition can be determined by looking at the order parameter itself, since the chiral condensate is the first derivative of the thermodynamic potential with respect to the quark mass.

The behavior of systems near first order transitions is qualitatively different from second order phase transitions and crossovers. A first order transition has latent heat, i.e., energy is released or absorbed during the transition. Furthermore, first order transitions allow for metastable phenomena, such as supercooling and overheating. Since there is a change of energy across a first order transition it is relatively easy to see in experiments. Second order transitions are more difficult to see, but at the transition, some correlation lengths diverge, leading to experimental consequences. In addition, near a second order phase transition, the system is scale-invariant and the phenomenon of criticality occurs. A crossover is even harder to find in experimental data, but if it is rapid enough (as a function of the parameter that is varied, usually the temperature), there is still a chance of measurable effects.

2.2 Phase diagram as function of μ_B and T

The question what happens to nuclear matter at high temperature and density was already raised by Fermi in the 1950s. He inferred the phase diagram shown in Fig. 2.1 using the knowledge of the constituents of matter at that time, protons, neutrons, and electrons.

In the 1970s it became clear that hadrons are not the basic constituents of matter, but that they are composed of quarks and gluons. At normal densities and temperatures, these are confined into hadrons, but Collins and Perry (1975), Cabibbo and Parisi (1975) argued that at high temperature and density, the hadrons will overlap and the quarks and gluons can move freely, a phase later called a quark-gluon plasma (QGP) (Shuryak, 1978). The fact that QCD has asymptotic freedom indicates that at (asymptotically) high temperatures and densities, the quarks and gluons are almost free. In such a system, the color charge is screened, just like in a normal plasma there is screening of electric charge. The inferred phase diagram is shown in Fig. 2.2, there are two phases, a confined and a deconfined one. Soon after, the possibility of color superconductivity was pointed out by Barrois (1977)

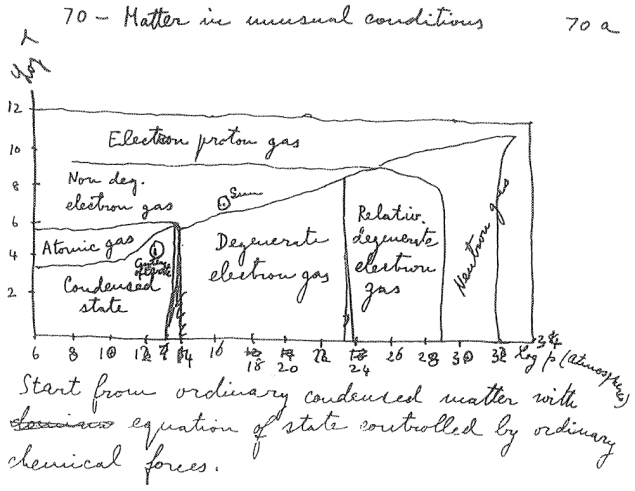

Figure 2.1: Phase diagram of nuclear matter conjectured by Fermi in his handwritten notes on "Matter under Unusual Conditions", taken from Bernardini and Bonolis (2004).

and Frautschi (1978), where quark pairs form a condensate, see Fig. 2.3. Other early work on color superconductivity was done by Bailin and Love (1984), but the whole subject of color superconductivity lay dormant for almost 20 years. The field was reopened by Alford, Rajagopal, and Wilczek (1998) and Rapp et al. (1998).

Apart from the deconfinement phase transition, it is also expected that at high temperature and also at high baryon chemical potential, chiral symmetry is restored. Often it

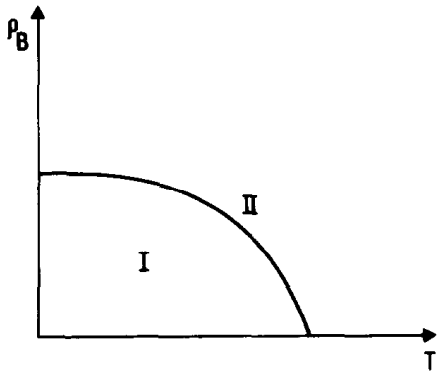

Figure 2.2: The phase diagram as a function of baryon density and temperature conjectured by Cabibbo and Parisi (1975).

2.2. Phase diagram as function of μ_B and T

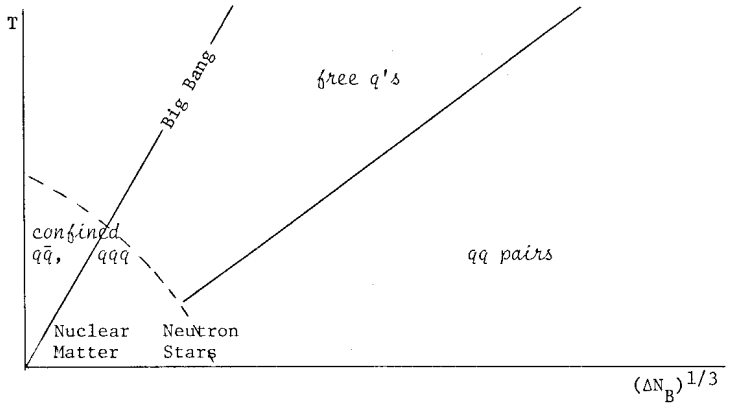

Figure 2.3: The phase diagram as a function of baryon density and temperature conjectured by Frautschi (1978), already including color superconductivity, the phase with the qq pairs.

is assumed that the two coincide, but this correlation is not necessarily true. Most lattice results suggest that the two phase transitions for the light quarks coincide at zero chemical potential (Cheng et al., 2006, 2008), but there are conflicting results (Aoki et al., 2006, 2009). The problem is that only in the case of infinite quark masses a (dis)order parameter for the deconfinement phase transition is known, the expectation value of the Polyakov loop. The deconfinement phase transition is connected to the breaking of the global $Z(3)$ center symmetry of $SU(3)$ in the deconfined phase corresponding to a nonzero value for the expectation value of the Polyakov loop (McLerran and Svetitsky, 1981b). For a review of the center symmetry of gauge theories and its relation to confinement, see Weiss (1993). No deconfinement order parameter is known for realistic quark masses, but usually the expectation value of the Polyakov loop is still used. The situation is similar to the restoration of chiral symmetry; $\langle\bar{\psi}\psi\rangle$ is only a real order parameter when the current quark masses are zero. The absence of real order parameters makes the discussion of the QCD phase transitions difficult, especially in determining whether they coincide or not.

As lattice calculations cannot be performed at large finite chemical potential (i.e. $\mu_B \geq T$), it is not clear whether the correlation between the two phase transitions continues at finite chemical potentials. McLerran and Pisarski (2007) have proposed a new phase, called the quarkyonic phase, using large N_c arguments. This quarkyonic phase is a confined phase with nonzero baryon number. It is conjectured that inside the quarkyonic phase the chiral phase transition occurs. Consequently, a chiral symmetric phase that confines exists and the phase transitions are decoupled. The conjectured phase diagram is shown in Fig. 2.4. At finite N_c the quarkyonic and chiral phase transition are probably coupled. The quarkyonic phase has been further investigated using model calculations by, for example, Fukushima (2008), McLerran, Redlich, and Sasaki (2009), and Abuki et al. (2008).

In this thesis we concentrate on the NJL model, which does not exhibit confinement and hence the deconfinement phase transition does not appear within the model. However, an extension of the NJL model exists which does incorporate a form of confinement, the Polyakov-NJL model, introduced by Fukushima (2004) and which is also studied in connection with the quarkyonic phase.

Let us now briefly discuss what is known about the phase diagram as a function of temperature and baryon chemical potential. In Fig. 2.5 an example of the modern view of the QCD phase diagram is displayed, including color superconductivity. The current view of the phase structure shows a rich structure. However, the form of this diagram is largely schematic, it is mostly based on theoretical arguments, which we will briefly discuss.

From lattice results it is expected that at zero chemical potential, no phase transition exists between the hadronic phase and the QGP, it is a crossover. Furthermore, most model calculations show that at zero temperature and finite chemical potential probably a first order phase transition should occur. Consequently, a critical point (i.e., a point where the first order phase transition ends and becomes a crossover) must exist, which could possibly be seen in heavy-ion collisions. However, the lattice results of de Forcrand and Philipsen (2007) suggest that the first order transition may not exist, contrary to theoretical expectations.

At high chemical potential color superconductivity occurs, where the quarks form Cooper pairs. Various color superconducting phases are possible, they differ in the pairing mechanisms. Using perturbation theory one can derive that at asymptotically high chemical potentials the color superconducting phase of color flavor locking (CFL) exists. In this phase the color and flavor of quarks become correlated. At lower chemical potential one has to rely on model calculations, for instance using the NJL model. For a review about color superconductivity see for example Alford et al. (2008). In this thesis we will not concentrate on deconfinement and color superconductivity, but on chiral symmetry breaking and phases that violate CP invariance.

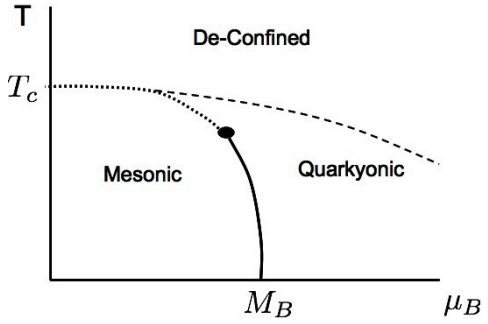

Figure 2.4: The QCD phase diagram including the quarkyonic phase and without color superconducting phases (McLerran, Redlich, and Sasaki, 2009).

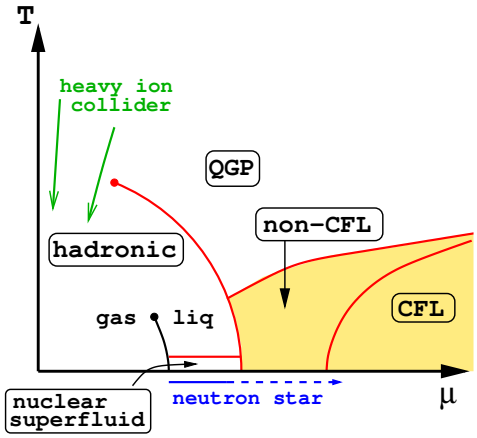

Figure 2.5: An example of a modern view of the QCD phase diagram as a function of baryon chemical potential and temperature (Alford et al., 2008).

2.3 Probes of the QCD phase diagram

The extreme conditions required to study the QCD phase diagram can be found in three different physical situations, the Big Bang, heavy-ion collisions and neutron stars. The Big Bang and heavy-ion collisions are described by high temperature and low baryon chemical potential, for neutron stars it is the other way around. Some heavy-ion collisions probe the intermediate regime, mainly to investigate the QCD critical point.

2.3.1 The Big Bang

The Universe was created approximately 14 billion years ago in the Big Bang. At first the Universe was very hot and dense. As the Universe evolved, it rapidly cooled down and expanded. During its evolution the Universe underwent several phase transitions, for example, after 10^{-10} s the electroweak phase transition occurred at a temperature of approximately 100 GeV $\approx 10^{15}$ K. In this phase transition the original $SU(2) \otimes U(1)$ symmetry of the electroweak theory broke down to the $U(1)$ symmetry of electromagnetism.

After approximately 10^{-5} s at a temperature of typically 200 MeV the confinement phase transition occurred. Lattice results indicate that the chiral phase transition occurred roughly at the same time as the confinement one. Before the transition the quarks and gluons could be described by a quark-gluon plasma. Afterwards, the phase structure is how we know it today, i.e., quarks and gluons confined into hadrons. One of the most important reasons to study the QCD phase diagram is to understand what happened during this transition.

2.3.2 Heavy-ion collisions

Experimentally, the phase diagram is studied using heavy-ion collisions. In some sense, these heavy-ion collisions can be seen as "little bangs" (McLerran, 1981), somewhat equivalent to the real big-bang. For recent reviews, see Gyulassy and McLerran (2005) and Braun-Munzinger and Stachel (2007).

The earliest experiments took place at the Alternating Gradient Synchroton (AGS) in Brookhaven and at the Super Proton Synchotron (SPS) at CERN. After these preliminary experiments, a special accelerator devoted to heavy-ion collisions was built in Brookhaven, the Relativistic Heavy-Ion collider (RHIC). At this collider gold and copper nuclei are collided with a center-of-mass energy per nucleon pair equal to $\sqrt{s_{NN}} = 200\text{GeV}$. In the near future also at the LHC heavy-ion collisions will take place. There lead ions will be used, with an expected center-of-mass energy of 5.5 TeV per nucleon pair.

In these experiments the nuclei collide and a "fireball" is created, which cools and expands until it hadronizes after passing the deconfinement temperature. As the energies in the experiments are much lower than the big bang, the timescales and baryon chemical potential are very different. It is expected that for about 10^{-22} s such a fireball exists, in which probably a quark-gluon plasma is formed.

The hadrons that emerge after a heavy-ion collision are very well described assuming that they are created from a thermally and chemically equilibrated state. Furthermore, the fireball expands hydrodynamically, which is also consistent with an equilibrated state. So it appears that equilibration takes place in such collisions in a remarkably short time, consequently temperature and chemical potential are well defined.

That hydrodynamics can be used in order to describe the fireball created in heavy-ion collision surprised theorists, because it indicates that the system is strongly coupled. It was generally believed that the system created in a heavy-ion collisions would be more like a gas, i.e. weakly coupled. Moreover, the calculations show that the created system behaves like a perfect liquid, without almost any viscosity.

Up to now, most experiments investigate the low baryon chemical potential regime, which resembles the early Universe. But there are planned experiments to look for the critical point at the SPS, RHIC and also at the future Facility for Antiproton and Ion Research (FAIR) at the heavy-ion research center GSI in Darmstadt (see e.g. Braun-Munzinger and Stachel, 2007).

Finally, we would like to mention that topological effects could be seen in heavy-ion collisions, which we already briefly discussed in the introduction. An example is that CP-violating bubbles are created, which behave as regions with an effective nonzero value for θ. Another example is the Chiral Magnetic Effect, discussed by Kharzeev, McLerran, and Warringa (2008), which is a combined effect of strong magnetic fields and variations of topology. In relation to this, Kharzeev, McLerran, and Warringa (2008) noted that in non-central heavy-ion collisions magnetic fields of magnitude 2×10^{19} G can be created. These variations of topology could for example be induced by instantons. The combined effects of instantons and magnetic fields on the phase structure of the NJL model will be investigated in detail in Chapter 6.

2.3.3 Neutron stars

The third system where extreme QCD matter is assumed to play a role is in the interior of neutron stars. Neutron stars are compact stars built mostly from neutrons, in which the neutron degeneracy pressure counterbalances the gravitational force leading to a hydrostatic equilibrium. The densities inside are probably large enough to allow for quark matter, maybe even for color superconductivity.

A neutron star is the end product of the evolution of a heavy star, which has a mass roughly between 2 – 8 solar masses. The fusion processes of such a star continues until an iron-nickel core has formed. Iron is the element which has the lowest nuclear binding energy, so fusion processes with iron atoms do not create energy. After the iron core has been formed, the temperature of the star will go down and with it the pressure. At some point, the pressure will be so low that it is not high enough anymore to counter the gravitational force and the star collapses until nuclear densities are achieved. During the collapse, the gravitational potential energy is released, which heats and expels the outer layers, resulting in a supernova. The core that remains continues cooling, resulting in a neutron star, or, if the density is even higher, a black hole.

The big question concerning neuron stars is what happens in the interior. Using the equation-of-state from different models and the Tolman-Oppenheimer-Volkoff relation (Tolman, 1939; Oppenheimer and Volkoff, 1939), mass-radius relations can be derived. The models for the equations-of-state that are used vary from ones containing neutrons and hyperons to ones that also contain quark matter and also hybrid models. Unfortunately it is very difficult to differentiate between the models as they give usually very similar results for observables in the relevant mass region.

Neutron stars are very dense, the density being comparable to the density that is obtained when the solar mass is squeezed into a sphere with a diameter of about 20 kilometer. Furthermore, they also spin very rapidly due to the conservation of angular momentum during the collapse. Finally we note that observations indicate that the magnetic fields of neutron stars are also very large, up to $10^{12} - 10^{13}$ G (Manchester et al., 2005). A special class of neutron stars have magnetic fields that even exceed those values, they have magnetic fields in the range $10^{14} - 10^{15}$G (Duncan and Thompson, 1992; Thompson and Duncan, 1993, 1996) and are known as magnetars. In the core even stronger magnetic fields could occur. These magnetic fields affect the matter inside the star considerably, for a recent review see Lattimer and Prakash (2007). Some aspects of the effect of magnetic fields on quark matter will be discussed in Chapter 6.

2.4 Theoretical techniques

There are several ways of attacking the problem of studying the phase diagram of QCD. The most straightforward one is perturbative QCD, which unfortunately only works at asymptotically high temperatures and chemical potentials, because only then the coupling constant of QCD becomes small as typical for a nonabelian gauge theory. Furthermore perturbative calculations indicate that the system is still not near the ideal gas limit at

temperatures of order $T \sim 1000T_c$, signalling that the system is rather strongly coupled up to these academically high temperatures (Andersen et al., 2002). Properties of a strongly coupled liquid could for instance be calculated using the AdS/CFT correspondence, which we will briefly discuss at the end of this section.

Another method that is in principle very reliable is lattice QCD. Creutz (1980) developed techniques to simulate QCD on the lattice. McLerran and Svetitsky (1981a,b), Kuti, Polonyi, and Szlachanyi (1981), and Engels et al. (1981) discussed how to implement finite temperature QCD on the lattice, for a review see Karsch (2002). But also in lattice calculations there are problems. The most severe one is that one cannot compute at finite baryon chemical potentials using the standard probabilistic methods to evaluate the functional integral, since the fermionic determinant becomes complex. Methods are developed to solve this problem, see for example Allton et al. (2005), but usually only work for a limited range of chemical potentials. For the same reason, lattice calculations at finite θ are also not possible. One can simulate however, the dependence on isospin chemical potentials, first noted by Son and Stephanov (2001), relevant for asymmetric quark matter that occurs in heavy-ion collisions and neutron stars. In this case the possibility of pion condensation arises, which we will discuss in some more detail in Chapter 4. Simulations of finite isospin were performed by Kogut and Sinclair (2002), Kogut and Sinclair (2004), Nishida (2004), de Forcrand, Stephanov, and Wenger (2007), Detmold et al. (2008). These results can then be compared with model calculations.

The method adopted in this thesis is to use low energy models for QCD. Different models can be used to study the phase diagram, all with some advantages and disadvantages. Chiral perturbation theory is the most reliable, as it is really an effective theory following the arguments of Weinberg (1979). However, the theory is only valid at temperatures lower than approximately 150 MeV (Gerber and Leutwyler, 1989). Therefore instead we use in this thesis two different models that describe chiral symmetry breaking, but that can also describe the restoration of chiral symmetry, namely the Nambu-Jona-Lasinio (NJL) model and the linear sigma model coupled to quarks (LSMq). The LSMq model is a hybrid model containing both mesons and quarks, the NJL model only contains quark degrees of freedom. Both of them describe the low energy meson spectrum of QCD quite well. In Chapters 3 and 5 we will give more elaborate introductions to the models.

As noted in Sect. 2.3.2, the matter created in heavy-ion collisions is a strongly coupled quark-gluon plasma. A final, quite modern method to investigate how such strongly coupled QCD matter behaves is by using the AdS/CFT correspondence (Maldacena, 1998). This method uses the conjectured correspondence of a string theory in anti-de Sitter space and a strongly coupled conformal field theory. Of course, QCD is neither conformal nor supersymmetric, so the correspondence gives at best hints about what is going on in a strongly coupled quark-gluon plasma. Currently much effort is put in trying to find the gravity dual of QCD, for example by Son and Stephanov (2004) and Erlich et al. (2005). One of the promising predictions of the AdS/CFT correspondence is that the pressure of a strongly coupled plasma equals 3/4 of the one found in the weak coupling limit (Gubser, Klebanov, and Tseytlin, 1998). Around a few times the critical temperature this value for the pressure is approached in lattice calculations, see Panero (2009).

2.5 Non-standard QCD phase diagrams

Apart from the usual phase diagram as a function of temperature and baryon chemical potential, it is also very illuminating to study the phase diagram as a function of other parameters. In this section we will discuss some of the possible diagrams, mainly those we will later refer to in this thesis. Some of the parameters discussed in this section are fixed in Nature, but varying their values can give us valuable insights in the phase structure of the strong interaction. In fact, that is what we do in this thesis. We study the QCD phase diagram as a function of θ, the strength of the instanton interaction, quark masses, isospin chemical potential and magnetic fields.

The order of the phase transition at finite temperature is strongly dependent on the parameters of QCD, for example, the number of active flavors and the values of the quark masses. For instance, in Fig 2.6 the phase diagram is shown as a function of the up, down, and strange current quark masses. The up and down current masses are taken degenerate. The order of the phase transition of the current quark masses was first studied this way by Brown et al. (1990), later in much more detail by for instance Karsch, Laermann, and Peikert (2001).

As from most lattice results it is assumed that the chiral phase transition roughly coincides with the deconfinement one at zero baryon chemical potential, they are not con-

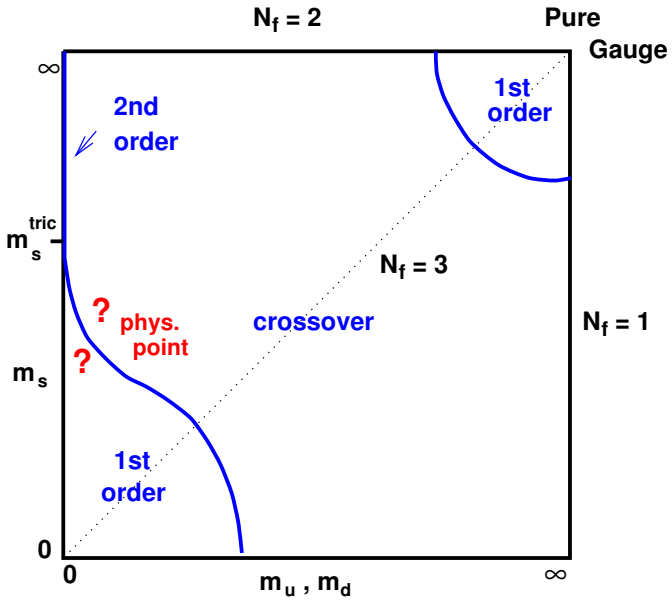

Figure 2.6: The phase diagram as a function of the quark masses, the up and down quark are taken degenerate (Peikert, Karsch, and Laermann, 2000).

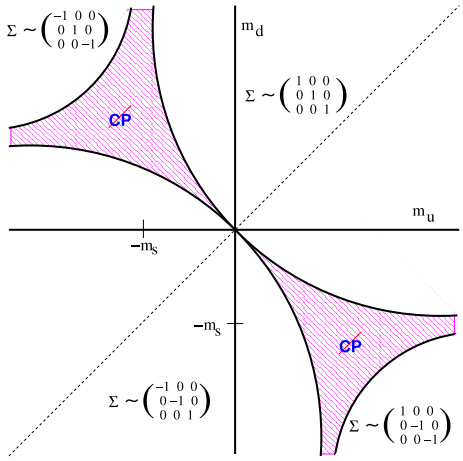

Figure 2.7: The phase diagram of three-flavor χPT as a function of the up and down quark mass (Creutz, 2004). The matrix Σ is the matrix U of Sect. 1.2.

sidered separately in Fig. 2.6. In the chiral limit ($m_u = m_d = m_s = 0$) it is expected that the chiral phase transition is of first order (Pisarski and Wilczek, 1984). At infinite quark masses, when the theory only contains gluons, lattice results indicate that the deconfinement transition is first order (Svetitsky and Yaffe, 1982a,b). At zero up and down quark mass and infinite strange quark mass the chiral phase transition is of second order, as this phase transition is expected to belong to the $O(4)$ universality class (Pisarski and Wilczek, 1984). If the up and down quark obtain a mass, the transition becomes a crossover. Lattice results suggest that the real world is in the crossover region of Fig. 2.6.

The phase diagram for negative up and/or down current quark masses with a fixed (positive) strange quark mass has been studied using chiral perturbation theory by Creutz (2004), the result is shown in Fig. 2.7. As discussed in Sect. 1.5 the case that one of the current quark masses is negative corresponds to $\theta = \pi$. In this diagram a large CP-violating region was found, Dashen's phenomenon.

The phase structure as a function of the up and down quark mass was also studied in the two-flavor case using a chiral Lagrangian by Tytgat (2000). Using his results, Fig. 2.8 can be obtained. One sees that also in the two flavor case a region of quark masses exists where the theory violates CP invariance. The shape of this region depends on the magnitude of the topological susceptibility with respect to the value of the chiral condensate. Chiral perturbation theory corresponds to the case $\tau \to \infty$ which shrinks the CP-violating region to the line of equal current quark masses. Note that one of the boundaries of the three-flavor case is missing in the two-flavor case. The phase structure as function of the up and down quark mass will be discussed in more detail for the two-flavor NJL model in Chapter 4. In that model also an upper boundary exists, similar to the three-flavor case discussed by Creutz (2004).

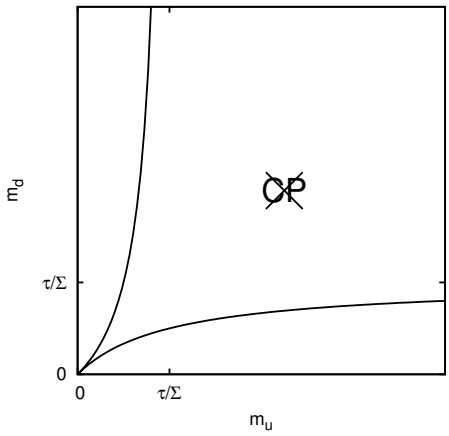

Figure 2.8: The phase diagram at $\theta = \pi$ as a function of the up and down quark mass using the two-flavor chiral Lagrangian.

The phase structure as a function of isospin chemical potential ($\mu_I = \mu_u - \mu_d$) has been studied to describe matter with unequal amounts of up and down quarks, which occurs in heavy-ion collisions and quark stars. From studies using chiral perturbation theory it is known that when the isospin chemical potential becomes larger than the pion mass, a condensate of charged pions is created (Son and Stephanov, 2001), which was also confirmed in the NJL model (Barducci et al., 2004; Barducci et al., 2003; He and Zhuang, 2005; Warringa, Boer, and Andersen, 2005). Metlitski and Zhitnitsky (2006) also studied the phase diagram as a function of isospin chemical potential, combined with the θ-dependence of the theory. The masses of the Goldstone bosons become θ-dependent, but the phase transition still occurs when the isospin chemical potential equals the mass of the Goldstone bosons. A similar relation will be considered in more detail in Chapter 4, with different results however.

2.6 Summary

In this chapter the phase structure of the strong interaction was discussed, which turns out to be very rich. For instance, at high densities and temperatures there exists a phase called the quark-gluon plasma, a state of matter with deconfined quarks and gluons. Also exotic phases exist, like color superconductivity at high chemical potential and low temperature.

In the literature, the phase structure has been investigated as a function of other parameters as well, such as the quark masses, the number of active flavors and the vacuum angle θ. In that case more possible phases emerge, including CP-violating ones. Some of these phases are only relevant for theoretical studies, while others can have consequences

for the structure of neutron stars, the Big Bang and the matter created in heavy-ion collisions.

We discussed four theoretical approaches to study QCD matter, namely perturbative methods, lattice calculations, the conjectured AdS/CFT correspondence and effective models. Perturbative methods only work at asymptotically high temperatures and chemical potentials. The applicability of lattice calculations is limited to very small chemical potentials. The AdS/CFT correspondence is expected to give only qualitative results as QCD is not conformal.

In the rest of this thesis we will use model calculations, which do not give exact results but do allow us to explore a large region in parameter space qualitatively. We will focus in particular on the role of instantons on the phase structure. These investigations are mainly performed in the framework of the NJL model, which we will introduce in the next chapter.

Chapter 3

The Nambu–Jona-Lasinio model

In this chapter the Nambu–Jona-Lasinio (NJL) model is introduced. It is mainly based on the reviews of Klevansky (1992) and Buballa (2005). In Sect. 3.1 the original NJL model is introduced, a model for interacting nucleons. We continue in Sect. 3.2 with the reinterpretation of the model as a quark model. Then the vacuum structure of the model at zero temperature and chemical potential is discussed in Sect. 3.3, including the bound states of the model, which can be interpreted as the mesons. Furthermore, some low-energy relations are derived. The chapter ends with Sect. 3.4, in which the values of the parameters that are used in this thesis are presented.

3.1 Introduction

The NJL model is a model for the strong interaction. It was first considered in 1961, before the discovery of quarks. In its original form, it was a model for interacting nucleons. In those days notions of chiral symmetry in the strong interaction were already known, leading to current algebra and the concept of a (partially) conserved axial vector current (PCAC). A model with (approximate) chiral symmetry is described by a Lagrangian with (almost) massless fermions. Inspired by superconductivity, Nambu and Jona-Lasinio (1961a,b) introduced their model, with the following Lagrangian

$$\mathscr{L} = \bar{\psi}\left(i\partial\!\!\!/ - m\right)\psi + G\left\{(\bar{\psi}\psi)^2 + (\bar{\psi}i\gamma_5\lambda_i\psi)^2\right\}. \tag{3.1}$$

Here ψ is a $SU(2)$ doublet describing the nucleons. The nucleons interact through a local four-fermion interaction with coupling constant G. This interaction is chirally symmetric (i.e., invariant under $SU(2)_L \otimes SU(2)_R$). The λ_i are the Pauli matrices and m is a small bare mass for the nucleons.

In the same way as the electrons form Cooper pairs in superconductivity, in the NJL model the nucleons form pairs with anti-nucleons and condense when G is strong enough. The condensate $\langle\bar{\psi}\psi\rangle$ becomes nonzero, signalling a breakdown of chiral symmetry. Following the Goldstone theorem, three massless pseudoscalar bosons should appear, since

the pions are much lighter than the nucleons and are pseudoscalars, they were interpreted as these Goldstone bosons. Results from current algebra could indeed be explained by this interpretation. Of course, pions are not really massless; the small mass of the pions comes from the explicit symmetry breaking by a small bare mass of the nucleons in the Lagrangian. Furthermore, the interaction creates a large self energy for the nucleons, even when the bare mass is taken to zero, and was seen as the explanation of the large mass of the nucleons, while being (almost) massless at the Lagrangian level.

3.2 The NJL model as quark model

After the discovery of QCD, the NJL model was reinterpreted as a quark model (Kleinert, 1976; Volkov, 1984; Hatsuda and Kunihiro, 1984). The fermion doublet becomes a doublet containing the up and down quark fields. In the new interpretation, the vacuum is not described by a nucleon-antinucleon condensate, but by a quark-antiquark condensate. However, the pions are still interpreted to represent the Goldstone bosons.

When the NJL model is used as a quark model, one has to be careful as some features of QCD are not contained within the model. First of all, the model does not contain gluons; this is resolved by the assumption that the gluons are "integrated out", leading to the four-quark interaction. In principle, this integrating-out would also lead to six and higher point interactions, but the coupling constants of these interactions are suppressed by Λ^{-6} and higher, where Λ is an ultraviolet cut-off. Secondly, the model contains four-fermion interactions, making it non-renormalizable. When viewed as an effective model, non-renormalizability is not a problem as there is natural a cut-off that limits the applicability. Lastly, the model does not implement confinement. In this thesis confinement will not play a role. This is clearly an omission, but many aspects of QCD can be described without considering confinement, especially chiral symmetry breaking and the light meson masses.

Since its introduction, the model has evolved along several lines. In the 1980s the model has been extended to also include the strange quark (Ebert and Reinhardt, 1986; Bernard, Jaffe, and Meissner, 1987; Hatsuda and Kunihiro, 1987). In the 1990s diquark interactions were incorporated in the NJL model. These interactions lead to color superconductivity; for a recent review see Alford et al. (2008). Color superconductivity is expected to arise at high baryon chemical potential and low temperatures. In this thesis we will not consider color superconductivity.

Apart from the form of the interaction used originally by Nambu and Jona-Lasinio, many more chirally symmetric interactions can be written down, for example, vector and axial-vector interaction terms. However, not all of these terms are independent, they are related via Fierz transformations (Klevansky, 1992; Buballa, 2005). Qualitatively, the vacuum structure of these models with more interaction terms behaves similarly to the version that only contains scalar and pseudoscalar interaction, therefore for simplicity in this thesis only the latter two will be taken into account. As a consequence, only scalar and pseudoscalar mesons will be considered.

Here the following form of the NJL model will be used

$$\mathscr{L}_{\mathrm{NJL}} = \bar{\psi}\left(i\gamma^{\mu}\partial_{\mu} + \gamma_0\mu\right)\psi - \mathscr{L}_{\mathrm{M}} + \mathscr{L}_{\bar{q}q} + \mathscr{L}_{\mathrm{det}}, \tag{3.2}$$

where the mass term of the Lagrangian is

$$\mathscr{L}_{\mathrm{M}} = \bar{\psi}M_0\psi, \tag{3.3}$$

and $\mu = (\mu_u, \mu_d)$ denotes the quark chemical potential. We choose an appropriate basis of quark fields, such that the mass-matrix M_0 is diagonal, i.e.,

$$\begin{pmatrix} m_u & 0 \\ 0 & m_d \end{pmatrix}. \tag{3.4}$$

Furthermore,

$$\mathscr{L}_{\bar{q}q} = G_1\left[(\bar{\psi}\lambda_a\psi)^2 + (\bar{\psi}\lambda_a i\gamma_5\psi)^2\right], \tag{3.5}$$

is the chirally symmetric interaction, similar to the one of Eq. (3.1). Actually, this interaction is equal to the attractive part of the $\bar{q}q$ channel of the Fierz transformed color current-current interaction (Buballa, 2005). Finally,

$$\begin{aligned}\mathscr{L}_{\mathrm{det}} =& 8G_2 e^{i\theta}\det\left(\bar{\psi}_R\psi_L\right) + \mathrm{h.c.}\\ =& G_2\cos\theta\left[(\bar{\psi}\lambda_0\psi)^2 + (\bar{\psi}\lambda_i i\gamma_5\psi)^2 - (\bar{\psi}\lambda_i\psi)^2 - (\bar{\psi}\lambda_0 i\gamma_5\psi)^2\right]\\ &- 2G_2\sin\theta\left[(\bar{\psi}\lambda_0\psi)(\bar{\psi}\lambda_0 i\gamma_5\psi) - (\bar{\psi}\lambda_i\psi)(\bar{\psi}\lambda_i i\gamma_5\psi)\right],\end{aligned} \tag{3.6}$$

is the 't Hooft determinant interaction which depends on the QCD vacuum angle θ ('t Hooft, 1976, 1986). This term is the effective interaction induced by instantons, it breaks the $U(1)_A$-symmetry (which is present in Eq. (3.5)).

Often G_1 and G_2 are taken equal, which at $\theta = 0$ means that the low energy spectrum consists of σ and $\boldsymbol{\pi}$ fields only. We will restrict ourselves to the two flavor case, using λ_a with $a = 0, ..., 3$ as generators of U(2).

The symmetry structure of the NJL model is very similar to that of QCD. In the absence of quark masses and the instanton interaction there is a global $SU(3)_c \times U(2)_R \times U(2)_L$-symmetry. The instanton interaction breaks it to $SU(3)_c \times SU(2)_L \times SU(2)_R \times U(1)_B$. For nonzero, but equal quark masses this symmetry is reduced to $SU(3)_c \times SU(2)_V \times U(1)_B$. For unequal quark masses and chemical potentials one is left with $SU(3)_c \times U(1)_B \times U(1)_I$, where B and I stand respectively for baryon number and isospin.

Because we want to investigate the effects of instantons on the vacuum, we are interested in its dependence on the strength of the determinant interaction, which is the effective instanton interaction. Frank, Buballa, and Oertel (2003) have investigated the effects of this interaction at $\theta = 0$, in particular flavor-mixing effects, on the QCD phase diagram, by choosing the following expressions for G_1 and G_2 (where our c is their α)

$$G_1 = (1 - c)G_0, \quad G_2 = cG_0. \tag{3.7}$$

In this way, the strength of the instanton interaction is controlled by the parameter c, while the value for the quark condensate at $\theta = 0$ (which is determined by the combination

Figure 3.1: The Schwinger-Dyson equation for the quark propagator in the Hartree approximation. The bare and dressed propagators are denoted by the thin and bold line respectively.

$G_1 + G_2$) is kept fixed. As mentioned, for $G_1 = G_2$, or equivalently $c = \frac{1}{2}$, only the σ and π mesons are present. In order for the model to have a stable ground state, $0 \leq c \leq \frac{1}{2}$, see Eq. (4.8)

3.3 Constituent quarks, mesons and low-energy theorems

In this section the vacuum properties of the NJL model are discussed; it is largely based on Buballa (2005). At zero temperature and density, the chiral symmetry that is present in the Lagrangian of the NJL model (and in QCD) is broken by a $\langle\bar{\psi}\psi\rangle$ condensate. Later in this thesis we will also allow for other pairing patterns, but let us stick for now to this condensate. The condensate gives a large self-energy to the quarks, usually calculated in the Hartree approximation. The corresponding self-consistent Schwinger-Dyson equation is shown in Fig. 3.1. The self-energy is p-independent in this approximation, i.e. it only shifts the mass of the quarks by a constant,

$$M = m + 2iG_0 \int \frac{\mathrm{d}^4 p}{(2\pi)^4} \mathrm{Tr}\, S(p), \tag{3.8}$$

where M is usually called the constituent mass as it behaves as an effective mass for the quarks. For simplicity we have set $m_u = m_d = m$ and $c = 0$. $S(p)$ is the dressed quark propagator, equal to $S(p) = (\not{p} - M + i\epsilon)^{-1}$. If G_0 is large enough, this equation has a nontrivial solution, where $M \neq m$. This equation is usually referred to as the gap equation, as it is analogous to the gap equation in superconductivity. Using the expression for $\langle\bar{\psi}\psi\rangle$

$$\langle\bar{\psi}\psi\rangle = -i \int \frac{\mathrm{d}^4 p}{(2\pi)^4} \mathrm{Tr}\, S(p) = \frac{M - m}{2G_0}, \tag{3.9}$$

it is clear that the appearance of a $\langle\bar{\psi}\psi\rangle$ condensate is intimately related to a large value of the constituent quark mass. The integral contained in Eq. (3.8) is divergent and needs to be regulated. The model is nonrenormalizable, so the results are scheme dependent. In this work a noncovariant three-dimensional UV cut-off Λ is employed. As discussed by Buballa (2005), such a cut-off is relatively simple and preserves the analytical structure of the integrals. Moreover, Buballa argues that the three-dimensional cut-off has the least impact on the medium parts of the integrals when performing calculations at finite temperature and chemical potential, as we will do in Chapter 4.

Meson properties are calculated within the NJL model by identifying the quark-antiquark T-matrix with meson exchange. The T matrix is usually calculated in the random-phase approximation (RPA). Graphically this identification is shown in Fig. 3.2. Here we will discuss the basic results and defer the details to Appendix A. As an example we discuss the pions, the other mesons go similarly.

The T-matrix in the pion channel is equal to

$$T_{\pi_i}(q^2) = \frac{2G_0}{1 - 2G_0\Pi_{\pi_i}(q^2)}, \tag{3.10}$$

where Π_{π_i} is the quark-antiquark polarization in the pion channel, equal to

$$\begin{aligned}\Pi_{\pi_i}(q^2) &= i\int \frac{\mathrm{d}^4p}{(2\pi)^4}\mathrm{Tr}\,\left[i\gamma_5\lambda_i S(p+q)i\gamma_5\lambda_i S(p)\right] \\ &= \frac{1}{2G_0}\left(1 - \frac{m}{M}\right) - \left(q^2 + 4M^2\right)I_0(q^2),\end{aligned} \tag{3.11}$$

where we have used the gap equation. The integral $I_0(q^2)$ is given by

$$I_0(q^2) = -4N_c i\int \frac{\mathrm{d}^4p}{(2\pi)^4}\frac{1}{\left[(p+q)^2 - M^2 + i\epsilon\right]\left[p^2 - M^2 + i\epsilon\right]}. \tag{3.12}$$

The T-matrix has a pole when the following relation holds, which can be viewed as the definition of the pion mass

$$1 - 2G_0\Pi_{\pi_i}(q^2 = m_\pi^2) = 0. \tag{3.13}$$

If we write

$$T_{\pi_i}(q^2) = \frac{-g_{\pi qq}^2}{q^2 - m_\pi^2}, \tag{3.14}$$

it follows that the coupling $g_{\pi qq}$ between the quarks and pion is given by

$$g_{\pi qq}^{-2} = \left.\frac{\mathrm{d}\Pi_{\pi_i}}{\mathrm{d}q^2}\right|_{q^2=m_\pi^2}. \tag{3.15}$$

Combining Eq. (3.13) with Eq. (3.11) and the gap equation leads to the following expression for the mass of the pion

$$m_\pi^2 = \frac{m}{M}\frac{1}{2G_0 I_0}, \tag{3.16}$$

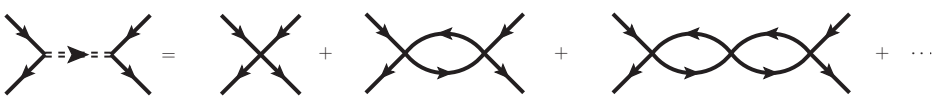

Figure 3.2: The T-matrix in the pion channel calculated in the RPA identified as pion exchange.

Figure 3.3: One-pion-to-vacuum matrix element in the RPA.

where we have made the assumption that $I_0(q^2)$ is a smooth and slowly varying function of q^2 (Klevansky, 1992), i.e. $I_0(q^2) \approx I_0(0) \equiv I_0$. Eq. (3.16) shows that the pions are massless in the chiral limit, as expected for Goldstone bosons. Furthermore, combining Eqs. (3.15) and (3.11) using the same approximation yields

$$g_{\pi qq}^{-2} = I_0, \tag{3.17}$$

thus the NJL model predicts a value for the coupling constant between quarks and mesons, an observation that will be of importance in Chapter 5.

Another important quantity related to pion physics is the pion decay constant. It is calculated from the matrix element $\langle 0| J_i^{5\mu} |\pi_j\rangle$, depicted graphically in Fig. 3.3 and which is equal to

$$\begin{aligned} f_\pi q^\mu \delta_{ij} &= g_{\pi qq} \int \frac{\mathrm{d}^4 p}{(2\pi)^4} \mathrm{Tr}\left[\gamma^\mu \gamma_5 \frac{\lambda_i}{2} S(p+q) i\gamma_5 \lambda_j S(p)\right] \\ &= g_{\pi qq} M q^\mu I_0(q^2) \delta_{ij}. \end{aligned} \tag{3.18}$$

Again neglecting the q^2-dependence of $I_0(q^2)$, we obtain

$$g_{\pi qq} f_\pi = M, \tag{3.19}$$

which is the quark level version of the π-nucleon Goldberger-Treiman relation (Goldberger and Treiman, 1958). Moreover, combining Eqs. (3.17) and (3.16) with Eq. (3.9) and expanding the result to first order in m gives the Gell-Mann–Oakes–Renner relation (Gell-Mann, Oakes, and Renner, 1968)

$$f_\pi^2 m_\pi^2 \approx -m \langle \bar{\psi}\psi \rangle . \tag{3.20}$$

To conclude this section, the NJL model reproduces the results of current algebra, which is to be expected, since these results are all consequences of chiral symmetry breaking. Because the model reproduces the low-energy theorems of current algebra, it can be used to describe low-energy QCD.

3.4 Choice of parameters

The NJL model employed in this thesis has five free parameters, G_0, the cut-off Λ, the current quark masses m_u and m_d, and the strength of the instanton interaction c. Using

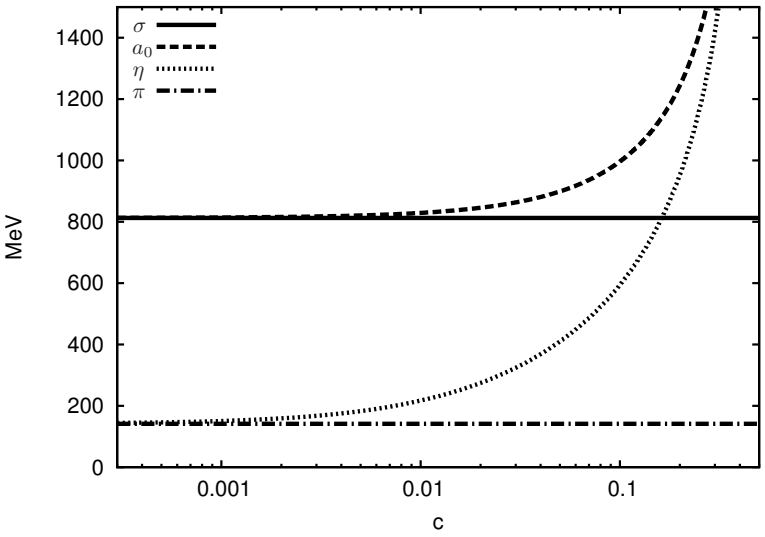

Figure 3.4: The c-dependence of the meson masses. The masses are calculated in the RPA.

the relations that were derived in the previous section, the first four parameters can be fitted to the pion decay constant f_π, the pion mass and the quark condensates $\langle\bar{u}u\rangle$ and $\langle\bar{d}d\rangle$. Following Frank, Buballa, and Oertel (2003) we choose for our numerical studies the following parameters, unless stated otherwise: $m = m_u = m_d = 6$ MeV in case of degenerate quark masses, a three-dimensional momentum cut-off $\Lambda = 590$ MeV/c and $G_0\Lambda^2 = 2.435$. These values corresponds to a pion mass of 140.2 MeV, a pion decay constant of 92.6 MeV and finally, a quark condensate $\langle\bar{u}u\rangle = \langle\bar{d}d\rangle = (-241.5\text{ MeV})^3$. These values are in reasonable agreement with experimental determinations.

For the last free parameter of the model, c, it is more difficult to obtain a realistic value. The parameter sets the amount of breaking of $U(1)_A$, consequently it determines the masses of the η and a_0 mesons. The c-dependence of the masses of the mesons calculated in the RPA are shown in Fig. 3.4. At $c = 0$, the $U(1)_A$ symmetry is restored and the mass of η equals the mass of the pions, for the same reason the mass of the sigma equals the mass of the a_0 mesons. When c is increased, the $U(1)_A$ symmetry gets broken and both the masses of η meson and the a_0 mesons increase monotonically. When c approaches $1/2$, the masses of those mesons go to infinity, which means that at $c = 1/2$ the spectrum only consists of σ and the pions, as mentioned in Sect. 3.2.

The problem now is to associate a mass to the η particle. In a pure $SU(2)$ world this would indeed be the physical η, leading to a value for c of 0.11. However, as discussed by Frank, Buballa, and Oertel (2003), it is unrealistic to describe the η meson without strange quarks. Using the $SU(3)$-version of the NJL model, they obtain a slightly higher estimate for c, between 0.16 and 0.21. Note that in the physical $N_f = 3$ world, η is not a flavor singlet. Furthermore, Frank, Buballa, and Oertel argue that as the instanton liquid

model is so successful in describing vacuum correlators, the instanton interaction is the dominant one, so one should choose an even higher value for c.

The parameter c is related to the topological susceptibility τ. Using expressions for the η mass, this relation can be made explicit. In the chiral limit, the relation between the η mass and τ is given by the Witten–Veneziano relation (Eq. (1.16)), which for $N_f = 2$ yields

$$\tau = \frac{f_\pi^2 m_\eta^2}{4}.$$

Using the procedure discussed in Sect. 3.3, one obtains the following expression for the η mass in the NJL model,

$$m_\eta^2 = \frac{c}{1-2c}\frac{-2\langle\bar{\psi}\psi\rangle M}{f_\pi^2}, \tag{3.21}$$

hence,

$$\tau \approx -\frac{1}{2}\frac{c}{1-2c}\langle\bar{\psi}\psi\rangle M. \tag{3.22}$$

From this expression we can infer that when $c \to \frac{1}{2}$, $\tau \to \infty$. In this work the value of c will be left free in order to study the influence of instantons.

Chapter 4

Spontaneous CP violation in the strong interaction at $\theta = \pi$

In this chapter the θ-dependence of the phase structure of the two-flavor NJL model will be discussed. The full θ-dependence of the vacuum will be studied (briefly), but the main focus is on the $\theta = \pi$-case, which allows for spontaneous CP violation. The dependence of the phase structure, and in particular of the CP-violating phase, on the quark masses, instanton interaction strength, temperature, baryon and isospin chemical potential is examined in detail. When available a comparison to earlier results from effective theories is made. From our results we conclude that spontaneous CP violation in the strong interaction is an inherently low-energy phenomenon. Furthermore, inside the CP-violating phase, the masses and the mixing of the mesons display some unusual features as a function of the instanton interaction strength. This chapter is partly based on Boer and Boomsma (2008).

4.1 Introduction

As discussed in Chapter 1, the possibility of spontaneous CP violation in the strong interaction, known as Dashen's phenomenon, is one of the reasons why the θ-dependence of this interaction has been studied. Furthermore, metastable states have been proposed to occur in heavy-ion collisions that violate CP invariance; such states would be described by an effective nonzero θ. It is very difficult to study finite θ in QCD due to the non-perturbative nature of the θ-term. Even in lattice QCD, studies are limited to small θ, because of the problem of how to deal with complex phases. Therefore, the θ-dependence of the strong interaction and Dashen's phenomenon have been studied extensively using low energy effective theories, such as chiral perturbation theory and using the chiral Lagrangian (Witten, 1980; di Vecchia and Veneziano, 1980; Smilga, 1999; Tytgat, 2000; Akemann, Lenaghan, and Splittorff, 2002; Creutz, 2004; Metlitski and Zhitnitsky, 2005, 2006), or by using specific models, such as the NJL model (Fujihara, Inagaki, and

Kimura, 2007). In a quark model, like the NJL model, the effects of instantons and the θ-term are incorporated via an effective interaction, the 't Hooft determinant interaction, see Sect. 3.2. In Sect. 1.2 it was argued that chiral perturbation theory can be expanded to include these effects in a similar way via a log determinant interaction (Witten, 1980; di Vecchia and Veneziano, 1980).

The discussion of chiral perturbation theory together with the log determinant interaction presented in Sect. 1.2 and 1.3 shows that whether or not the strong interaction exhibits spontaneous CP violation at $\theta = \pi$ depends on the topological susceptibility τ, the chiral condensate Σ and on the values of the quark masses. We will now discuss this dependence in some more detail. Two limiting cases were considered in the literature. Witten (1980), who studied the lowest order (LO) chiral Lagrangian, argued that when τ/Σ is nonzero but much smaller than the quark masses, the theory always exhibits spontaneous CP violation at $\theta = \pi$, independent of the values of the quark masses and number of flavors. The opposite case (Witten, 1980; di Vecchia and Veneziano, 1980; Tytgat, 2000), i.e. when the masses of the quarks are much smaller than τ/Σ, leads to different results. In this case it does depend on the values of the quark masses. In the two-flavor case for $\tau \to \infty$ (which means no η meson is included and thus corresponds to chiral perturbation theory), spontaneous CP violation only occurs for degenerate quark masses. For finite $\tau/\Sigma \gg m_u, m_d$ spontaneous CP violation also occurs for nondegenerate quark masses in a finite interval of m_d/m_u around 1, as was shown by Tytgat (2000), see Fig. 2.8. In the three-flavor case, a region exists in the (m_u, m_d)-plane where the theory spontaneously violates CP invariance (Creutz, 2004), as shown in Fig. 2.7. The asymptotes depend on the value of the strange quark mass.

When performing calculations with the LO chiral Lagrangian there are only a few parameters, namely the quark masses, the pion decay constant, the value of the quark condensate and the strength of the determinant interaction. It is therefore interesting to study CP violation in a somewhat richer situation, such as chiral perturbation theory beyond leading order, which has been studied by Smilga (1999) and corresponds to $\tau \to \infty$. In this chapter we will make a comprehensive study of the θ-dependence and especially spontaneous CP violation at $\theta = \pi$ within the framework of the two-flavor NJL model in the mean-field approximation. We will study the dependence on the effective instanton interaction strength c, not only in the two limiting cases, but for all possible values. This c is related to the topological susceptibility τ as given in Eq. (3.22).

We find that there is a critical value of the interaction strength at $\theta = \pi$ above which spontaneous CP violation occurs and which depends linearly on the quark masses, as expected from axial anomaly considerations. As will be discussed, the two-flavor NJL model allows for Dashen's phenomenon also for nondegenerate quark masses (as is the case for chiral perturbation theory only at next-to-leading order (Tytgat, 2000)). We find a region in the (m_u, m_d)-plane very similar to the three-flavor LO chiral perturbation theory result shown in Fig. 2.7. However, for the two-flavor NJL model the asymptotes are determined by the strength of the instanton induced interaction, instead of m_s.

Next we study the influence of nonzero temperature and baryon and isospin chemical potential. It has been suggested that in those cases the Vafa-Witten theorem may no longer apply (see for instance Cohen (2001) for some explicit arguments, but also Ein-

horn and Wudka (2003) for counterarguments). But even if it does apply, spontaneous CP violation at finite temperature or baryon chemical potential (through metastable states) has been considered in the literature (Lee, 1973; Morley and Schmidt, 1985; Kharzeev, Pisarski, and Tytgat, 1998; Buckley, Fugleberg, and Zhitnitsky, 2000) and possible experimental signatures in heavy ion collisions have been put forward (Kharzeev and Pisarski, 2000; Voloshin, 2004; Kharzeev and Zhitnitsky, 2007; Kharzeev, McLerran, and Warringa, 2008). This would also be relevant in the early universe, when possibly θ was nonzero and later relaxed to zero, for example via a Peccei-Quinn-like mechanism (Peccei and Quinn, 1977b,a; Wilczek, 1978). We therefore wish to check the Vafa-Witten theorem and the possible presence of CP-violating local minima in the NJL model at finite temperature and density.

Spontaneous CP violation at $\theta = \pi$ within the two-flavor NJL model including temperature dependence has been considered before in Fujihara, Inagaki, and Kimura (2007), but only for a very limited range of quark masses: $|m_u \pm m_d| < 6$ MeV at $c = \frac{1}{2}$ and without chemical potentials.

In Metlitski and Zhitnitsky (2006) the phase diagram as a function of θ and isospin chemical potential has been investigated within first-order chiral perturbation theory for two flavors. We will compare this to our results at nonzero isospin chemical potential, where a modification of the pattern of charged pion condensation is observed at $\theta = \pi$.

In this chapter the ground state is obtained by minimizing the effective potential, an approach equivalent to the one discussed in the previous chapter, i.e. solving the gap equation, which is convenient when discussing the bound states of the model. The effective potential will be calculated in the mean-field approximation, the minimization is done numerically.

This chapter is organized as follows, first we discuss the effect of chiral transformations on the model, which is relevant for the calculation of the effective potential and for a comparison to earlier results from the literature. We continue with a discussion of the θ-dependence of the ground state, including temperature effects and nonzero baryon and isospin chemical potential. Also we discuss the c-dependence of the meson masses and mixing in the CP-violating phase. We end with conclusions and a further discussion of the results.

4.2 Chiral transformations in the NJL model

In Sect. 1.5 we discussed the relation between a negative quark mass and QCD with $\theta = \pi$. Here we extend this discussion to the NJL model. The NJL model is not a gauge theory, so the fermion measure is invariant under chiral rotations. But now the Lagrangian contains two terms that are not invariant under chiral transformations, the mass-term and the determinant interaction. The latter is θ-dependent. Like for QCD, this θ-dependence can be absorbed in the up-quark mass using a chiral rotation. So the analysis for the NJL model is similar to the one for QCD, but instead of a noninvariant measure we have a noninvariant effective interaction.

The calculation of the ground state of the NJL-model is more conveniently done with

the θ-dependence in the up-quark mass term, i.e. we use in Eq. (3.2)

$$\begin{aligned}\mathscr{L}'_{\mathrm{M}} &= \bar{u}'_R m_u e^{-i\theta} u'_L + \bar{d}'_R m_d d'_L + \text{h.c.},\\ \mathscr{L}'_{\mathrm{det}} &= 8G_2 \det(\bar{\psi}'_R \psi'_L) + \text{h.c.},\end{aligned} \tag{4.1}$$

with

$$\begin{aligned}u_L &= e^{-i\theta/2} u'_L,\\ u_R &= e^{i\theta/2} u'_R.\end{aligned} \tag{4.2}$$

Therefore, below we will calculate the effective potential using the transformed (primed) fields, but discuss the ground state phase structure solely in terms of the condensates in terms of the original fields. Only in the latter case the $SU(2)_V$ symmetry among the three pions (and among the a_0-mesons) is manifest when we consider degenerate quark masses for instance.

4.3 Calculation of the ground state

In Chapter 3 the ground state of the NJL model was calculated at zero temperature and chemical potential, and with equal current masses for the up and down quark. The method used in that chapter to obtain the ground state was to solve the gap equation, the approach originally used by Nambu and Jona-Lasinio. In this section an equivalent method will be presented, namely minimizing the effective potential. This approach generalizes much easier to other pairing mechanisms than the one when only $\langle\sigma\rangle$ becomes nonzero.

The ground state of a theory is obtained by finding the state that minimizes the free energy Ω. Very often it is assumed that the ground state does not depend on position, which corresponds to translational invariance and allows for the introduction of the effective potential $\mathcal{V}$

$$\mathcal{V} = T\frac{\Omega}{\mathscr{V}} = -T\frac{\ln Z}{\mathscr{V}}, \tag{4.3}$$

where $\mathscr{V}$ is the volume of space, T is temperature and Z is the grand canonical partition function. In the case of a ground state that does not depend on position, one has to minimize the effective potential.

We will calculate the effective potential in the mean-field approximation, which is equivalent to the Hartree approximation and in this case leading order in the $1/N_c$ expansion. In order to perform this calculation a Hubbard-Stratonovich transformation will be performed. First we introduce 8 real auxiliary fields α_a and β_a in Eq. (3.2) as follows

$$\mathscr{L}'_{\mathrm{NJL}} \to \mathscr{L}'_{\mathrm{NJL}} - \frac{\alpha'^2_0 + \beta'^2_i}{4(G_1+G_2)} - \frac{\alpha'^2_i + \beta'^2_0}{4(G_1-G_2)}. \tag{4.4}$$

Shifting these auxiliary fields according to

$$\begin{aligned}&\alpha'_0 \to \alpha'_0 + 2(G_1+G_2)\bar{\psi}'\lambda_0\psi' && \alpha'_i \to \alpha'_i + 2(G_1-G_2)\bar{\psi}'\lambda_i\psi'\\ &\beta'_0 \to \beta'_0 + 2(G_1-G_2)\bar{\psi}'\lambda_0 i\gamma_5\psi' && \beta'_i \to \beta'_i + 2(G_1+G_2)\bar{\psi}'\lambda_i i\gamma_5\psi'\end{aligned} \tag{4.5}$$

eliminates the four-quark interactions and the Lagrangian becomes quadratic in the fermion fields

$$\mathscr{L}'_{\mathrm{NJL}} = \bar{\psi}' \left(i\gamma^\mu \partial_\mu - M'_0 - \alpha'_a \lambda_a - i\gamma_5 \beta'_a \lambda_a \right) \psi' - \frac{\alpha_0'^2 + \beta_i'^2}{4(G_1 + G_2)} - \frac{\alpha_i'^2 + \beta_0'^2}{4(G_1 - G_2)}. \tag{4.6}$$

The integration over the quark fields is straightforward to perform. In the mean-field approximation fluctuations of the auxiliary fields are not taken into account, which means that in Eq. (4.6) the auxiliary fields are replaced by their vacuum expectation values (VEVs). From now on, α_a and β_a will denote the VEVs of the corresponding fields. These vev's are directly related to the quark condensates

$$\begin{aligned} \alpha'_0 &= -2(G_1 + G_2) \langle \sigma' \rangle , & \boldsymbol{\alpha}' &= -2(G_1 - G_2) \langle \boldsymbol{a}'_0 \rangle , \\ \beta'_0 &= -2(G_1 - G_2) \langle \eta' \rangle , & \boldsymbol{\beta}' &= -2(G_1 + G_2) \langle \boldsymbol{\pi}' \rangle . \end{aligned} \tag{4.7}$$

All quantities in this section refer to the primed fields, but for notational convenience we will drop the primes from now on *in this section only*. Results presented in the subsequent sections will refer exclusively to the unprimed quantities.

One obtains the following expression for the thermal effective potential $\mathcal{V}$ in the mean-field approximation (see e.g. Warringa, Boer, and Andersen, 2005)

$$\mathcal{V} = \frac{\alpha_0^2 + \beta_i^2}{4(G_1 + G_2)} + \frac{\alpha_i^2 + \beta_0^2}{4(G_1 - G_2)} - T\, N_c \sum_{p_0 = (2n+1)\pi T} \int \frac{\mathrm{d}^3 p}{(2\pi)^3} \log\det K \tag{4.8}$$

where K is a matrix in flavor and Dirac space,

$$K = \mathbb{1}_{\mathrm{f}} \otimes (i\gamma_0 p_0 + \gamma_i p_i) - \mu \otimes \gamma_0 - \mathscr{M} \tag{4.9}$$

is the inverse quark propagator, and

$$\begin{aligned} \mathscr{M} = {} & m_u (\cos\theta\, \lambda_u \otimes \mathbb{1}_{\mathrm{d}} + \sin\theta\, \lambda_u \otimes i\gamma_5) + m_d \lambda_d \otimes \mathbb{1}_{\mathrm{d}} + \alpha_a \lambda_a \otimes \mathbb{1}_{\mathrm{d}} \\ & + \beta_a \lambda_a \otimes i\gamma_5, \end{aligned} \tag{4.10}$$

with $\lambda_u = (\lambda_0 + \lambda_3)/2$ and $\lambda_d = (\lambda_0 - \lambda_3)/2$.

The values of the condensates are found by minimizing the effective potential with respect to these condensates. By exploiting U(1) flavor symmetry one only has to study the condensates $\alpha_0, \alpha_1, \alpha_3, \beta_0, \beta_1$, and β_3. Warringa, Boer, and Andersen (2005) ignored the β_0 and β_3 condensates based on the Vafa-Witten theorem. As we wish to check the validity of this theorem at finite temperature and density in our model calculation, we do take these condensates into account.

In order to calculate the effective potential, it is convenient to multiply K with $\mathbb{1}_{\mathrm{f}} \otimes \gamma_0$ which leaves the determinant invariant and yields a new matrix $\tilde{K}$ with ip_0's on the diagonal. The determinant of K can be calculated as $\det K = \prod_{i=1}^{8} (\lambda_i - ip_0)$, where λ_i are the eigenvalues of $\tilde{K}$ with $p_0 = 0$. After performing the sum over the Matsubara frequencies, we obtain

$$T \sum_{p_0 = (2n+1)\pi T} \log\det K = \sum_{i=1}^{8} \left[\frac{|\lambda_i|}{2} + T \log\left(1 + e^{-|\lambda_i|/T} \right) \right]. \tag{4.11}$$

Finally we need to integrate over the three-momenta p up to the ultraviolet cutoff Λ to determine the effective potential.

Minimizing $\mathcal{V}$ implies solving the equations

$$\frac{\partial \mathcal{V}}{\partial x_i} = 0, \tag{4.12}$$

where $x = \{\alpha_0, \alpha_1, \alpha_3, \beta_0, \beta_1, \beta_3\}$. The derivatives of the effective potential can be calculated from the expression (Warringa, 2006)

$$T \frac{\partial}{\partial x_j} \sum_{p_0=(2n+1)\pi T} \log\det K = \frac{1}{2} \sum_{i=1}^{8} b_{ij} \left(1 - \frac{2}{e^{|\lambda_i|/T} + 1}\right) \mathrm{sgn}\,(\lambda_i)\,, \tag{4.13}$$

where $b_{ij} = \left(U^\dagger \partial \tilde{K}(p_0 = 0)/\partial x_j U\right)_{ii}$. Here U is a unitary matrix which contains in the i-th column the normalized eigenvector of $\tilde{K}$ with eigenvalue λ_i. Again, one has to integrate over p to obtain the complete derivative. Since this calculation does not use the finite distance method, the derivatives can be determined very accurately. Also, it is very efficient as one needs the eigenvalues of $\tilde{K}$ anyway in order to calculate the effective potential.

When a solution to Eq. (4.12) has been found, it has to be checked whether the solution is indeed a minimum and not a maximum or saddle-point. This is checked by verifying that the Hessian of the solution only has positive eigenvalues. If more than one minimum is found, the one with the lowest value is chosen. Also the continuity of the effective potential is checked.

The speed of the calculation mainly depends on how fast the eigenvalues of $\tilde{K}$ can be calculated. To speed up the evaluation of the calculation of the eigenvalues, one can make use of the fact that the determinant of $\tilde{K}$ is invariant under the interchanging of rows and columns. This can be used to bring $\tilde{K}$ to a block-diagonal form of two 4×4-matrices. This reduces the computing time to determine the eigenvalues with a factor of four as the time to numerically calculate the eigenvalues scales cubically with the dimension of the matrix. Another way of improving the speed of the calculation is to choose $\mathbf{p}$ to lie along the z-direction, exploiting the fact that $\det \tilde{K}$ does not depend on the direction of $\mathbf{p}$.

As we said in the beginning of this section, the method presented here is equivalent to solving the gap equation, discussed in Chapter 3 for zero temperature and chemical potential. In that case we can assume that only α_0 becomes nonzero (if we also take $m_u = m_d = m$ and $\theta = 0$). The absolute values of the λ_i become all equal to $|\lambda_i| = \sqrt{\mathbf{p}^2 + (\alpha_0 + m)^2}$. Consequently it is straightforward to evaluate Eq. (4.12), only $x_i = \alpha_0$ has to be taken into account

$$\frac{\partial \mathcal{V}}{\partial \alpha_0} = \frac{\alpha_0}{2(G_1 + G_2)} - 4N_c N_f \int \frac{\mathrm{d}^3 p}{(2\pi)^3} \frac{\alpha_0 + m}{\sqrt{\mathbf{p}^2 + (\alpha_0 + m)^2}} = 0, \tag{4.14}$$

which is equivalent to Eq. (3.8) after performing the trace and p_0-integration. Note that $\alpha_0 + m$ equals the constituent quark mass.

One final remark we have to make regarding Eq. (4.8) is the fact that in order for the effective potential to have a minimum at finite values for the condensates, the coupling

G_2 has to satisfy $-G_1 \leq G_2 \leq G_1$, and correspondingly, $-\frac{1}{2} \leq c \leq \frac{1}{2}$. From Eq. (3.6) we can see that a negative value for G_2 corresponds to shifting $\theta \to \theta + \pi$, implying that the minimum of the theory will be at $\theta = \pi$, in violation of the Vafa-Witten theorem at zero temperature and density. Therefore, we will restrict to $0 \leq c \leq \frac{1}{2}$. The case $c = \frac{1}{2}$ is special, because then only the σ' and $\boldsymbol{\pi}'$ fields are present in the theory, which means at $\theta = 0$ the σ and $\boldsymbol{\pi}$ mesons and at $\theta = \pi$ the η and $\boldsymbol{a}_0$ mesons.

4.4 Convexity of the effective potential

A well known result from statistical physics is that the effective potential is convex. But if one calculates the effective potential in the mean-field approximation, sometimes local minima arise and hence a non-convex effective potential is found. In textbooks such as Peskin and Schroeder (1995) and Weinberg (1996) it is shown how one obtains a convex effective potential from a nonconvex one. Here we will briefly repeat the argument, which is a field-theoretical analogue to a Maxwell construction.

Let us discuss for simplicity a scalar field theory with field operator Φ. We assume that the effective potential as a function of vacuum expectation value of the field ϕ has the form of Fig. 4.1, which has a concave region. The expectation values of the minima are ϕ_1 and ϕ_2. Now consider that for states between the two minima, the state is a linear combination of the two minimizing states, i.e.

$$|\phi\rangle = \sqrt{x}\,|\phi_1\rangle + \sqrt{1-x}\,|\phi_2\rangle\,, \quad 0 < x < 1. \tag{4.15}$$

For the value of the expectation value ϕ between the two minima we obtain (Peskin and Schroeder, 1995)

$$\phi = x\phi_1 + (1-x)\phi_2, \tag{4.16}$$

leading to an effective potential between the two minima of the form

$$\mathcal{V}(\phi) = x\mathcal{V}(\phi_1) + (1-x)\mathcal{V}(\phi_2), \tag{4.17}$$

as interference terms vanish in the infinite volume limit (Weinberg, 1996). The potential of Eq. (4.17) has a lower value between the two minima. Weinberg (1996) states that the effective potential is defined as: $\mathcal{V}(\phi)$ *is the minimum of the expectation value of the energy density for all states constrained by the condition that the scalar field* Φ *has expectation value* ϕ. Using this definition we see that Eq. (4.17) corresponds to the "real" effective potential, which obtains the form given in Fig. 4.2, indeed a convex function. In other words, the convexity applies to the equilibrium effective potential.

The solution to the convexity problem that we just presented is a formal one, one of its consequences is that metastable states are not possible. However, in physical systems metastable phases do arise. How can these states be described? The important assumption when discussing the formal effective potential is that one assumes that all quantum fluctuations are taken into account, including ones that are very long-ranged and take a very long time, like tunneling effects. In real physical situations, like in heavy-ion collisions, not all fluctuations ought to be taken into account as the system has finite size and

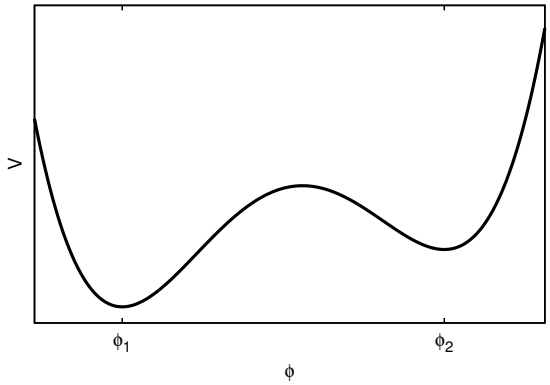

Figure 4.1: A possible form of the effective potential as a function of the expectation value of the field ϕ (Peskin and Schroeder, 1995).

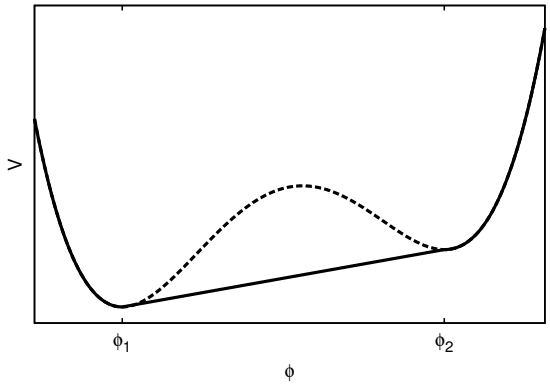

Figure 4.2: The "convex" potential obtained from Fig. 4.1 by using Eq. (4.17).

exists for a finite amount of time. The "physical" (coarse-grained) effective potential, is consequently not necessarily convex.

The situation is analogous to the phenomenon of phase separation in thermodynamics, if the system is in the concave region it is unstable and phase separation will take place. If the system is in a convex region (but not in the global minimum), the system stays there for some time until a large fluctuation takes the system to the global minimum. The point where the curvature of the effective potential flips sign is called a spinodal, it represents the end-point of stability of a certain phase.

Another indication that local minima have a physical interpretation is that they can become the global one when changing external parameters like θ, T, μ, etcetera, usually connected to a first order transition. The latter suggests that the local minima are indeed metastable states. However, the physics of a metastable state cannot be described by effec-

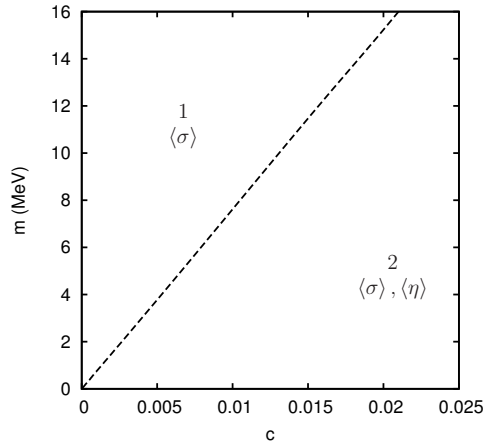

Figure 4.3: The (c, m) phase diagram at $\theta = \pi$.

tive potential considerations alone, as it is inherently a non-stable and non-homogeneous situation. For example, for the calculation of the lifetime of a metastable state one would need to perform a calculation using the effective action. We will not do this for the local minima that we encounter, hence no conclusions about the lifetime of metastable states will be reached.

4.5 The ground state of the NJL model

This section deals with our results for the ground state of the NJL model. First we discuss the θ-dependence of the condensates and the effective potential. It turns out that for nonzero c, two different situations can be distinguished: below a certain critical c value (c_{crit}) no spontaneous CP violation takes place at $\theta = \pi$, whereas for c larger than this critical value it does take place. The value of this c_{crit} depends on the values of the quark masses. In Fig. 4.3 we show the phase diagram at $\theta = \pi$ in the (c, m)-plane for degenerate quark masses $m_u = m_d = m$, two phases can be distinguished,

1. $\langle\sigma\rangle \neq 0$, the ordinary chiral condensate.

2. $\langle\sigma\rangle \neq 0, \langle\eta\rangle \neq 0$, the CP-violating phase.

The phase transition corresponds to c_{crit} and is of second order. A linear relation exists between the quark mass and c_{crit} (more on this in Sect. 4.7.1). Note that the value of the $\langle\sigma\rangle$ condensate in phase 2 is significantly smaller than its value in phase 1, except close to the phase transition.

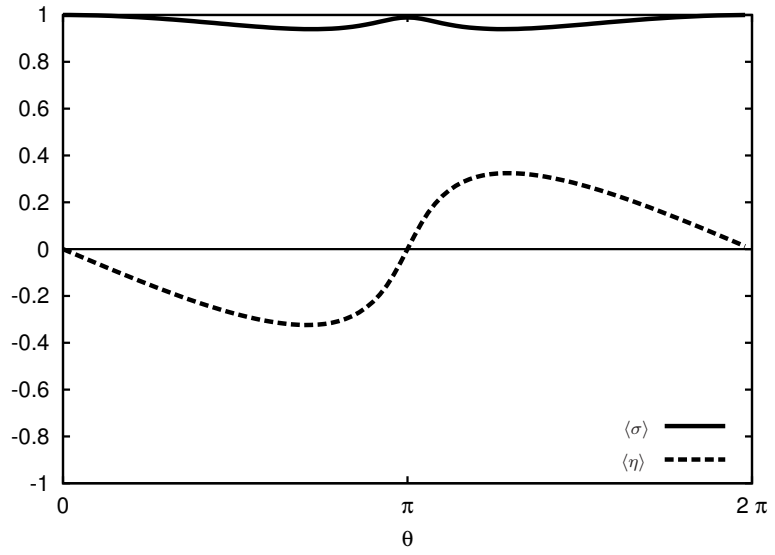

Figure 4.4: The θ-dependence of the normalized condensates, with $c = 0.005 < c_{\text{crit}}$.

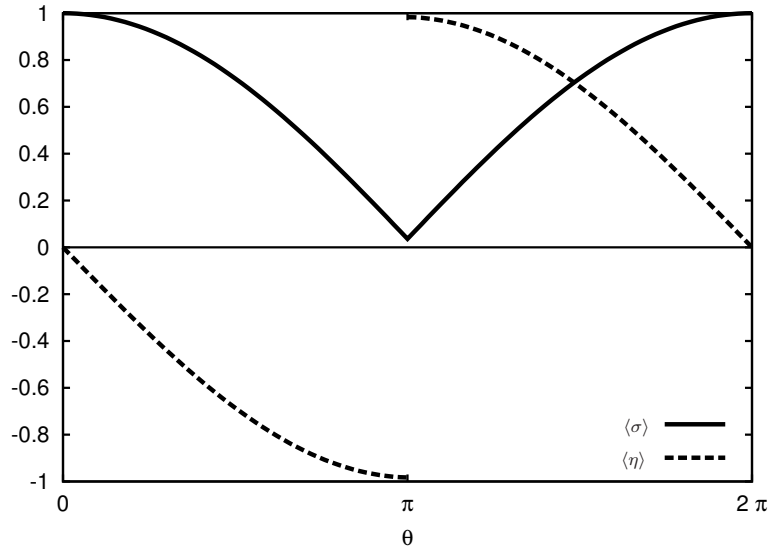

Figure 4.5: The θ-dependence of the normalized condensates, with $c = 0.2 > c_{\text{crit}}$.

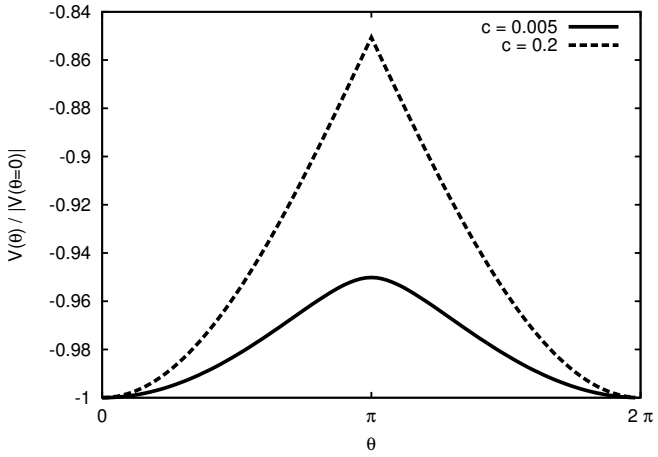

Figure 4.6: The θ-dependence of the normalized effective potential at $c = 0.005$ and $c = 0.2$.

4.5.1 The θ-dependence of the vacuum

When the determinant interaction is turned off, there is no θ-dependence. In terms of the unprimed fields, only the σ condensate is nonzero.

In Fig. 4.4 we show the θ-dependence of the various condensates for the case $c = 0.005$, which for our choice $m_u = m_d = 6\,\mathrm{MeV}$ is below $c_{\mathrm{crit}} \approx 0.008$. As can be seen, no spontaneous CP violation occurs, since $\langle\eta\rangle = 0$ at $\theta = \pi$. Explicit CP violation for other values of θ does occur, as expected. In this figure the condensates are normalized with respect to $\langle\sigma\rangle$ at $\theta = 0$. Both $\langle\boldsymbol{\pi}\rangle$ and $\langle\boldsymbol{a}_0\rangle$ are zero for all θ and this remains true for c above c_{crit} for degenerate quark masses.

Fig. 4.5 shows the case of $c = 0.2$. Spontaneous CP violation is clearly visible, as $\langle\eta\rangle$ is nonzero at $\theta = \pi$. As can be seen two degenerate vacua then exist, with opposite signs for $\langle\eta\rangle$. These two degenerate vacua differ by a CP transformation. This is known as Dashen's phenomenon (Dashen, 1971) and is also apparent from the θ-dependence of the effective potential. In Fig. 4.6 we show the effective potential as a function of θ normalized to its value at $\theta = 0$, for the two cases $c = 0.005$ and $c = 0.2$. In both cases, the minimum of the effective potential is at $\theta = 0$, in agreement with the Vafa-Witten theorem. Furthermore, it can be seen that the case with spontaneous CP violation has a cusp at $\theta = \pi$, and therefore a left and a right derivative which differ by a sign. Due to the axial anomaly, the θ-derivative of the effective potential is proportional to $\langle\eta\rangle$. This explains the occurrence of two values for the η condensate.

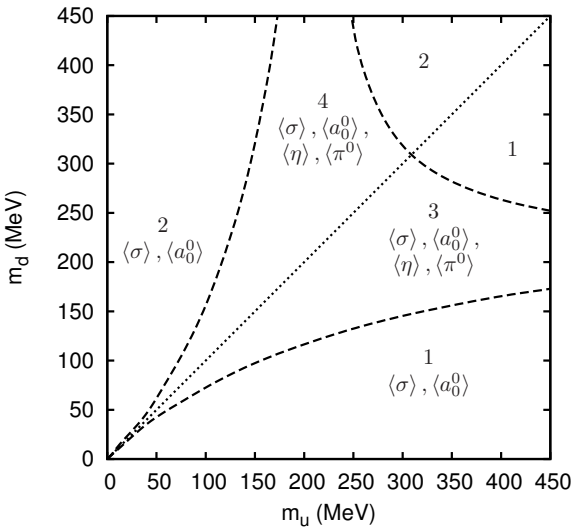

Figure 4.7: The (m_u, m_d) phase diagram of the NJL at $\theta = \pi$ with $c = 0.4$. The dashed lines denote second order phase transitions and the dotted line a crossover.

4.5.2 Phase structure at $\theta = \pi$

In this section we concentrate further on the case $\theta = \pi$. We will start with a discussion of the mass-dependence of the ground state. From Creutz (2004) we know that in three-flavor chiral perturbation theory a region exists in the (m_u, m_d)-plane where CP is spontaneously violated, cf. Fig. 2.7. In that case the shape of the CP-violating region depends on the strange quark mass. In the present case it depends on the choice of c. Finally we note that in the calculation when using the two-flavor chiral Lagrangian the shape of the region is set by the topological susceptibility τ, cf. Fig. 2.8.

In Fig. 4.7 we show the phase diagram of the NJL model at $\theta = \pi$ with $c = 0.4$ in the (m_u, m_d)-plane. Four phases can be distinguished

1. $\langle\sigma\rangle < 0, \langle a_0^0\rangle < 0$
2. $\langle\sigma\rangle < 0, \langle a_0^0\rangle > 0$
3. $\langle\sigma\rangle < 0, \langle a_0^0\rangle < 0, \langle\eta\rangle \neq 0, \langle\pi^0\rangle \neq 0$
4. $\langle\sigma\rangle < 0, \langle a_0^0\rangle > 0, \langle\eta\rangle \neq 0, \langle\pi^0\rangle \neq 0$

In phases 3 and 4 two degenerate vacua exist with opposite signs for both $\langle\eta\rangle$ and $\langle\pi^0\rangle$. The phase transitions between the CP-conserving phases 1 and 2 to the CP-violating phases 3 and 4 are second order. The phases 1 and 2 only differ in the sign for the $\langle a_0^0\rangle$-condensate, the same holds for the phases 3 and 4. The phase transition between the phases 3 and 4 is a crossover, as is the case for the phase transition between phase 1 and 2 for large m_u

and m_d. Exactly at the crossover, $\langle a_0^0 \rangle$ vanishes and in the CP-violating region the same applies to $\langle \pi^0 \rangle$, but not to $\langle \eta \rangle$. The fact that a_0^0-condensation (and π^0-condensation in the CP-violating region) occurs when the masses are not equal simply reflects the explicit breaking of $SU(2)_V$ which occurs for nondegenerate quark masses.

The shape of the CP-violating region is determined by the asymptotes, which are proportional to c. We conclude that in contrast to two-flavor LO chiral perturbation theory (the case of $m_s \to \infty$ in Creutz (2004), such that the asymptotes are moved to $m_u = m_d = \infty$), the NJL model does have a spontaneous CP-violating phase for two nondegenerate quark flavors. This is in accordance with the analysis using the LO chiral Lagrangian of Tytgat (2000) in the large N_c limit and for finite $\tau/\Sigma \gg m_u, m_d$. There is however an important difference between the NJL model and the results obtained from the two-flavor LO chiral Lagrangian, in the latter case there is always CP violation when m_u and m_d are larger than τ/Σ, cf. Fig. 2.8, which is not the case in the NJL model.

4.6 Finite temperature and baryon chemical potential

In this section we turn to the changes in the phase structure at nonzero temperature and density. Fujihara, Inagaki, and Kimura (2007) states that the CP-violating phase at $\theta = \pi$ does not exist at high temperatures, i.e. a critical temperature exists above which the CP-violating condensates are zero. Fujihara, Inagaki, and Kimura only considered the case $c = \frac{1}{2}$ and small mass. Here we generalize their results to other c values. In Fig. 4.8 the (T, c) phase diagram is shown for degenerate quark masses. The following three phases arise

1. $\langle \sigma \rangle \neq 0$, the ordinary chiral condensate.
2. $\langle \sigma \rangle \neq 0, \langle \eta \rangle \neq 0$, the CP-violating phase.
3. $\langle \sigma \rangle \approx 0$, the (almost) chiral symmetry restored phase.

The phase structure at $T = 0$ can be understood from Fig. 4.7: for degenerate quark masses the two phases are encountered on its diagonal. The phase transition occurs at that particular value of $m_u = m_d$ for which $c = 0.4$ is the critical c. The phase transition between phases 1 and 2 is of second order for all temperatures. This second order transition is in disagreement with the analysis of Mizher and Fraga (2009), who studied the same phase transition in the linear sigma model coupled to quarks. In Chapter 5 we will study this discrepancy in detail.

For nondegenerate quark masses the phases 1 and 2 would correspond to phases 1 and 3 or 2 and 4 of Fig. 4.7 depending on whether m_u is larger or smaller than m_d, respectively. In that case two second order phase transitions are present.

Above a certain temperature one observes in Fig. 4.8 an approximate restoration of chiral symmetry (phase 3). Note that the chiral symmetry is not fully restored due to the nonzero current quark masses. The phase transition between phases 1 and 3 is a crossover, like it is at $\theta = 0$. The crossover line is defined by the inflection points $\partial^2 \langle \sigma \rangle / \partial T^2 = 0$.

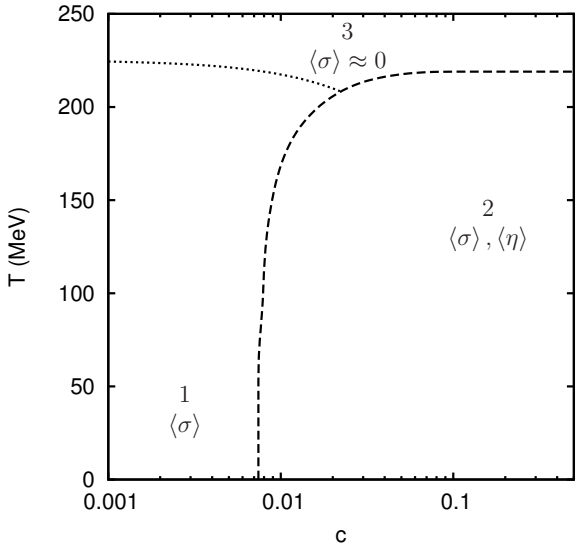

Figure 4.8: The (T, c) phase diagram of the NJL model at $\theta = \pi$. The dotted line represents a crossover, which is defined by the inflection points $\partial^2 \langle\sigma\rangle / \partial T^2 = 0$.

At high temperature also the CP-violating phase disappears. This is consistent with the fact that at high temperature instanton effects become exponentially suppressed (Gross, Pisarski, and Yaffe, 1981). The CP-violating phase is after all realized due to the instanton induced interaction. The maximum value of the critical temperature as function of c is 219 MeV.

The analysis can be extended to nondegenerate quark masses, shown in Figs. 4.9 and 4.10, where the phase diagram is shown as a function of the up and down current quark masses at temperatures of respectively 120 MeV and 150 MeV. It is mainly the high mass regime that is affected by a nonzero temperature. As the temperature increases, the region with broken CP invariance gets smaller and the phase transition that crosses the $m_u = m_d$ line, referred to as the upper boundary of the CP-violating region, moves to smaller values of the masses. The amount of CP violation decreases with temperature. It is interesting to see that it is mainly the upper boundary that is affected by the temperature, as it is not present in LO chiral perturbation theory with anomaly effects, see Fig. 2.8 and is consequently not taken into account in the discussions of Kharzeev, Pisarski, and Tytgat (1998). The other 2 boundaries hardly change with temperature, which may indicate that τ/Σ (their asymptotic value at $T = 0$) is only weakly dependent on T, in contrast to the assumption in Kharzeev, Pisarski, and Tytgat, discussed in Sect. 1.4. Note however that Kharzeev, Pisarski, and Tytgat considered the three-flavor case.

We have verified that also for nonzero temperature the minimum of the effective potential is at $\theta = 0$, which means the Vafa-Witten theorem ($\mathcal{V}(\theta = 0) \leq \mathcal{V}(\theta \neq 0)$) continues to hold in the NJL model at nonzero temperature. The same applies to finite baryon and

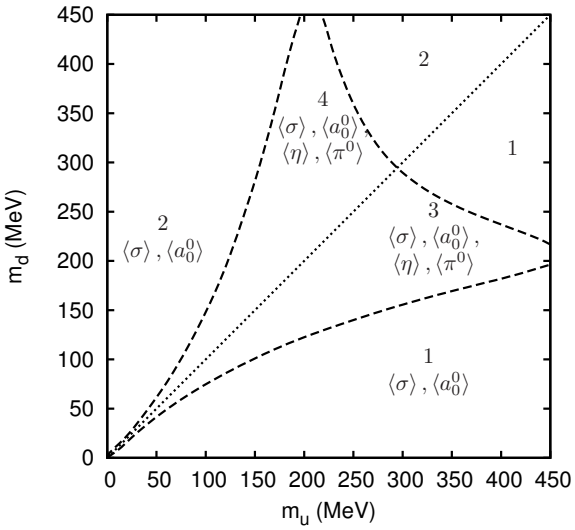

Figure 4.9: The (m_u, m_d) phase diagram of the NJL at $\theta = \pi$ with $c = 0.4$ and $T = 120\,\text{MeV}$.

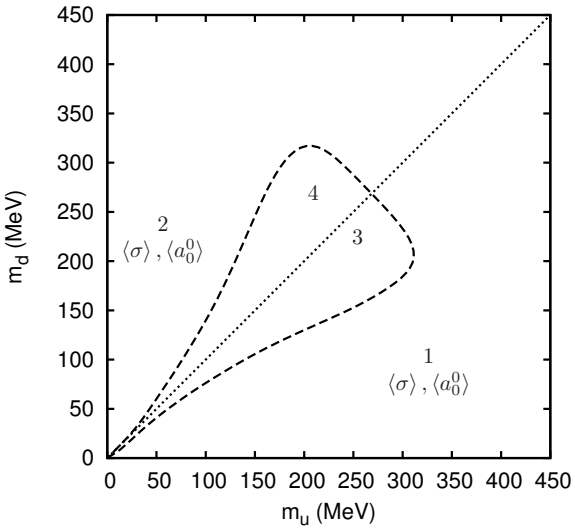

Figure 4.10: Same as Fig. 4.9, now for $T = 150\,\text{MeV}$.

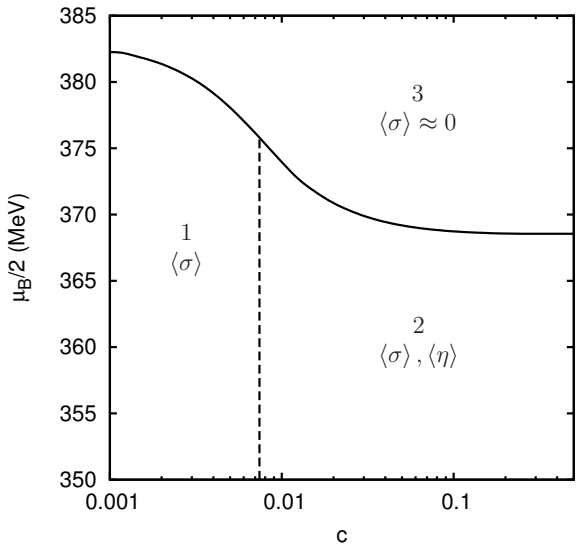

Figure 4.11: The (μ_B, c) phase diagram of the NJL model at $\theta = \pi$.

isospin chemical potential. We also have checked whether there are any local minima in the effective potential at nonzero temperature and density, but we found none. Our results indicate that τ/Σ may be T-independent, but θ-dependent. Probably the θ-dependence of τ/Σ closes the small window around T_c that allows for metastable states, cf. the discussion of Sect. 1.4. The two-flavor NJL model in the mean-field approximation therefore does not support the suggestion of Kharzeev, Pisarski, and Tytgat (1998).

Now we will briefly consider nonzero baryon chemical potential $\mu_B = \mu_u + \mu_d$, where $\mu_{u,d}$ denote the u, d quark chemical potentials. The (μ_B, c) phase diagram is displayed in Fig. 4.11 for a restricted range of μ_B values. The same phases occur as in the (T, c) phase diagram, but now the phase transition to the (almost) chiral symmetry restored phase is of first order, like for $\theta = 0$. Furthermore, the first-order phase transition has a small c dependence (note the suppressed zero). As always, the phase transition from phase 1 to phase 2 is of second order.

4.7 Nonzero isospin chemical potential

In quark matter systems equilibrium and neutrality conditions can require that $\mu_u \neq \mu_d$. Son and Stephanov (2001) observed that charged pion condensation can occur for nonzero isospin chemical potential $\mu_I = \mu_u - \mu_d$. At $\theta = 0$ this second order phase transition between the ordinary phase of broken chiral symmetry ($\langle\sigma\rangle \neq 0$) to the pion condensed phase (which also breaks chiral symmetry) occurs when μ_I equals the vacuum pion mass. In this subsection we address this issue at $\theta = \pi$.

In Fig. 4.12 we show the phase diagram of the NJL model in the (μ_I, c)-plane, for

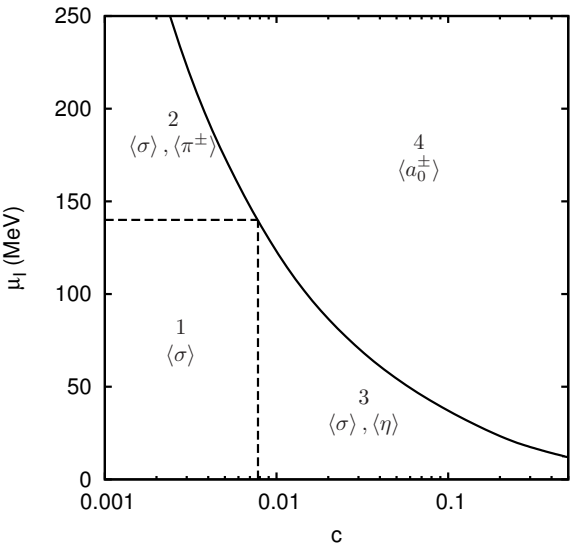

Figure 4.12: The (μ_I, c) phase diagram of the NJL model at $\theta = \pi$.

$m_u = m_d = 6$ MeV. The solid line indicates a first-order phase transition, the dashed lines indicate second-order phase transitions. The four phases are characterized as follows

1. $\langle\sigma\rangle \neq 0$
2. $\langle\sigma\rangle \neq 0, \langle\pi^{\pm}\rangle \neq 0$
3. $\langle\sigma\rangle \neq 0, \langle\eta\rangle \neq 0$
4. $\langle a_0^{\pm}\rangle \neq 0$

Phase 4 is a novel phase characteristic of $\theta = \pi$. This phase also has a small nonzero $\langle\sigma\rangle$-condensate (not indicated), due to the explicit breaking by the quark masses.

For $c < c_{\text{crit}}$ a nonzero $\langle\pi^{\pm}\rangle$-condensate exists above a certain μ_I value. Like at $\theta = 0$ the second-order phase transition turns out to be at $\mu_I = m_\pi$, where m_π is the vacuum pion mass. In addition, there is a second phase transition, of first order this time, at larger μ_I, where charged pion condensation makes way for charged a_0 condensation. For $c > c_{\text{crit}}$ no nonzero $\langle\pi^{\pm}\rangle$-condensate exists, only nonzero $\langle a_0^{\pm}\rangle$. The phase transition between phases 3 and 4 is of first order. The question arises what determines the value of μ_I at this phase transition to charged meson condensation? To answer this question, the meson masses need to be calculated using the methods presented in Sect. 3.3.

4.7.1 The c-dependence of the meson masses and mixing

As said, at $\theta = 0$ charged pion condensation occurs when μ_I is larger than or equal to the vacuum ($\mu_I = 0$) pion mass. For the NJL model this has been studied extensively in

Barducci et al. (2004, 2005), He and Zhuang (2005), and Warringa, Boer, and Andersen (2005). This condition is independent of c. To see what happens in the $\theta = \pi$ case, we calculate the c-dependence of the meson masses, with $\mu_I = 0$. The results are shown in Fig. 4.13. Clearly, at $\theta = \pi$ the situation is quite different from $\theta = 0$, shown in Fig. 3.4.

At $c = 0$ (no instanton interactions) the η and $\boldsymbol{\pi}$ masses are equal and also the σ and $\boldsymbol{a}_0$ masses. This follows from the symmetry of the Lagrangian at $c = 0$, which has a $\mathrm{U}(2)_L \otimes \mathrm{U}(2)_R$-symmetry that is spontaneously broken by the chiral condensate (ignoring the explicit breaking by the quark masses) to $\mathrm{U}(2)_V$. This means there are four (pseudo-) Goldstone bosons, with the same (small) masses: the η and $\boldsymbol{\pi}$ mesons. The instanton interactions remove the degeneracy for $c \neq 0$.

When $c > c_{\mathrm{crit}}$, i.e. when $\langle \eta \rangle \neq 0$, a complication arises: the mass eigenstates are not CP or P eigenstates any longer. The occurrence of the η condensate results in mixing of the σ-particle with its parity partner, the η-particle. Similarly, the pions mix with their parity partners, the $\boldsymbol{a}_0$'s. The mixing is to be expected because when the ground state is not CP-conserving, there is no need for the excitations, i.e. the mesons, to be CP eigenstates or states of definite parity in case of charged mesons.

The mass eigenstates, denoted with a tilde, are defined in the following way

$$\begin{aligned} |\tilde{\sigma}\rangle &= \cos\theta_\eta \, |\sigma\rangle + \sin\theta_\eta \, |\eta\rangle \,, \\ |\tilde{\eta}\rangle &= \cos\theta_\eta \, |\eta\rangle - \sin\theta_\eta \, |\sigma\rangle \,, \\ |\tilde{\boldsymbol{a}}_0\rangle &= \cos\theta_{\boldsymbol{\pi}} \, |\boldsymbol{a}_0\rangle + \sin\theta_{\boldsymbol{\pi}} \, |\boldsymbol{\pi}\rangle \,, \\ |\tilde{\boldsymbol{\pi}}\rangle &= \cos\theta_{\boldsymbol{\pi}} \, |\boldsymbol{\pi}\rangle - \sin\theta_{\boldsymbol{\pi}} \, |\boldsymbol{a}_0\rangle \,, \end{aligned} \tag{4.18}$$

where θ_η and $\theta_{\boldsymbol{\pi}}$ are the mixing angles. The states on the r.h.s. are the usual states of definite parity. In Fig. 4.14 the c-dependence of the mixing is shown.

The calculation of the mixing and the resulting masses is similar to the mixing of η_0 and η_8 in the three-flavor NJL-model, which was discussed in great detail in Klevansky (1992) using the random phase approximation (RPA), which we present in Appendix A. As a side remark we mention that we also calculate the curvature of the effective potential at the minimum. This should be proportional to the RPA masses, which we check explicitly in Appendix A.

When $c < c_{\mathrm{crit}}$ no mixing takes place and the tilde fields are equal to their counterparts without tilde. When $c > c_{\mathrm{crit}}$ mixing occurs. The mixing between η and σ increases rapidly as c increases, reaching a maximum at $c = 0.09$, where $\tilde{\sigma}$ is almost completely η and vice versa. For larger c the mixing, however, decreases rapidly again, so that when $c = \frac{1}{2}$, $\tilde{\sigma}$ ($\tilde{\eta}$) is again equal to σ (η).

The mixing between $\boldsymbol{a}_0$ and the pions behaves differently; here the mixing angle increases rapidly to become 90° at $c = \frac{1}{2}$, i.e. $\tilde{\boldsymbol{\pi}}$ becomes $\boldsymbol{a}_0$ and vice versa.

Now we return to the behavior of the tilde-meson masses, which also display unusual features as function of c, see Fig. 4.13. When $c < c_{\mathrm{crit}}$, the $\tilde{\boldsymbol{\pi}}$ masses are constant, and equal to the ordinary pion masses. Furthermore, the $\tilde{\eta}$ mass decreases with increasing c. This is peculiar to $\theta = \pi$, because at $\theta = 0$ the η mass increases with increasing c. The $\tilde{\eta}$ mass has its lowest, nonzero value at c_{crit}. This is in contrast to three-flavor lowest order chiral perturbation theory (Creutz, 2004), where the η mass (in Creutz (2004) actually the

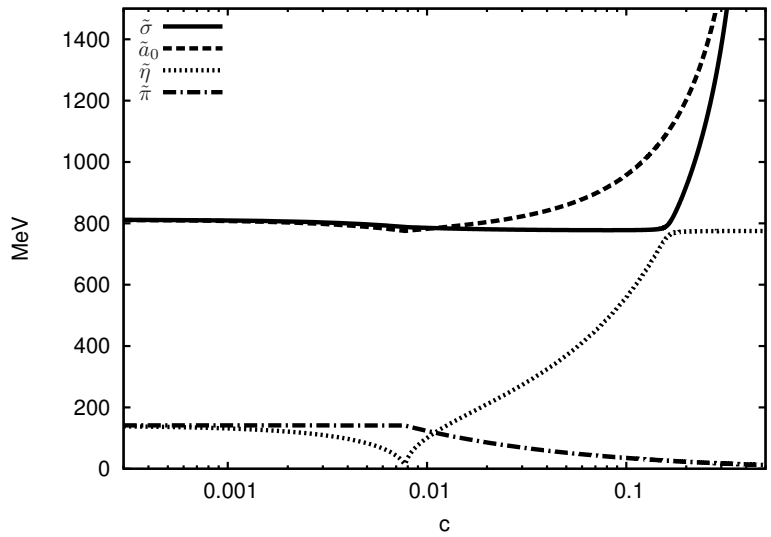

Figure 4.13: The c-dependence of the meson masses at $\theta = \pi$. The masses are calculated in the RPA.

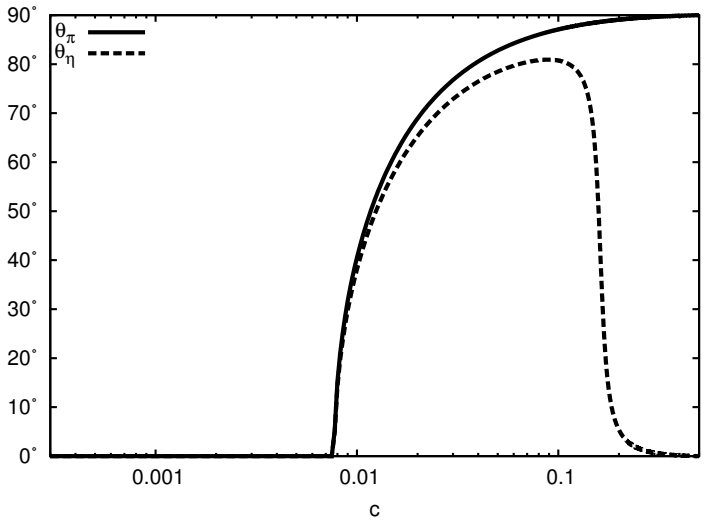

Figure 4.14: The c-dependence of the mixing-angle of the mesons at $\theta = \pi$. The mixing is calculated in the RPA.

π^0 mass using the primed theory) vanishes at the phase transition. Finally, also the masses of the $\boldsymbol{a}_0$'s and σ decrease slightly with increasing c. From the fact that $m_\eta \approx 0$ at c_{crit}, the current quark mass dependence of c_{crit} as discussed in Sect. 4.5 can be deduced. The mass of the η meson (Eq. (3.21)) at $\theta = \pi$ for small c is given by

$$m_\eta^2 \approx \frac{m}{M}\frac{1}{2G_0 I_0} - \frac{c}{G_0 I_0}, \tag{4.19}$$

resulting in the following expression for c_{crit}

$$c_{\text{crit}} \approx \frac{m}{2M}. \tag{4.20}$$

This confirms the linear dependence on m found in Fig. 4.3, which indeed has a slope approximately equal to $1/2M \approx 1/800\,\text{MeV}$, where M is the constituent quark mass at $c = 0$.

When $c > c_{\text{crit}}$ the c-dependence of the masses changes dramatically. The $\tilde{\boldsymbol{\pi}}$ mass now decreases monotonically with increasing c, whereas the $\tilde{\boldsymbol{a}}_0$ and $\tilde{\sigma}$ mass both increase monotonically to infinity towards $c = \frac{1}{2}$. The latter can be understood, because when $c = \frac{1}{2}$, G_1 equals G_2, which as mentioned means for $\theta = \pi$ that there are no $\boldsymbol{\pi}$ and σ mesons in the spectrum.

Another striking feature is that the $\tilde{\eta}$ mass rises until it almost reaches the $\tilde{\sigma}$ mass, after which it remains approximately constant. The behavior of the $\tilde{\sigma}$ mass is opposite, first it is almost constant and when it becomes almost equal to the $m_{\tilde{\eta}}$ mass it increases to infinity. The masses of $\tilde{\sigma}$ and $\tilde{\eta}$ cannot cross when there are interactions that mix the two states, which is similar to level repulsion in quantum mechanics. The point where both masses are almost equal corresponds to a mass that is twice the constituent quark mass. This forms the threshold to decay into two quarks, which makes one of the two mesons unstable when $c > c_{\text{crit}}$.

Fig. 4.13 strengthens the conclusion that Nature is not described by $\theta = \pi$. From Bég (1971) we know that no CP-violating condensate is present in the vacuum, so if θ would be equal to π, c has to be smaller than c_{crit}. But when $c < c_{\text{crit}}$ and $\theta = \pi$, the mass of the η meson is always smaller than the mass of the pions and the decay of η into pions is prohibited, as opposed to the case $\theta = 0$. This decay is observed in Nature, meaning that the physical η mass is much larger than the pion mass, hence we can conclude that the NJL model also indicates that $\theta \approx 0$ in Nature, a conclusion already reached by Baluni (1979), Crewther et al. (1979), and Kawarabayashi and Ohta (1981) by looking at the electric dipole moment of the neutron, see Sect. 1.2.

Now we turn again to the original question concerning the charged meson condensation phase transition. From the calculation of the masses of the tilde-mesons, we infer that the condition for charged meson condensation at $\theta = \pi$ is $\mu_I \geq m_{\tilde{\pi}}(c)$. For $c < c_{\text{crit}}$, the phase transition takes place when μ_I equals $m_{\tilde{\pi}} = m_\pi$, as it does at $\theta = 0$. For $c > c_{\text{crit}}$ it takes place at the mass of $\tilde{\boldsymbol{\pi}}$, which is now a mixed state of $\boldsymbol{\pi}$ and $\boldsymbol{a}_0$. At $c = \frac{1}{2}$ this means at the mass of the $\boldsymbol{a}_0$. The latter observation is in agreement with a result of Metlitski and Zhitnitsky (2006), where the (μ_I, θ) phase diagram of degenerate two-flavor chiral perturbation theory is investigated to lowest order at effectively $c = \frac{1}{2}$ (due to the absence of the

η meson). There it is observed that charged pion condensation occurs when μ_I is equal to the θ-dependent pion mass $m_\pi(\theta)$. In Metlitski and Zhitnitsky (2006) all θ-dependence resides in the mass matrix, with both quarks having a θ-dependent mass. Hence, their θ-dependent pion field corresponds to what we call π', which at $\theta = \pi$ is the $\boldsymbol{a}_0$ field in the original, unprimed theory, leading to an agreement with our finding.

The second phase transition for $c < c_{\text{crit}}$ from the charged pion condensed phase to the charged $\boldsymbol{a}_0$ condensed phase does not correspond to μ_I being equal to a meson mass calculated at $\mu_I = 0$. Although we have not found a condition in terms of the calculated masses, μ_I at this first-order phase transition follows a line that is the smooth continuation of the $\tilde{\pi}$ mass in the region $c > c_{\text{crit}}$ to infinity at $c = 0$. A calculation of the meson masses at nonzero μ_I, such as performed by He and Zhuang (2005) for the $\theta = 0$-case, might resolve this open issue.

4.8 Conclusion and discussion

The θ-dependence of the ground state of the two-flavor NJL model is investigated in the mean-field approximation. The main focus is on the case $\theta = \pi$, when spontaneous CP violation is possible. The θ-dependence of the theory is found to strongly depend on the strength of the 't Hooft determinant interaction. When the strength of this interaction, which is governed by the parameter c, is small or zero, no spontaneous CP violation takes place at $\theta = \pi$. The low-energy physics is then almost the same as at $\theta = 0$, except that the η mass is smaller than the pion mass at $\theta = \pi$. At larger c however, spontaneous CP violation does take place at $\theta = \pi$. So the phenomenon of spontaneous CP violation is governed by the 't Hooft determinant interaction, which describes the effect of instantons in the effective theory. The question whether c is sufficiently large for CP violation to occur at $\theta = \pi$ depends on the quark masses. In other words, spontaneous CP violation requires instantons, but its actual realization depends on the size of their contribution w.r.t. the quark masses. This is also expected to be the case in QCD, where it can be phrased in terms of the low-energy theorem identity $\sum_q 2im_q \langle \bar{q}\gamma_5 q \rangle = -N_f \langle g^2 F^a_{\mu\nu} \tilde{F}^{\mu\nu}_a \rangle / 8\pi^2$ (cf. e.g. Metlitski and Zhitnitsky (2005)), which relates $\langle \eta \rangle$ to the first derivative of the effective potential w.r.t. θ. Depending on m_q the coupling constant g needs to be sufficiently large for spontaneous CP violation to take place. Or in other words, the energy needs to be sufficiently low. The latter observation is in agreement with the disappearance of the CP violation at temperatures above a certain critical temperature or density. Therefore, we conclude that spontaneous CP violation in the strong interaction is an inherently low-energy phenomenon.

We have checked that the Vafa-Witten theorem holds in the NJL model also at finite temperature and density and found that no local minima arise, indicating the absence of metastable CP-violating states in the NJL model. We have confirmed several previous results that were obtained in two-flavor chiral perturbation theory. We found (in accordance with the results of Tytgat (2000)) that two-flavor lowest-order chiral perturbation theory (i.e. $\tau \to \infty$) is in general not rich enough to yield results that one might expect to hold in QCD too. It leads for instance to the conclusion that only for $m_u = m_d$ spontaneous

CP violation occurs, without a critical strength of the instanton induced interaction. In contrast, the phase diagram of the two-flavor NJL model is very similar to that of three-flavor chiral perturbation theory (Creutz, 2004), where spontaneous CP violation arises for specific ranges of quark masses.

We also found that the presence of a nonzero η-condensate has a strong effect on the c-dependence of the meson masses and gives rise to mixing among the states of definite parity, as expected when CP invariance is not a symmetry anymore. As a result, the pions mix with their parity partners, the $\boldsymbol{a}_0$'s, and the η meson mixes with its parity partner, the σ meson. Unlike the mixing discussed as a function of θ, (i.e. the "primed" fields of Eq. (1.31)), which is just a matter of consistently naming the states in order to be able to compare to results obtained with negative quark masses and which does not affect physical results, the mixing as function of c does change the physics. For instance, the condition for charged pion condensation at nonzero isospin chemical potential becomes modified. At $\theta = \pi$ for $c < c_{\text{crit}}$, a second-order phase transition takes place when μ_I equals m_π, just as at $\theta = 0$ found by Son and Stephanov. However, we find that for $c > c_{\text{crit}}$ it becomes a first-order phase transition to a novel phase of charged $\boldsymbol{a}_0$ condensation that takes place at the mass of $\tilde{\boldsymbol{\pi}}$, which is a mixed state of $\boldsymbol{\pi}$ and $\boldsymbol{a}_0$. At $c = \frac{1}{2}$ it is entirely $\boldsymbol{a}_0$. Charged $\boldsymbol{a}_0$ condensation also arises for $c < c_{\text{crit}}$ and $\mu_I > m_\pi$, but it appears there is no condition in terms of vacuum meson masses for this second phase transition.

We expect the presented two-flavor NJL model results to remain valid when going beyond the mean-field approximation, but this remains to be studied. The three flavor case would also be interesting to study, as in that case in the chiral limit the high temperature chiral phase transition is of first order, see Sect. 2.5. This is connected to the $U(1)_A$-anomaly, see Sano, Fujii, and Ohtani (2009) for a related study in a chiral random matrix model. Finally, it would be very useful if the results could in the future be compared to lattice QCD results on the low-energy physics at $\theta = \pi$.

Chapter 5

The high temperature CP-restoring phase transition at $\theta = \pi$

In the previous chapter the phase structure of the 2-flavor NJL model at $\theta = \pi$ was discussed, in particular the conditions for spontaneous CP violation, known as Dashen's phenomenon were considered. It was found that this CP violation disappears as a second order phase transition as a function of temperature. In this chapter we will study the temperature dependence of Dashen's phenomenon in detail in comparison to another model, the linear sigma model coupled to quarks (LSMq), which has been studied by Mizher and Fraga (2009). Despite being very similar to the NJL model, it predicts a first order phase transition. In this chapter, we will see that the origin of the difference is a nonanalytic vacuum term present in the NJL model, but usually not included in the LSMq model. This chapter is largely based on Boomsma and Boer (2009).

5.1 Introduction

Both the NJL model and the linear sigma model coupled to quarks are models that aim to describe the low-energy phenomenology QCD, especially chiral symmetry breaking. Furthermore, in both models the effects of instantons are included through an additional interaction, the 't Hooft determinant interaction ('t Hooft, 1976, 1986). Both models exhibit Dashen's phenomenon, which turns out to be temperature dependent. This is to be expected, because at high temperature the effects of instantons, which are needed for the CP violation, are exponentially suppressed (Gross, Pisarski, and Yaffe, 1981). In both models the spontaneous CP violation at $\theta = \pi$ disappears at a critical temperature between 100 and 200 MeV. However, the order of the phase transition differs, in the NJL model the transition is of second order, whereas in the LSMq model it is first order. This difference

is important, because a first order transition allows for metastable phases, in contrast to a second order transition.

Although the NJL and LSMq model are not the same, they are closely related. Eguchi (1976) has shown that one can derive a linear sigma model from the NJL model, a procedure known as bosonization (discussed in Sect. 5.4). However, the effects of quarks are treated differently in the two models, which was already discussed by Scavenius et al. (2001) at $\theta = 0$. In the case of the LSMq model the effects of the quarks are usually only taken into account for nonzero temperatures, whereas in the NJL model their effects are necessarily incorporated also at zero temperature. Scavenius et al. (2001) found that the order of the chiral symmetry restoring phase transition at $\theta = 0$ was the same in both models, but the critical temperatures differ. While the qualitative aspects of the phase transition are similar at $\theta = 0$, this is not the case for the high temperature CP-restoring phase transition at $\theta = \pi$ as we will discuss in detail. We should mention here that the situation at $\theta = 0$ depends on the amount of explicit chiral symmetry breaking. Schaefer and Wambach (2007) observed that when the pion mass is reduced in order to study the chiral limit, neglecting the effects of the quarks at zero temperature can affect the order of the high temperature phase transition at $\theta = 0$ too.

Although there is a CP-restoring phase transition at high chemical potential also, in this chapter we will restrict ourselves to the temperature dependence of this phase transition at $\theta = \pi$, because there the differences between the two models are most pronounced. The chapter is organized as follows. First, the effective potentials of both models are analyzed analytically, which will allow the determination of the order of the phase transitions using standard Landau-Ginzburg type of arguments. A comparison to numerical results obtained earlier corroborates these conclusions. Subsequently, we will discuss the bosonization procedure of Eguchi, which relates the NJL model to a linear sigma model and allows us to further pinpoint the origin of the similarities and differences with the LSMq model. We end with some brief comments about chiral perturbation theory and QCD.

5.2 The NJL model

As discussed in Chapter 4, to calculate the ground state of the theory, the effective potential has to be minimized. In the following we will only consider the case of unbroken isospin symmetry, such that only nonzero $\langle\bar{\psi}\psi\rangle$ and/or $\langle\bar{\psi}i\gamma_5\psi\rangle$ can arise. At $\theta = 0$ only $\langle\bar{\psi}\psi\rangle$ becomes nonzero. A nonzero $\langle\bar{\psi}i\gamma_5\psi\rangle$ signals that CP invariance is broken, i.e., it serves as an order parameter for the CP-violating phase.

To obtain the effective potential in the mean-field approximation we start with Eq. (3.2) and "linearize" the interaction terms in the presence of the $\langle\bar{\psi}\psi\rangle$ and $\langle\bar{\psi}i\gamma_5\psi\rangle$ condensates (this is equivalent to the procedure with a Hubbard-Stratonovich transformation used in

Chapter 4)

$$\begin{aligned}(\bar{\psi}\psi)^2 &\simeq 2\langle\bar{\psi}\psi\rangle\,\bar{\psi}\psi - \langle\bar{\psi}\psi\rangle^2\,,\\ (\bar{\psi}i\gamma_5\psi)^2 &\simeq 2\langle\bar{\psi}i\gamma_5\psi\rangle\,\bar{\psi}i\gamma_5\psi - \langle\bar{\psi}i\gamma_5\psi\rangle^2\,,\\ (\bar{\psi}\psi)(\bar{\psi}i\gamma_5\psi) &\simeq \langle\bar{\psi}\psi\rangle\,\bar{\psi}i\gamma_5\psi + \langle\bar{\psi}i\gamma_5\psi\rangle\,\bar{\psi}\psi - \langle\bar{\psi}\psi\rangle\,\langle\bar{\psi}i\gamma_5\psi\rangle\,,\end{aligned} \tag{5.1}$$

leading to

$$\mathscr{L}^{\text{vac}}_{\text{NJL}} = \bar{\psi}\left(i\gamma^\mu\partial_\mu - \mathscr{M}\right)\psi - \frac{(G_1 - G_2\cos\theta)\alpha_0^2}{4(G_1^2 - G_2^2)} - \frac{(G_1 + G_2\cos\theta)\beta_0^2}{4(G_1^2 - G_2^2)} - \frac{(G_2\sin\theta)\alpha_0\beta_0}{2(G_1^2 - G_2^2)}, \tag{5.2}$$

where $\mathscr{M} = (m + \alpha_0) + \beta_0 i\gamma_5$ and

$$\begin{aligned}\alpha_0 &= -2(G_1 + G_2\cos\theta)\,\langle\bar{\psi}\psi\rangle + 2G_2\sin\theta\,\langle\bar{\psi}i\gamma_5\psi\rangle\,,\\ \beta_0 &= -2(G_1 - G_2\cos\theta)\,\langle\bar{\psi}i\gamma_5\psi\rangle + 2G_2\sin\theta\,\langle\bar{\psi}\psi\rangle\,.\end{aligned} \tag{5.3}$$

Note that we have kept the θ-dependence in the determinant interaction term. This Lagrangian is quadratic in the quark fields, so the integration can be performed. After going to imaginary time the thermal effective potential in the mean-field approximation is obtained (Warringa, Boer, and Andersen, 2005)

$$\mathcal{V}^{\text{vac}}_{\text{NJL}} = \frac{\alpha_0^2(G_1 - G_2\cos\theta)}{4(G_1^2 - G_2^2)} + \frac{\beta_0^2(G_1 + G_2\cos\theta)}{4(G_1^2 - G_2^2)} + \frac{G_2\alpha_0\beta_0\sin\theta}{2(G_1^2 - G_2^2)} + \mathcal{V}_q, \tag{5.4}$$

with

$$\mathcal{V}_q = -T\,N_c \sum_{p_0=(2n+1)\pi T} \int \frac{\mathrm{d}^3p}{(2\pi)^3}\log\det K, \tag{5.5}$$

and where K is the inverse quark propagator,

$$K = (i\gamma_0 p_0 + \gamma_i p_i) - \mathscr{M}\,. \tag{5.6}$$

In order to calculate the effective potential, it is convenient to multiply K with γ_0, like we did in Chapter 4. This multiplication does not change the determinant, but gives a new matrix $\tilde{K}$ with ip_0's on the diagonal. It follows that $\det K = \prod_{i=1}^{8}(\lambda_i - ip_0)$, where λ_i are the eigenvalues of $\tilde{K}$ with $p_0 = 0$. Because of the symmetries of the inverse propagator, half of the eigenvalues are equal to $E_{\mathbf{p}} = \sqrt{\mathbf{p}^2 + M^2}$ and the other half to $E_{\mathbf{p}} = -\sqrt{\mathbf{p}^2 + M^2}$, with $M^2 = (m + \alpha_0)^2 + \beta_0^2$. After the summation over the Matsubara frequencies, we obtain

$$\mathcal{V}_q = -8N_c \int \frac{\mathrm{d}^3p}{(2\pi)^3}\left[\frac{E_{\mathbf{p}}}{2} + T\log\left(1 + e^{-E_{\mathbf{p}}/T}\right)\right]. \tag{5.7}$$

At $T = 0$ this integral can be performed analytically. A conventional non-covariant three-dimensional UV cut-off is used to regularize the integral and yields:

$$\mathcal{V}_q^{T=0} = \nu_q|M|\frac{M^3\log\left(\frac{\Lambda}{M} + \sqrt{1 + \frac{\Lambda^2}{M^2}}\right) - \Lambda\left(M^2 + 2\Lambda^2\right)\sqrt{1 + \frac{\Lambda^2}{M^2}}}{32\pi^2}, \tag{5.8}$$

where the degeneracy factor $\nu_q = 24$.

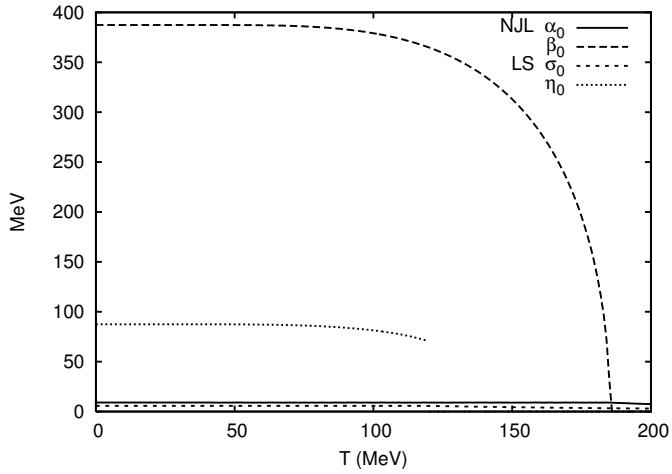

Figure 5.1: The temperature dependence of the condensates in the NJL and linear sigma model.

5.2.1 The CP-restoring phase transition

In this section the high-T CP-restoring phase transition at $\theta = \pi$ is investigated in detail. As was shown in Chapter 4 the phenomenon of spontaneous CP violation is governed by the strength c of the 't Hooft determinant interaction. It will be assumed that c is 0.2, which following the arguments of Frank, Buballa, and Oertel (2003) is considered realistic. But in fact, the critical temperature is to very good approximation c-independent for c above ~ 0.05, as can be seen from the (T, c) phase diagram given in Chapter 4.

We will start with a numerical minimization as a function of the temperature, the results of which, together with those for the LSMq model, are shown in Fig. 5.1. One observes that the critical temperature of the NJL model is significantly larger than the one of the linear sigma model, in agreement with the results of Scavenius et al. (2001) for the chiral phase transition at $\theta = 0$. Furthermore, the order of the phase transition is clearly different, contrary to the results of Scavenius et al. (2001) for $\theta = 0$.

Next we will derive an analytic expression for the effective potential for the NJL model. Two important observations which can be made from the numerical study will be helpful. First, we note that α_0 is very small and constant as long as β_0 is nonzero, which allows us to approximate $M^2 \approx \beta_0^2$. Furthermore, β_0 and hence M can be considered much smaller than πT and Λ, allowing expansions. These observations simplify our study considerably.

The phase transition occurs for M much smaller than Λ, so Eq. (5.8) can be expanded in M/Λ at $T = 0$:

$$\mathcal{V}_q^{T=0} = \nu_q \left[-\frac{M^4 \log M^2}{64\pi^2} + \frac{M^4 \log\left(4\Lambda^2\right)}{64\pi^2} - \frac{M^4}{128\pi^2} - \frac{\Lambda^2 M^2}{16\pi^2} - \frac{\Lambda^4}{16\pi^2} + \cdots \right]. \qquad (5.9)$$

For the phase transition, the non-analytic term $M^4 \log M^2$ turns out to be very important. We will see that it is exactly the *absence* of this term at finite temperatures in the NJL model that causes the differences between the two models.

Usually the temperature-dependent part of the potential has to be evaluated numerically, however when $M < \pi T$ the integral can be expanded in M/T. As can be inferred from Fig. 5.1 it is exactly this regime which is relevant for the phase transition. Note that the temperature-dependent part of the potential is UV finite, which means that for this part the cut-off can be taken to infinity. In Chapter 4 this was not done, leading to a slightly larger critical temperature. Performing the expansion, we obtain (Kapusta and Gale, 2006)

$$\mathcal{V}_q^T = -\nu_q \int \frac{\mathrm{d}^3 p}{(2\pi)^3} T \log\left(1 + e^{-E_{\mathbf{p}}/T}\right) = \nu_q \Bigg[-\frac{7\pi^2 T^4}{720} + \frac{M^2 T^2}{48} + \frac{M^4}{32\pi^2}\left(\gamma_E - \frac{3}{4} + \frac{1}{2}\log\frac{M^2}{T^2} - \log\pi\right) + \cdots \Bigg]. \quad (5.10)$$

From this expansion one can see that also the temperature dependence contains a logarithmic term, that will precisely cancel the one of Eq. (5.9) when added together.

Using that $M^2 \approx \beta_0^2$, we end up with the effective potential

$$\mathcal{V}_{\mathrm{NJL}}^{\mathrm{vac}}(T) = A_{\mathrm{NJL}}(T) + B_{\mathrm{NJL}}(T)\beta_0^2 + C_{\mathrm{NJL}}(T)\beta_0^4, \quad (5.11)$$

where

$$A_{\mathrm{NJL}}(T) = -\frac{\left(7\pi^4 T^4 + 45\Lambda^4\right)\nu_q}{720\pi^2}, \quad (5.12)$$

$$B_{\mathrm{NJL}}(T) = \frac{\left(\pi^2 T^2 - 3\Lambda^2\right)\nu_q}{48\pi^2} + \frac{1}{4G_0}, \quad (5.13)$$

$$C_{\mathrm{NJL}}(T) = \frac{\left(\log\left(4\Lambda^2\right) - \log T^2\right)\nu_q}{64\pi^2} + \frac{(-1 + \gamma_E - \log\pi)\nu_q}{32\pi^2}. \quad (5.14)$$

One observes that the $\log M^2$-term at zero temperature is cancelled by the $\log M^2$-term in the temperature-dependent part of the potential. Hence, as long as $\beta_0 < \pi T, \Lambda$ the potential contains no logarithms and is fully analytic. We note that the potential of Eq. (5.11) is the same as the one in the chiral limit at $\theta = 0$, with β_0 replaced by α_0.

The phase transition occurs when $B_{\mathrm{NJL}}(T)$ changes sign. As the potential is symmetric and quartic in the order parameter, we conclude (following Landau-Ginzburg arguments) that the phase transition is of second order, which the numerical analysis corroborates. The critical temperature is equal to

$$T_c^{\mathrm{NJL}} = \sqrt{\frac{3\nu_q G_0 \Lambda^2 - 12\pi^2}{G_0 \pi^2 \nu_q}} = 185\ \mathrm{MeV}. \quad (5.15)$$

As long as $T < \frac{2\Lambda}{\pi}\exp(-1+\gamma_E) = 246\,\mathrm{MeV}$, C_{NJL} is positive, indicating that higher order terms in β_0 are not needed in the analysis.

5.3 The LSMq model

The linear sigma model coupled to quarks, like the NJL model, is an effective low-energy model for QCD (Pisarski, 1996; Scavenius et al., 2001; Paech, Stoecker, and Dumitru, 2003; Schaefer and Wambach, 2007) similar in form to the Gell-Mann-Lévy model (Gell-Mann and Lévy, 1960). It is a hybrid model that includes both meson and constituent quark degrees of freedom, the latter only at nonzero temperature however. As was the case in the NJL model, the effects of instantons are included via the 't Hooft determinant interaction ('t Hooft, 1976, 1986). In this chapter the analysis of Mizher and Fraga (2009) is followed.

We will start with the $T = 0$ case, when only mesons are considered. The Lagrangian, which contains all Lorentz invariant terms allowed by symmetry and renormalizability has the following form, using a slightly different notation than Mizher and Fraga (2009)

$$\begin{aligned}\mathscr{L}_{LS} = &\frac{1}{2}\mathrm{Tr}(\partial_\mu\phi^\dagger\partial^\mu\phi) + \frac{\mu^2}{2}\mathrm{Tr}(\phi^\dagger\phi) - \frac{\lambda_1}{4}[\mathrm{Tr}(\phi^\dagger\phi)]^2 - \frac{\lambda_2}{4}\mathrm{Tr}[(\phi^\dagger\phi)^2] \\ &+ \frac{\kappa}{2}[e^{i\theta}\det(\phi) + e^{-i\theta}\det(\phi^\dagger)] + \frac{1}{2}\mathrm{Tr}[\frac{H}{\sqrt{2}}(\phi+\phi^\dagger)]\,,\end{aligned} \tag{5.16}$$

where ϕ is the chiral field, defined as

$$\phi = \frac{1}{\sqrt{2}}(\sigma + i\eta) + \frac{1}{\sqrt{2}}(\boldsymbol{a}_0 + i\boldsymbol{\pi})\cdot\boldsymbol{\lambda}\,. \tag{5.17}$$

The Lagrangian incorporates both spontaneous and explicit breaking of chiral symmetry, the latter through the term proportional to H. To study this symmetry breaking, we can concentrate on the potential corresponding to Eq. (5.16), expressed in the meson fields

$$\begin{aligned}\mathcal{V}_{\mathrm{LS}}^{T=0} = &-\frac{\mu^2}{2}(\sigma^2 + \boldsymbol{\pi}^2 + \eta^2 + \boldsymbol{a}_0^2) \\ &- \frac{\kappa}{2}\cos\theta\,(\sigma^2 + \boldsymbol{\pi}^2 - \eta^2 - \boldsymbol{a}_0^2) \\ &+ \kappa\,\sin\theta\,(\sigma\eta - \boldsymbol{\pi}\cdot\boldsymbol{a}_0) - H\sigma \\ &+ \frac{1}{4}(\lambda_1 + \frac{\lambda_2}{2})(\sigma^2 + \eta^2 + \boldsymbol{\pi}^2 + \boldsymbol{a}_0^2)^2 \\ &+ \frac{2\lambda_2}{4}(\sigma\boldsymbol{a}_0 + \eta\boldsymbol{\pi} + \boldsymbol{\pi}\times\boldsymbol{a}_0)^2\,.\end{aligned} \tag{5.18}$$

The spontaneous symmetry breaking manifests itself through nonzero σ and η condensates and are obtained by minimizing the potential. We allow for these condensates by shifting the fields

$$\sigma \to \sigma_0 + s, \quad \eta \to \eta_0 + h, \tag{5.19}$$

where σ_0 and η_0 are the values that minimize the potential and s and h are the fluctuations. These σ_0 and η_0 are proportional to the condensates α_0 and β_0 of the NJL model, respectively.

The potential can now be split in two parts, a vacuum part and one that depends on the fluctuations, i.e.,

$$\mathcal{V}_{\rm LS}^{T=0} = \mathcal{V}_{LS}^{{\rm vac},T=0} + \mathcal{V}_{\rm LS}^{\rm fluc}\,. \tag{5.20}$$

First we concentrate on the vacuum part, which is given by the following expression:

$$\mathcal{V}_{LS}^{{\rm vac},T=0} = \frac{\lambda}{4}(\sigma_0^2 - v_\theta^2)^2 - H\sigma_0 + \frac{\lambda}{4}(\eta_0^2 - u_\theta^2)^2 + \kappa\,\sin\theta\,\sigma_0\eta_0 + \frac{\lambda}{2}\sigma_0^2\eta_0^2 - \frac{\lambda}{4}(v_\theta^4 + u_\theta^4), \tag{5.21}$$

where we have defined the combination of couplings $\lambda \equiv \lambda_1 + \lambda_2/2$, and follow the notation of Mizher and Fraga (2009):

$$v_\theta^2 \equiv \frac{\mu^2 + \kappa\,\cos\theta}{\lambda} \quad ; \quad u_\theta^2 \equiv v_\theta^2 - \frac{2\kappa}{\lambda}\cos\theta\,. \tag{5.22}$$

This part of the potential determines the phase structure and has to be compared with the NJL expression (5.9). The main difference is that this potential is fully analytic and does not contain any logarithmic terms.

The part of the potential that depends on the fluctuations is used to determine the parameters μ^2, κ, H, λ_1 and λ_2 in Eq. (5.16). They are obtained by fitting the masses contained in $\mathcal{V}_{\rm LS}^{\rm fluc}$ and the pion decay constant at $\theta = 0$ such that the model reproduces the low-energy phenomenology of QCD. At $\theta = 0$ $\mathcal{V}_{\rm LS}^{\rm fluc}$ has the following form

$$\begin{aligned}\mathcal{V}_{\rm LS}^{\rm fluc} = {}& \frac{1}{2}\left[m_{\boldsymbol{\pi}}^2\boldsymbol{\pi}^2 + m_\sigma^2 s^2 + m_\eta^2\eta^2 + m_{\boldsymbol{a}_0}^2\boldsymbol{a}_0^2\right] + \left(\lambda_1 + \frac{1}{2}\lambda_2\right)\sigma_0 s\left(s^2 + \boldsymbol{\pi}^2 + \eta^2\right) \\ & + \left(\lambda_1 + \frac{3}{2}\lambda_2\right)\sigma_0 s\boldsymbol{a}_0^2 + \lambda_2\sigma_0\eta\boldsymbol{\pi}\cdot\boldsymbol{a}_0 + \left(\frac{1}{4}\lambda_1 + \frac{1}{8}\lambda_2\right)\left(s^2 + \boldsymbol{\pi}^2 + \eta^2 + \boldsymbol{a}_0^2\right)^2 \\ & + \frac{1}{2}\lambda_2\left[(s\boldsymbol{a}_0 + \eta\boldsymbol{\pi})^2 + (\boldsymbol{\pi}\times\boldsymbol{a}_0)^2\right].\end{aligned} \tag{5.23}$$

The masses depend on the parameters of the model as follows:

$$\begin{aligned} m_{\boldsymbol{\pi}}^2 &= -\mu^2 - \kappa + \frac{1}{2}(2\lambda_1 + \lambda_2)\sigma_0^2, \\ m_\sigma^2 &= -\mu^2 - \kappa + \frac{3}{2}(2\lambda_1 + \lambda_2)\sigma_0^2, \\ m_{\boldsymbol{a}_0}^2 &= -\mu^2 + \kappa + (\lambda_1 + \frac{3}{2}\lambda_2)\sigma_0^2, \\ m_\eta^2 &= -\mu^2 + \kappa + (\lambda_1 + \frac{1}{2}\lambda_2)\sigma_0^2. \end{aligned} \tag{5.24}$$

The mass values used are: $m_{\boldsymbol{\pi}} = 138\,\text{MeV}$, $m_\sigma = 600\,\text{MeV}$, $m_{\boldsymbol{a}_0} = 980\,\text{MeV}$, and $m_\eta = 574\,\text{MeV}$.

At nonzero θ, η_0 becomes nonzero, which alters the mass relations. Furthermore, cross terms like $\sigma\eta$ become nonzero, signalling that the mass eigenstates are no longer CP eigenstates, as discussed for the NJL model in Chapter 4. As a consequence, the σ-field mixes with the η-field and the $\boldsymbol{\pi}$-field mixes with the $\boldsymbol{a}_0$-field. We will not give these expressions explicitly here.

5.3.1 Spontaneous CP violation at $\theta = \pi$

Similarly to the NJL model and chiral perturbation theory, for a range of values of the parameters the linear sigma model violates CP invariance at $\theta = \pi$. In this section we will discuss this violation in the same way as we have done in the NJL model, i.e. varying the instanton interaction, but keeping the masses of the pions and σ meson fixed. In the case of the linear sigma model, this means that the combination $\mu_0^2 = \mu^2 + \kappa$ is kept fixed. It turns out that a critical value of κ exists, below which there is no spontaneous CP violation at $\theta = \pi$. For values of κ larger that the critical value, the model exhibits spontaneous CP violation at $\theta = \pi$. The critical value of κ will be denoted as κ_{crit}.

In order to find the ground state, $\mathcal{V}_{\text{LS}}^{T=0}$ has to be minimized, which at $\theta = \pi$ boils down to solving the following two equations

$$\begin{aligned}\frac{\partial \mathcal{V}_{\text{LS}}^{T=0}}{\partial \sigma_0} &= \sigma_0 \left(\lambda\left(\eta_0^2 + \sigma_0^2\right) + 2\kappa - \mu_0^2\right) - H = 0,\\ \frac{\partial \mathcal{V}_{\text{LS}}^{T=0}}{\partial \eta_0} &= \eta_0 \left(\lambda\left(\eta_0^2 + \sigma_0^2\right) - \mu_0^2\right) = 0.\end{aligned} \tag{5.25}$$

When κ is small, the following values of the condensates minimize the potential

$$\begin{aligned}\sigma_0 &= \frac{Y^2 - X}{3\lambda Y},\\ \eta_0 &= 0,\end{aligned} \tag{5.26}$$

where we have introduced

$$\begin{aligned}X &= 6\kappa\lambda - 3\lambda\mu_0^2,\\ Y &= \sqrt[3]{\frac{1}{2}\sqrt{729H^2\lambda^4 + 4X^3} + \frac{27}{2}H\lambda^2}.\end{aligned} \tag{5.27}$$

This solution corresponds to a CP-conserving ground state. When κ is large, the minimum corresponds to the following values of the condensates

$$\begin{aligned}\sigma_0 &= \frac{H}{2\kappa},\\ \eta_0 &= \frac{\sqrt{4\mu_0^2\kappa^2 - H^2\lambda}}{2\kappa\sqrt{\lambda}}.\end{aligned} \tag{5.28}$$

In case $\eta_0 \neq 0$, this solution violates CP invariance. When this solution obtains a real value for η_0, i.e. $\kappa \geq \kappa_{\text{crit}} = H\sqrt{\lambda}/(2\mu_0)$, it becomes the global minimum. The value of κ chosen in this chapter is higher than κ_{crit}, consequently the model spontaneously violates CP invariance at $\theta = \pi$. The CP restoring phase transition is second order as function of κ. Next we will look at the order as function of T.

5.3.2 Nonzero temperature

In the LSMq model the quarks start to contribute at nonzero temperatures. In fact, it is assumed that all the temperature dependence comes from the quarks. Scavenius et al. (2001) argued that this approach is more justified for studying high T phenomena than considering only thermal fluctuations of the meson fields, because at high T constituent quarks become light and mesonic excitations heavy. For the study of the chiral phase transition at $\theta = 0$ this approach yields results that are qualitatively similar to those of the NJL model.

The part of the LSMq Lagrangian that depends on the quark fields is:

$$\mathscr{L}_q = \bar{\psi}\left[i\partial\!\!\!/ - g\left(\sigma + i\gamma_5\eta + \boldsymbol{a}_0 \cdot \boldsymbol{\lambda} + i\gamma_5\boldsymbol{\pi} \cdot \boldsymbol{\lambda}\right)\right]\psi. \tag{5.29}$$

The quark thermal fluctuations are incorporated in the effective potential for the mesonic sector, by means of integrating out the quarks to one loop (Mizher and Fraga, 2009). The resulting quark contribution to the potential is given by

$$\mathcal{V}_q^T = -\nu_q \int \frac{\mathrm{d}^3 p}{(2\pi)^3} T \log\left(1 + e^{-E_{\mathbf{p}}/T}\right). \tag{5.30}$$

This expression is equal to the temperature dependent part of the NJL model Eq. (5.10), with again $E_{\mathbf{p}} = \sqrt{\mathbf{p}^2 + M^2}$ and the constituent quark mass M depends on the vacuum expectation values of the meson fields in the following way: $M = g\sqrt{\left(\sigma_0^2 + \eta_0^2\right)}$, where g is the Yukawa coupling between the quarks and the mesons. A reasonable value for the constituent quark mass at $\theta = 0$ fixes this coupling constant. In Mizher and Fraga (2009) (and here) $g = 3.3$ is used, which leads to a cross-over for the chiral phase transition as a function of temperature at $\theta = 0$ and to a constituent quark mass of approximately $1/3$ of the nucleon mass.

5.3.3 The phase transition

With all parameters fixed, we can study the CP-restoring phase transition at $\theta = \pi$ in the LSMq model. This was studied in detail, along with other values for θ, by Mizher and Fraga (2009). There also the effect of a magnetic field was discussed, which we will not take into account in this chapter.

We are now going to follow the same procedure as for the NJL model to study the details of the phase transition. Again, we start the discussion with numerical results of the minimization of the effective potential, this time the results of Mizher and Fraga (2009), shown in Fig. 5.1. From this figure, two simplifying assumptions can be inferred. First, as was the case for the NJL model, in the neighborhood of the phase transition $M < \pi T$, allowing Eq. (5.30) to be expanded in M/T as in Eq. (5.10). Secondly, σ_0 is much smaller than η_0 which means that we can neglect the σ_0-dependence. This assumption leads to a small error near $\eta_0 \approx 0$, but as we checked explicitly this is not important since the structure of the extrema of the potential is not altered.

Summing the contributions at zero and nonzero temperature gives the following form for the effective potential

$$\mathcal{V}_{\mathrm{LS}}^{\mathrm{vac}}(T) = A_{\mathrm{LS}}(T) + B_{\mathrm{LS}}(T)\eta_0^2 + C_{\mathrm{LS}}(T)\eta_0^4 + D_{\mathrm{LS}}\eta_0^4 \log \eta_0^2, \tag{5.31}$$

where

$$A_{\mathrm{LS}}(T) = -\frac{7}{720}\pi^2 T^4 \nu_q, \tag{5.32}$$

$$B_{\mathrm{LS}}(T) = \frac{1}{48}\left(g^2 T^2 \nu_q - 24(\mu^2 + \kappa)\right), \tag{5.33}$$

$$C_{\mathrm{LS}}(T) = \frac{1}{32}\left(\frac{\nu_q\left(\log\left(\frac{g}{\pi T}\right) + \gamma_E - \frac{3}{4}\right)g^4}{\pi^2} + 8\lambda\right), \tag{5.34}$$

$$D_{\mathrm{LS}} = \frac{g^4 \nu_q}{64\pi^2}. \tag{5.35}$$

The form of this potential is clearly different from the one of the NJL model Eq. (5.11), the difference being the uncanceled logarithmic term. This term proportional to D_{LS} will always cause the phase transition to be of first order. As observed for the NJL model, also in this case the potential is exactly the same as the chiral limit at $\theta = 0$, with η_0 replaced by σ_0. Beyond the chiral limit the explicit symmetry breaking term $\sim H\sigma_0$ (which has no analogue at $\theta = \pi$) will change the first order transition into a cross-over, unless the Yukawa coupling g is increased sufficiently (Paech, Stoecker, and Dumitru, 2003; Schaefer and Wambach, 2007). We conclude that the absence of explicit CP violation through a linear term in η_0 at $\theta = \pi$ lies at the heart of the difference between the observations made here and those by Scavenius et al. (2001).

Like in the NJL model, it is the sign flip of B_{LS} that modifies the structure of the minima. But instead of a phase transition, now a meta-stable state develops at $\eta_0 = 0$. When $B_{\mathrm{LS}}(T)$ becomes larger than $2D_{\mathrm{LS}} \exp(-\frac{3}{2} - \frac{C_{\mathrm{LS}}(T)}{D_{\mathrm{LS}}})$ the original minimum disappears. Between the two spinodals the minimum jumps, signalling a first order transition.

When the parameters of Mizher and Fraga (2009) are used, we obtain the following values for the spinodals: 118 MeV and 129 MeV. To find the exact point of the phase transition, the potential has to be minimized numerically, giving a critical temperature of 126.4 MeV. As already noted, this is significantly lower than T_c^{NJL}, but the specific values depend on the parameter choices made. As should be clear from the previous discussion, choosing different parameters would not affect the conclusion about the different orders of the phase transition, at least as long as $M < \pi T, \Lambda$ and $\kappa > -\mu^2$ (equivalently, $m_\sigma^2 > 3m_\pi^2$ at $T = 0$).

5.4 Relation between the models

As mentioned, the LSMq model is a hybrid model for mesons, which are coupled to quarks at nonzero temperature, and the NJL model is a quark model, where the bosonic states of quark-antiquark fields are interpreted as mesons. Eguchi (1976) has shown how

to derive from the Lagrangian of the NJL model a Lagrangian for the mesonic excitations for $G_2 = 0$. This bosonization procedure is reviewed in Klevansky (1992). Here the corresponding meson Lagrangian will be derived for $G_2 \neq 0$, which was also studied by Dmitrasinovic (1996) in the chiral limit.

The situation will be reviewed for $\theta = 0$, when only the $\bar{\psi}\psi$ receives a vacuum expectation. The case $\theta = \pi$ is very similar, then also $\langle\bar{\psi}i\gamma_5\psi\rangle$ becomes nonzero, which approximately doubles the number of terms one has to incorporate. However, the structure one obtains remains the same. We start with the Lagrangian given in Eq. (3.2). The generating functional is given by the standard expression

$$Z[\bar{\xi},\xi] = \frac{1}{N}\int \mathcal{D}\psi\mathcal{D}\bar{\psi}\exp\left(i\int \mathrm{d}^4x\left[\mathscr{L}_{\mathrm{NJL}}(\bar{\psi},\psi) + \bar{\psi}\xi + \bar{\xi}\psi\right]\right), \tag{5.36}$$

where $\bar{\xi}$ and ξ are the antifermion and fermion sources and N is a normalization factor which will be suppressed from now on. Next we introduce auxiliary fields σ, η, $\boldsymbol{\pi}$ and $\boldsymbol{a}_0$ and a new Lagrangian $\mathscr{L}'$ such that the effective potential can be written as

$$Z[\bar{\xi},\xi] = \int \mathcal{D}\psi\mathcal{D}\bar{\psi}\mathcal{D}\sigma\mathcal{D}\eta\mathcal{D}\boldsymbol{\pi}\mathcal{D}\boldsymbol{a}_0\exp\left(i\int \mathrm{d}^4x\left[\mathscr{L}'_{\mathrm{NJL}}(\bar{\psi},\psi) + \bar{\psi}\xi + \bar{\xi}\psi\right]\right), \tag{5.37}$$

with

$$\begin{aligned}\mathscr{L}'_{\mathrm{NJL}} = \bar{\psi}\left[i\partial\!\!\!/ - m - g\left(\sigma + i\gamma_5\eta + \boldsymbol{a}_0\cdot\boldsymbol{\lambda} + i\gamma_5\boldsymbol{\pi}\cdot\boldsymbol{\lambda}\right)\right]\psi \\ - \frac{1}{2}\delta\mu_1^2\left(\sigma^2 + \boldsymbol{\pi}^2\right) - \frac{1}{2}\delta\mu_2^2\left(\eta^2 + \boldsymbol{a}_0^2\right),\end{aligned} \tag{5.38}$$

and

$$\delta\mu_1^2 = \frac{g^2}{2(G_1+G_2)}, \quad \delta\mu_2^2 = \frac{g^2}{2(G_1-G_2)}. \tag{5.39}$$

Here g is again the Yukawa coupling between the quarks and mesons, which in the case of the NJL model can be evaluated and indicates that the NJL model is in this respect less general than the LSMq model. The following value is obtained

$$g^{-2} = -4N_c i\int\frac{\mathrm{d}^4p}{(2\pi)^4}\frac{1}{(p^2-M^2)^2}, \tag{5.40}$$

which requires some regularization.

Integrating out the quarks gives the following generating functional

$$\begin{aligned}Z[\bar{\xi},\xi] = \int \mathcal{D}\sigma\mathcal{D}\eta\mathcal{D}\boldsymbol{\pi}\mathcal{D}\boldsymbol{a}_0\exp\Bigg(i\mathcal{S}_{\mathrm{NJL}} \\ + i\int \mathrm{d}^4x\,\bar{\xi}\frac{1}{i\partial\!\!\!/ - m - g\left(s + i\gamma_5\eta + \boldsymbol{a}_0\cdot\boldsymbol{\lambda} + i\gamma_5\boldsymbol{\pi}\cdot\boldsymbol{\lambda}\right)}\xi\Bigg)\end{aligned} \tag{5.41}$$

where the action $\mathcal{S}_{\rm NJL}$ is given by

$$\mathcal{S}_{\rm NJL} = \int \mathrm{d}^4x \left[-\frac{1}{2}\delta\mu_1^2 \left(\sigma^2 + \boldsymbol{\pi}^2\right) - \frac{1}{2}\delta\mu_2^2 \left(\eta^2 + \boldsymbol{a}_0^2\right) \right] - i\mathrm{Tr}\,\log\left[i\partial\!\!\!/ - m - g\left(\sigma + i\gamma_5\eta + \boldsymbol{a}_0\cdot\boldsymbol{\lambda} + i\gamma_5\boldsymbol{\pi}\cdot\boldsymbol{\lambda}\right)\right]. \quad (5.42)$$

Assuming that only the σ-field receives a vacuum expectation value σ_0, i.e., $\sigma = \sigma_0 + s$, the action can be split into a vacuum part and a part that depends on the fluctuations, which are the mesons $s, \eta, \boldsymbol{\pi}, \boldsymbol{a}_0$:

$$\mathcal{S}_{\rm NJL} = \mathcal{S}_{\rm NJL}^{\rm vac} + \mathcal{S}_{\rm NJL}^{\rm fluc}, \quad (5.43)$$

with

$$\begin{aligned}
\mathcal{S}_{\rm NJL}^{\rm vac} &= \int \mathrm{d}^4x \left[-\frac{1}{2}\delta\mu_1^2\sigma_0^2 \right] - i\mathrm{Tr}\,\log\left[i\partial\!\!\!/ - M\right], \\
\mathcal{S}_{\rm NJL}^{\rm fluc} &= \int \mathrm{d}^4x \left[-\frac{1}{2}\delta\mu_1^2 \left(s^2 + 2\sigma_0 s + \boldsymbol{\pi}^2\right) - \frac{1}{2}\delta\mu_2^2 \left(\eta^2 + \boldsymbol{a}_0^2\right) \right] \\
&\quad - i\mathrm{Tr}\,\log\left[1 - \frac{1}{i\partial\!\!\!/ - M} g\left(s + i\gamma_5\eta + \boldsymbol{a}_0\cdot\boldsymbol{\lambda} + i\gamma_5\boldsymbol{\pi}\cdot\boldsymbol{\lambda}\right)\right], \quad (5.44)
\end{aligned}$$

and the constituent quark mass $M = m + g\sigma_0$. In order to obtain a local action for the meson fields, the nonlocal fermionic determinant in $\mathcal{S}_{\rm NJL}^{\rm fluc}$ is rewritten using a derivative expansion:

$$-i\mathrm{Tr}\,\log\left[1 - \frac{1}{i\partial\!\!\!/ - M} g\left(s + i\gamma_5\eta + \boldsymbol{a}_0\cdot\boldsymbol{\lambda} + i\gamma_5\boldsymbol{\pi}\cdot\boldsymbol{\lambda}\right)\right] = \sum_{n=1}^{\infty} U^{(n)}, \quad (5.45)$$

where

$$U^{(n)} = \frac{1}{n}\mathrm{Tr}\left(\frac{1}{i\partial\!\!\!/ - M} g\left(s + i\gamma_5\eta + \boldsymbol{a}_0\cdot\boldsymbol{\lambda} + i\gamma_5\boldsymbol{\pi}\cdot\boldsymbol{\lambda}\right)\right)^n. \quad (5.46)$$

From power counting we note that $U^{(n)}$ with $n \geq 5$ are convergent and the rest is divergent. Only the divergent parts of the $U^{(n)}$ with $n = 1, 2, 3, 4$ will be taken into account. As an example, we will present the calculation of the scalar contribution to $U^{(2)}$, following Klevansky (1992).

We start with the expression for the scalar contribution to $U^{(2)}$, which is shown diagrammatically in Fig. 5.2 and is equal to

$$\begin{aligned}
U_s^{(2)} &= g^2 \frac{i}{2}\mathrm{Tr} \int \frac{\mathrm{d}^4p}{(2\pi)^4} \langle p| \frac{1}{i\partial\!\!\!/ - M} s \frac{1}{i\partial\!\!\!/ - M} s |p\rangle \\
&= 2ig^2 N_f N_c \int \frac{\mathrm{d}^4p}{(2\pi)^4} \frac{\mathrm{d}^4p'}{(2\pi)^4} \mathrm{d}^4x\, \mathrm{d}^4y \\
&\quad \times e^{i(p-p')\cdot(x-y)} \frac{p'\cdot p + M^2}{(p^2 - M^2)(p'^2 - M^2)} s(x)s(y). \quad (5.47)
\end{aligned}$$

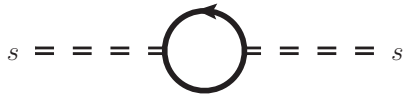

Figure 5.2: The scalar contribution to $U^{(2)}$, the double dashed lines denote the s-field.

Now we Taylor expand the field $s(y)$

$$s(y) = s(x) + (y-x)^\mu \partial_\mu s(x) + \frac{1}{2}(y-x)^\mu (y-x)^\nu \partial_\mu \partial_\nu s(x) + \cdots, \tag{5.48}$$

and insert this expansion in Eq. (5.47)

$$U_s^{(2)} = U_s^{(2)}\big|_{s^2} + U_s^{(2)}\big|_{s\partial_\mu s} + U_s^{(2)}\big|_{s\partial_\mu\partial_\nu s} + \cdots. \tag{5.49}$$

The first term is given by

$$\begin{aligned} U_s^{(2)}\big|_{s^2} &= 2ig^2 N_f N_c \int \frac{\mathrm{d}^4p}{(2\pi)^4}\frac{\mathrm{d}^4p'}{(2\pi)^4}\,\mathrm{d}^4x\,\mathrm{d}^4y \\ &\quad \times e^{i(p-p')\cdot(x-y)}\frac{p'\cdot p + M^2}{(p^2-M^2)(p'^2-M^2)}s(x)^2 \\ &= 2ig^2 N_c N_f \int \frac{\mathrm{d}^4p}{(2\pi)^4}\,\mathrm{d}^4x\,\frac{p^2+M^2}{p^2-M^2}s(x)^2 \\ &= (g^2 I_2 - 2M^2 g^2 I_0)\int \mathrm{d}^4x\, s(x)^2, \end{aligned} \tag{5.50}$$

where we have put $N_f = 2$ and introduced the following two (divergent) integrals

$$\begin{aligned} I_0 &= -4N_c i \int \frac{\mathrm{d}^4p}{(2\pi)^4}\frac{1}{(p^2-M^2)^2}, \\ I_2 &= 4N_c i \int \frac{\mathrm{d}^4p}{(2\pi)^4}\frac{1}{p^2-M^2}, \end{aligned} \tag{5.51}$$

which will be regularized using the three-dimensional UV cut-off. Note that $I_0 = g^{-2}$. The second term is linear in the derivative and vanishes. The last divergent term is the third one, which is given by

$$\begin{aligned} U_s^{(2)}\big|_{s\partial_\mu\partial_\nu s} &= ig^2 N_f N_c \int \frac{\mathrm{d}^4p}{(2\pi)^4}\frac{\mathrm{d}^4p'}{(2\pi)^4}\,\mathrm{d}^4x\,\mathrm{d}^4y \\ &\quad \times e^{i(p-p')\cdot(x-y)}\frac{p'\cdot p + M^2}{(p^2-M^2)(p'^2-M^2)}s(x)(y-x)^\mu(y-x)^\nu\partial_\mu\partial_\nu s(x) \\ &= ig^2 N_f N_c \int \frac{\mathrm{d}^4p}{(2\pi)^4}\frac{\mathrm{d}^4p'}{(2\pi)^4}\,\mathrm{d}^4x\,\mathrm{d}^4z \\ &\quad \times e^{i(p-p')\cdot z}\frac{p'\cdot p + M^2}{(p^2-M^2)(p'^2-M^2)}s(x)z^\mu z^\nu\partial_\mu\partial_\nu s(x), \end{aligned} \tag{5.52}$$

where $z = x - y$. Using $z^\mu e^{i(p-p')\cdot z} = i\frac{\partial}{\partial p'_\mu} e^{i(p-p')\cdot z} \equiv i\partial^\mu_{p'} e^{i(p-p')\cdot z}$ and performing the integration over z gives

$$U_s^{(2)}\big|_{s\partial_\mu\partial_\nu s} = ig^2 N_f N_c \int \frac{\mathrm{d}^4p}{(2\pi)^4}\frac{\mathrm{d}^4p'}{(2\pi)^4}\,\mathrm{d}^4x \times s(x)\partial_\mu\partial_\nu s(x)\frac{p'\cdot p + M^2}{(p^2-M^2)(p'^2-M^2)}\partial^\mu_{p'}\partial^\nu_{p'}\delta(p-p'), \tag{5.53}$$

which after the p'-integration can be brought to the following form, only taking the divergent term into account

$$\begin{aligned} U_s^{(2)}\big|_{s\partial_\mu\partial_\nu s} &= ig^2 N_c N_f \int \frac{\mathrm{d}^4p}{(2\pi)^4}\mathrm{d}^4x\, s(x)\partial_\mu\partial_\nu s(x)\frac{g^{\mu\nu}}{(p^2-M^2)^2} \\ &= \frac{1}{2}g^2 I_0 \int \mathrm{d}^4x\,\partial_\mu s(x)\partial^\mu s(x). \end{aligned} \tag{5.54}$$

The other divergent $U^{(n)}$-terms can be evaluated in the same way. The following Lagrangian is obtained after the summation of these $U^{(n)}$, which integrated over space-time, yields $\mathcal{S}^{\mathrm{fluc}}_{\mathrm{NJL}}$:

$$\begin{aligned} \mathscr{L}^{\mathrm{fluc}}_{\mathrm{NJL}} = {} & \frac{1}{2}\left[(\partial_\mu s)^2 + (\partial_\mu\eta)^2 + (\partial_\mu \boldsymbol{a}_0^2)^2 + (\partial_\mu\boldsymbol{\pi})^2\right] - \frac{1}{2}\left[m^2_{\boldsymbol{\pi}}\boldsymbol{\pi}^2 + m^2_\sigma s^2 + m^2_\eta\eta^2 + m^2_{\boldsymbol{a}_0}\boldsymbol{a}_0^2\right] \\ & - g_3 s\left(s^2+\boldsymbol{\pi}^2+\eta^2+3\boldsymbol{a}_0^2\right) - 2g_3\eta\boldsymbol{\pi}\cdot\boldsymbol{a}_0 - \frac{1}{2}g_4\left(s^2+\boldsymbol{\pi}^2+\eta^2+\boldsymbol{a}_0^2\right)^2 \\ & - 2g_4\left[(s\boldsymbol{a}_0+\eta\boldsymbol{\pi})^2 + (\boldsymbol{\pi}\times\boldsymbol{a}_0)^2\right]. \end{aligned} \tag{5.55}$$

The masses and coupling constants have the following values

$$\begin{aligned} m^2_{\boldsymbol{\pi}} &= \frac{1}{2G_0I_0} - 2\frac{I_2}{I_0} = \frac{m}{M}\frac{1}{2G_0I_0}, \\ m^2_\sigma &= m^2_{\boldsymbol{\pi}} + 4M^2, \\ m^2_\eta &= \frac{1}{2(1-2c)G_0I_0} - 2\frac{I_2}{I_0}, \\ m^2_{\boldsymbol{a}_0} &= m^2_\eta + 4M^2, \\ g_3 &= \frac{2M}{I_0^{1/2}} = 2Mg_4^{1/2}, \\ g_4 &= \frac{1}{I_0}, \\ g &= \frac{1}{I_0^{1/2}}, \end{aligned} \tag{5.56}$$

The resulting masses (when the integrals are regularized using a three-dimensional UV cut-off) are equal to the ones obtained using the random phase approximation used in

Chapter 4 (where the dependence on the external momentum of the generalized I_0 defined in, for example, Klevansky (1992) has been neglected). The Lagrangian (5.55) without the $\boldsymbol{a}_0$ and η-fields was also given in Ebert and Volkov (1983). In the chiral limit the results agree with those of Dmitrasinovic (1996).

Eq. (5.55) is equal to the fluctuation part of the linear sigma model Lagrangian (5.16) using the following parameters

$$\begin{aligned}
\lambda_1 &= 0, \\
\lambda_2 &= 4/I_0, \\
\mu^2 &= 2M^2 - \frac{c}{2(1-2c)G_0 I_0}, \\
\kappa &= \frac{c}{2(1-2c)G_0 I_0}, \\
H &= \frac{m}{2G_0 I_0^{1/2}}.
\end{aligned} \tag{5.57}$$

Although the bosonization of the NJL model yields $\lambda_1 = 0$, this is of no consequence for the order of the phase transition, as the effective potential at zero temperature is a quartic polynomial irrespective of whether $\lambda_1 = 0$ or not. It does however, affect the masses of the mesons. If $\lambda_1 = 0$, the following relation holds: $m_\sigma^2 - m_{\boldsymbol{\pi}}^2 = m_{\boldsymbol{a}_0}^2 - m_\eta^2 = 4M^2$, a property of the NJL model already noted in Dmitrasinovic (1996). Clearly, the bosonized NJL model does not yield the most general linear sigma model. However, it gives additional contributions to the vacuum that usually are not taken into account in the linear sigma model coupled to quarks (Scavenius et al., 2001; Mizher and Fraga, 2009). Schaefer and Wambach (2007) noted that upon inclusion of fluctuations using a renormalization group flow equation, the transition becomes second order. This boils down to including quark loop effects at zero temperature too and is consistent with our findings.

To conclude, the mesonic part of this bosonized NJL Lagrangian is equal to the mesonic part of the LSMq model. So the mesons are treated in same way in the two models, but the vacuum contributions are treated differently.

It is straightforward to bosonize the NJL model for $\theta \neq 0$ when also $\langle \bar{\psi} i\gamma_5 \psi \rangle$ can become nonzero, leading to cross terms that mix the σ-field with the η-field and $\boldsymbol{a}_0$-field with the $\boldsymbol{\pi}$-field, but we do not give the expressions here as they do not lead to any additional insights.

5.5 The phase transition in chiral perturbation theory

In this chapter we compared the NJL model with the linear sigma model coupled to quarks. It would be very useful to also compare our results with chiral perturbation theory, which is the most general low-energy effective theory of the strong interaction. Gasser and Leutwyler (1987a,b) and Gerber and Leutwyler (1989) have shown how to incorporate finite temperature in chiral perturbation theory. For instance, they show how the chiral condensate decreases as a function of temperature. Unfortunately, their approach is a low-temperature one, which means that the difference between the condensate

at nonzero and zero temperature is treated as small. This approximation breaks down in the vicinity of the critical point (Gasser and Leutwyler, 1987a). Moreover, in the vicinity of the critical point massive states, such as kaons, the η meson and vector mesons, start to become relevant (Gerber and Leutwyler, 1989), also a signal of the breakdown of the approximation. Finally, the value of the condensate at zero temperature (both at $\theta = 0$ and $\theta = \pi$), which is set by the parameter f_π, needs to be fixed. No minimization takes place to obtain f_π, hence chiral perturbation theory does not contain information about the structure of the minima of the effective potential as a function of f_π.

From these considerations we can conclude that is not possible to use the chiral Lagrangian to study the order of the CP restoring phase transition at $\theta = \pi$.

5.6 Conclusions

In this chapter the high-T CP-restoring phase transition at $\theta = \pi$ was discussed for two different models which aim to describe the low-energy QCD phenomenology, the NJL model and the linear sigma model coupled to quarks. Although the models are related, the philosophy of how the mesons are treated is quite different in both models. In the NJL model they are bosonic states of quark-antiquarks, whereas in the LSMq model they are the fundamental degrees of freedom, interacting with quarks at nonzero temperature. Using the bosonization procedure of Eguchi, one can show that a bosonized NJL model gives a linear sigma model, in which mesons are treated in the same way as in the LSMq model. However, the vacuum contributions arising from the quark degrees of freedom are different. The LSMq model was motivated for high temperatures, when constituent quarks are light and mesons are heavy. Therefore, it is assumed that quarks only play a role at nonzero temperature and do not affect the vacuum contributions at zero temperature. On the other hand, in the NJL model contributions by the quarks are necessarily taken into account also at zero temperature. The temperature dependent contributions to the effective potential are equal in these two models, coming exclusively from the quarks. In the end, the effective potentials of the models only differ in their zero temperature contributions. Nevertheless, this directly affects the nature of the phase transition at high temperature at $\theta = \pi$.

The temperature dependence of the ground states of the two models was investigated using a Landau-Ginzburg analysis. The difference between the models is that the potential as a function of the order parameter of the LSMq model contains a non-analytic logarithmic term, whereas the potential of the NJL model is a quartic polynomial near the phase transition. It is this logarithm that makes the difference, because it affects the order of the phase transition. The logarithm comes from the contribution of the quarks at zero temperature, but neglecting these contributions will affect the high temperature results qualitatively at $\theta = \pi$. A similar effect occurs for the chiral symmetry restoration phase transition at $\theta = 0$ close to the chiral limit, i.e. for sufficiently small explicit symmetry breaking. The absence of explicit CP violation is therefore an important aspect of the physics at $\theta = \pi$.

Since neither model is directly derived from QCD, it is not straightforward to draw

a conclusion about the order of the phase transition expected in QCD. However, as we explained, chiral perturbation theory cannot be used either. If the NJL model is viewed as a model for the microscopic theory underlying the low energy mesonic theory, it would not seem justified to neglect the logarithmic term at zero temperature.

Chapter 6

The combined influence of strong magnetic fields and instantons

Both in heavy-ion collisions and in magnetars very strong magnetic fields are generated, which has its influence on the phases of matter involved. In this chapter we investigate the effect of strong magnetic fields ($B \sim 5m_\pi^2/e = 1.7\times10^{19}$G) on the chiral symmetry restoring phase transition at $\theta = 0$ using the Nambu-Jona-Lasinio model. It is observed that the pattern of phase transitions depends on the relative magnitude of the magnetic field and the instanton interaction strength. We study two specific regimes in the phase diagram, high chemical potential and zero temperature and vice versa, which are of relevance for neutron stars and heavy-ion collisions respectively. In order to shed light on the behavior of the phase transitions we study the dependence of the minima of the effective potential on the occupation of Landau levels. We observe a near-degeneracy of multiple minima with different Landau occupation numbers, of which some become the global minimum upon changing the magnetic field or the chemical potential. These minima differ considerably in the amount of chiral symmetry breaking and in some cases also of isospin breaking. Throughout this chapter we consider $\theta = 0$. This chapter is largely based on Boomsma and Boer (2010).

6.1 Introduction

Recently it has been noted that very strong magnetic fields can be produced in heavy-ion collisions (Selyuzhenkov, 2006; Kharzeev, 2006; Kharzeev, McLerran, and Warringa, 2008). Estimates are that at RHIC magnetic fields are created of magnitude $5m_\pi^2/e = 1.7\times 10^{19}$ G and at LHC of $6m_\pi^2/e = 2\times10^{19}$ G, and there are even higher estimates (Skokov, Illarionov, and Toneev, 2009). Also, certain neutron stars called magnetars exhibit strong magnetic fields, between $10^{14} - 10^{15}$ G (Duncan and Thompson, 1992; Thompson and Duncan, 1993, 1996). These fields occur at the surface, probably in the much denser interior even higher fields are present. Using the virial theorem it can be derived that the

maximal strength is $10^{18} - 10^{19}$ G (Lai and Shapiro, 1991). If one assumes that the star is bound by the strong interaction instead of by gravitation, this limit can be even higher.

As discussed in Chapter 2, both in neutron stars and in heavy-ion collisions it is expected that quark matter plays a role. Therefore it is interesting to study how this form of matter behaves in a strong magnetic field. Two different regions in the QCD phase diagram are of relevance here. Heavy-ion collisions probe the low chemical potential and high temperature regime, for neutron stars it is the other way around. In this chapter the effect of very strong magnetic fields will be investigated in both regimes.

Much work has been done on how an external magnetic field changes nuclear matter, for a review see Lattimer and Prakash (2007). The behavior of ordinary quark matter has been studied using the Nambu-Jona-Lasinio (NJL) model, see for example Klevansky (1992), Gusynin, Miransky, and Shovkovy (1994, 1995a,c, 1996), Ebert et al. (2000), Ebert and Klimenko (2003), Klimenko and Zhukovsky (2008), Inagaki, Kimura, and Murata (2004), and Menezes et al. (2009a) and recently also in the linear sigma model coupled to quarks (Fraga and Mizher, 2008). Most studies investigate the one and two-flavor cases, but recently also the three-flavor case has been investigated (Osipov et al., 2007; Menezes et al., 2009b). At high quark chemical potential, it is believed that the ground state is a color superconducting phase. The effects of an external magnetic field on such a phase are discussed by Ferrer, de la Incera, and Manuel (2005, 2006), Ferrer and de la Incera (2006, 2007a,b), Noronha and Shovkovy (2007), and Fukushima and Warringa (2008). Here color superconductivity will not be considered.

In this chapter we study the chiral symmetry restoring phase transition, which is strongly influenced by an external magnetic field. From studies in the NJL model it is known that a magnetic field enhances the chiral symmetry breaking (Klevansky, 1992), which is related to the phenomenon of magnetic catalysis of chiral symmetry breaking, introduced by Klimenko (1992a,b, 1991), further studied for the NJL model by Gusynin, Miransky, and Shovkovy (1994, 1995a,c, 1996), Ebert et al. (2000), Ebert and Klimenko (2003), Klimenko and Zhukovsky (2008) and for QED by e.g. Gusynin, Miransky, and Shovkovy (1995b), Lee, Leung, and Ng (1998, 1997), and Ferrer and de la Incera (2009, 2010), where also the generation of an anomalous magnetic moment was pointed out (Ferrer and de la Incera, 2009, 2010). This enhancement can be understood as follows. The B-field anti-aligns the helicities of the quarks and antiquarks, which are then more strongly bound by the NJL-interaction (Klevansky, 1992). The phenomenon of magnetic catalysis of chiral symmetry breaking leads to interesting behavior, since it allows for phases with broken chiral symmetry and nonzero nuclear density for a range of chemical potentials and magnetic fields (Ebert et al., 2000; Ebert and Klimenko, 2003;Inagaki, Kimura, and Murata, 2004). In such a phase nonperiodic magnetic oscillations occur, which means that the constituent quark masses are strongly dependent on the magnetic field, and consequently also other thermodynamic parameters, analogous to the de Haas-van Alphen effect.

In all studies of the influence of magnetic fields on chiral symmetry breaking up to now, the effects of instantons have not been studied explicitly, i.e. as a function of instanton interaction strength. Magnetic fields and instantons can lead to combined effects. Kharzeev, McLerran, and Warringa (2008) have shown that variations in topologi-

cal charge, which induce variations of net chirality, in a strong magnetic field gives rise to an electrical current. This effect is known as the chiral magnetic effect and could perhaps be observed in heavy-ion collisions (Abelev et al., 2009a,b). Variations of topological charge can for instance be created by instantons.

Here a related study will be performed. We will investigate the combined effect of instantons and a strong magnetic field on quark matter using the NJL model. In this model instantons induce an extra interaction, the 't Hooft determinant interaction, which leads to a mixing between the different quark flavors. Following the analysis of Chapter 3, the strength of the instanton interaction is set by the dimensionless parameter c. For $c = 0$ there is no contribution and there is no mixing. Because of the difference in charge of the quarks, the phase transitions are decoupled. The other extreme case is $c = 1/2$, which is actually the most studied case. The quarks are then fully mixed, the constituent quark masses are equal and the phase transitions will always coincide. Ebert et al. (2000) studied this case in the chiral limit. It is observed that for a range of typical values of the coupling constant, phases with broken chiral symmetry and nonzero nuclear density arise.

In general there is a competition between the magnetic field, which tends to differentiate the constituent quark masses for different flavors, and the instanton interaction which favors equal constituent quark masses. In this chapter this competition is studied. Apart from studying the ground state as a function of the magnetic field and the chemical potential for various characteristic values of c, we also look at the local minima of the effective potential and the corresponding occupation of Landau levels. It is found that in the neighborhood of the chiral phase transition the phase diagram develops metastable phases, differing in the number of filled Landau levels. Some of these local minima become the global one upon increasing the magnetic field or chemical potential, but not all of them do. These phases can have rather different values for the constituent quark masses, in other words, display significantly different amounts of chiral symmetry breaking. Unlike in the case of $c = 1/2$ which is isospin symmetric, in these phases the values of the two constituent quark masses can be very distinct, which corresponds to large isospin violation. Furthermore, we find that for a realistic choice of parameters, appearance of phases of broken chiral symmetry and nonzero nuclear density requires not too large instanton interaction strength, i.e. $c \lesssim 0.1$.

As mentioned, we also investigate the role of nonzero temperature at zero chemical potential, which is of relevance for heavy-ion collisions. Without magnetic field the chiral symmetry restoring phase transition at finite temperature is a crossover. In the linear sigma model coupled to quarks it has been observed that the magnetic field turns it into a first order transition (Fraga and Mizher, 2008). We will see that this is not the case for the NJL model, similar to the CP restoring phase transition at $\theta = \pi$, discussed in the previous chapter.

This chapter is organized as follows. First we derive the effective potential of the NJL model in the mean-field approximation in a magnetic background. Then we discuss the phase diagram as a function of chemical potential, concentrating on the phase with nonzero nuclear density and chiral symmetry breaking. We continue with discussing the temperature dependence and end with conclusions.

6.2 Effective potential of the NJL model with a magnetic field

In this section we discuss how a constant external magnetic field can be incorporated in the NJL model. We choose the external magnetic field along the z-direction and use the potential $A_\mu = Bx_1\delta_{\mu 2}$. In the following we will assume that $B > 0$. The Lagrangian then becomes equal to

$$\mathscr{L}^B_{\text{NJL}} = \bar{\psi}\left(i\gamma^\mu\partial_\mu - q_f\lambda_f B\gamma^2 x_1 - m - \mu\gamma_0\right)\psi + \mathscr{L}_{\bar{q}q} + \mathscr{L}_{\text{det}}, \tag{6.1}$$

where $\mathscr{L}_{\bar{q}q}$ and $\mathscr{L}_{\text{det}}$ are the four-quark interactions, as given in Chapter 3. q_f denotes the charge of quark flavor f. Degenerate current quark masses are used, $m_u = m_d = m$. Finally, μ denotes the quark chemical potential, which we take equal for both quarks.

In order to obtain the ground state of the model, the effective potential has to be minimized. We will again use the mean-field approximation. Furthermore, we will assume that only the charge-neutral condensates $\langle\bar{\psi}\lambda_0\psi\rangle$ and $\langle\bar{\psi}\lambda_3\psi\rangle$ can become nonzero. To obtain the effective potential in the mean-field approximation, we use the procedure used in Chapter 5, we "linearize" the interaction terms in the presence of the condensates, this time the $\langle\bar{\psi}\lambda_0\psi\rangle$ and $\langle\bar{\psi}\lambda_3\psi\rangle$ condensates, as follows

$$(\bar{\psi}\lambda_a\psi)^2 \simeq 2\langle\bar{\psi}\lambda_a\psi\rangle\bar{\psi}\lambda_a\psi - \langle\bar{\psi}\lambda_a\psi\rangle^2, \tag{6.2}$$

leading to

$$\mathscr{L}^B_{\text{NJL}} = \bar{\psi}\left(i\gamma^\mu\partial_\mu - q_f\lambda_f B\gamma^2 x_1 - \mathscr{M} - \mu\gamma_0\right)\psi - \frac{(M_0 - m)^2}{4G_0} - \frac{M_3^2}{4(1-2c)G_0}, \tag{6.3}$$

where $\mathscr{M} = M_0\lambda_0 + M_3\lambda_3$ and

$$\begin{aligned} M_0 &= m - 2G_0\langle\bar{\psi}\lambda_0\psi\rangle = m + \alpha_0, \\ M_3 &= -2(1-2c)G_0\langle\bar{\psi}\lambda_3\psi\rangle = \alpha_3. \end{aligned} \tag{6.4}$$

The Lagrangian is now quadratic in the quark fields, so we can perform the fermion integration. This is a little more complicated than in the previous chapters, due to the external magnetic field. The external magnetic field causes quantization of the momenta in the plane perpendicular to the magnetic field, known as Landau quantization (Landau and Lifshitz, 1977). This quantization changes the dispersion relation of the quarks into

$$p_{0n}^2 = p_3^2 + M_f^2 + (2n + 1 - \sigma)|q_f|B, \tag{6.5}$$

where n is the quantum number labelling the discrete orbits and σ the spin of the quark. M_f is the constituent quark mass of flavor f, related to M_0 and M_3 by $M_u = M_0 + M_3$ and $M_d = M_0 - M_3$.

The asymptotic quark states are different when a constant magnetic field is present (see e.g. Ritus, 1972, 1978; Leung et al., 1996; Ferrer and de la Incera, 1998). In Appendix B

we show how the fermion integration is performed using these new asymptotic states. The result is

$$\begin{aligned}\mathcal{V} &= \frac{(M_0-m)^2}{4G_0} + \frac{M_3^2}{4(1-2c)G_0} + \sum_{f=u}^{d} \log \mathrm{Det}\left(i\gamma^\mu\partial_\mu - q_f B\gamma^2 x_1 - M_f - \mu\gamma_0\right) \\ &= \mathcal{V}_0 + \mathcal{V}_1(B) + \mathcal{V}_2(B,\mu,T),\end{aligned} \tag{6.6}$$

where Det denotes a functional determinant and

$$\begin{aligned}\mathcal{V}_0 &= \frac{(M_0-m)^2}{4G_0} + \frac{M_3^2}{4(1-2c)G_0} - \frac{N_c}{8\pi^2}\sum_{f=u}^{d}|M_f|\Bigg(M_f^3\ln\left(\frac{\Lambda}{M_f}+\sqrt{1+\frac{\Lambda^2}{M_f^2}}\right) \\ &\quad - \Lambda\left(M_f^2+2\Lambda^2\right)\sqrt{1+\frac{\Lambda^2}{M_f^2}}\Bigg), \\ \mathcal{V}_1(B) &= -\frac{N_c}{2\pi^2}\sum_{f=u}^{d}(|q_f|B)^2\left[\zeta'(-1,x_f) - \frac{1}{2}(x_f^2-x_f)\ln x_f + \frac{x_f^2}{4}\right], \\ \mathcal{V}_2(B,\mu,T) &= -\frac{N_c}{2\pi}\sum_{k,f}(2-\delta_{k0})|q_f|B\int\frac{\mathrm{d}p_3}{2\pi}\Big\{T\ln\left[1+e^{-\left[E_{p,k}(T)+\mu\right]/T}\right] \\ &\quad + T\ln\left[1+e^{-\left[E_{p,k}(T)-\mu\right]/T}\right]\Big\},\end{aligned} \tag{6.7}$$

where we have defined $x_f = \frac{M_f^2}{2|q_f|B}$ and $\zeta'(-1,x_f) = \frac{d\zeta(z,x_f)}{dz}|_{z=-1}$ with $\zeta(z,x_f)$ the Hurwitz zeta function. We have neglected x_f-independent terms in $\mathcal{V}_1(B)$ (including a UV divergent one). Furthermore, $E_{p,k} = \sqrt{p_3^2+M_f^2+2k|q_f|B}$ and k denotes the Landau levels, which have degeneracy $(2-\delta_{k0})$.

The expression $\zeta'(-1,x_f)$ in $\mathcal{V}_1(B)$ can be written in a more convenient form by differentiating and integrating the function with respect to x_f:

$$\zeta'(-1,x_f) = \zeta'(-1,0) + \frac{x_f^2}{2} - \frac{x_f}{2} - \frac{x_f}{2}\log(2\pi) + \psi^{(-2)}(x_f), \tag{6.8}$$

where $\psi^{(m)}(x_f)$ is the m-th polygamma function. The term $\zeta'(-1,0)$ is independent of x_f and will therefore not be taken into account. The remaining expression is amenable to numerical evaluation.

At zero temperature, $\mathcal{V}_2$ can be simplified to

$$\begin{aligned}\mathcal{V}_2(B,\mu,0) &= -\frac{N_c}{2\pi}\sum_{k,f}(2-\delta_{k0})\int\frac{\mathrm{d}p_3}{2\pi}\theta(\mu-E_{p,k})\left[\mu-E_{p,k}\right]\\ &= \sum_{f=u}^{d}\sum_{k=0}^{k_{f,\max}}(2-\delta_{k0})\,\theta\left(\mu-s_f(k,B)\right)\frac{|q_f|BN_c}{4\pi^2}\\ &\quad\times\left\{\mu\sqrt{\mu^2-s_f^2(k,B)}-s_f^2(k,B)\ln\left[\frac{\mu+\sqrt{\mu^2-s_f^2(k,B)}}{s_f(k,B)}\right]\right\},\end{aligned} \tag{6.9}$$

where $s_f(k,B)=\sqrt{M_f^2+2|q_f|Bk}$ and $k_{f,\max}$ is the upper Landau level, defined as

$$k_{f,\max}=\left\lfloor\frac{\mu^2-M_f^2}{2|q_f|B}\right\rfloor, \tag{6.10}$$

where the brackets indicate the floor of the enclosed quantity.

We will now use these expressions in a numerical study of the minima of the effective potential, performed along the lines discussed in Chapter 4.

6.3 Results

We start with considering the case of $\mu=0, T=0$, and $c=0$. Fig. 6.1 shows the results for this unmixed case. The magnetic field enhances M_u and M_d, which are proportional to $\langle\bar{u}u\rangle$ and $\langle\bar{d}d\rangle$, respectively, consequently the chiral symmetry breaking is enhanced (Klevansky, 1992). Because of the charge difference of the quarks, the B-dependence of the constituent quark masses is not equal. Nonzero c will cause mixing and will bring the masses closer to each other. As discussed, at $c=1/2$ the constituent quark masses are exactly equal.

6.3.1 Nonzero chemical potential

In this section we turn to the phase structure near the phase transition at nonzero chemical potential and zero temperature. From Klein, Toublan, and Verbaarschot (2003), Toublan and Kogut (2003), and Barducci et al. (2003, 2004) it is known that when the isospin chemical potential is nonzero, it is possible to have two phase transitions at low temperature and high baryon chemical potential. Here we study a similar case, instead of nonzero isospin chemical potential, we allow for nonzero magnetic field. Then we will see that also here the possibility of separate phase transitions for the two quarks arises. We will take equal chemical potentials for the quarks, but the magnetic field acts effectively like a nonzero isospin chemical potential due to the difference in charge of the quarks. Instantons cause mixing between the quarks; if the mixing is strong enough, the two separate

phase transitions merge into one. This was extensively investigated by Klein, Toublan, and Verbaarschot (2003) for the nonzero isospin chemical potential case.

From Ebert et al. (2000), Ebert and Klimenko (2003), and Inagaki, Kimura, and Murata (2004), where the NJL model in the chiral limit was studied, it is known that Landau quantization induces a more complex phase structure. Apart from the usual phase of broken chiral symmetry with zero nuclear density, there is also the possibility of such a phase with nonzero nuclear density. Here we perform a more detailed study of this case, which is a characteristic phenomenon at nonzero chemical potential and sufficiently strong magnetic fields, (cf. Eq. (6.11) below).

The $c = 0$ case

When the determinant interaction is turned off, the up and down quarks are decoupled. This leads to the possibility of separate phase transitions for the quarks. In Figs. 6.2 and 6.3 we show the constituent quark mass of the up and down quarks respectively as a function of quark chemical potential and magnetic field. As expected, the two quarks have decoupled behavior.

Let us first discuss the behavior of the up quark. At low chemical potential we have the "standard" chiral symmetry breaking NJL ground state with empty Landau levels (LL). Following the nomenclature of Ebert et al. (2000) and Ebert and Klimenko (2003) where the $c = 1/2$ case was studied in the chiral limit, this is called phase B. Note that this phase always has zero nuclear density. At high chemical potential chiral symmetry is restored, up to the explicit breaking. In this approximately symmetric phase magnetic oscillations

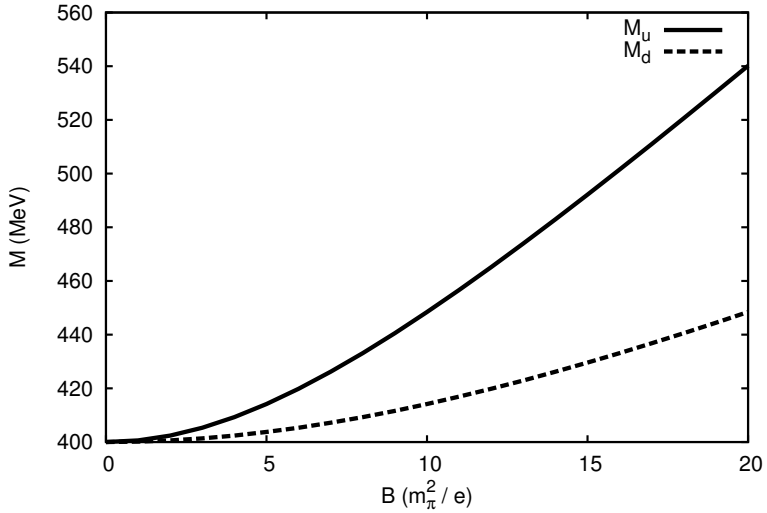

Figure 6.1: The dependence of the constituent quark masses M_u and M_d on the magnetic field B.

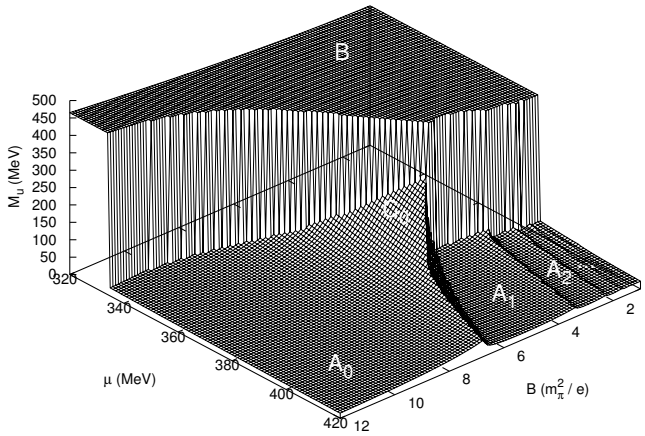

Figure 6.2: The dependence of the constituent up-quark mass on B and μ. A_i, B and C_0 denote the different phases using the scheme of Ebert et al. (2000) and Ebert and Klimenko (2003). Chiral symmetry is broken in phases B and C_0, phases A_0 and C_0 have nonzero nuclear density.

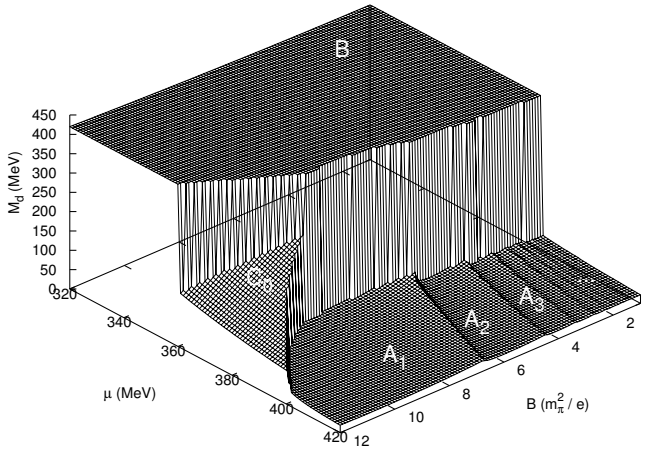

Figure 6.3: Same as Fig. 6.2, now for the down quark.

can be seen in the constituent quark masses, which are caused by Landau quantization. These oscillating phases are denoted by A_i, where i gives the number of filled LL. As these phases have occupied LL, they have nonzero nuclear density. The nuclear density of level k is given by (Menezes et al., 2009a)

$$\rho_{f,k}(B,\mu) = (2-\delta_{k0})\theta(\mu - s_f(k,B))\frac{|q_f|BN_c}{6\pi^2}\sqrt{\mu^2 - s_f^2(k,B)}. \tag{6.11}$$

In the chiral limit the constituent quark masses vanish in the A_i phases.

The oscillations are similar to the de Haas-van Alphen effect, which in QED and in the two-flavor NJL model for $c = 1/2$ in the chiral limit lead to second order transitions between the A_i phases (Ebert et al., 2000). However, with our choice of parameters the transitions are weakly first order. In the chiral limit they become second order, like for $c = 1/2$, as can for instance be seen in the nuclear density. For completeness, we mention that in the color superconducting case of Noronha and Shovkovy (2007) and Fukushima and Warringa (2008) the oscillations in the gap parameter are seen to be continuous, but second order transitions can occur when neutrality conditions are imposed.

For B larger than $4.5m_\pi^2/e$ an interesting intermediate phase arises, where the up-quark jumps as a function of μ first to a phase with a still rather large constituent mass and then to phase A_1. This intermediate phase is called C_0 in the language of Ebert et al. (2000) and Ebert and Klimenko (2003) and corresponds to a phase of broken chiral symmetry having nonzero nuclear density and a filled zeroth LL. So the essential difference between this phase and A_0 is the breaking of chiral symmetry. For smaller values of the coupling constant G_0 also the phases C_k with $k > 0$ (which are similar to C_0 but with more occupied LL) occur. The transitions between the C_k are first order, furthermore, they are nonperiodic in the sense that the difference between the transitions is B-dependent as the constituent mass strongly depends on B (Ebert et al., 2000). If we are in this phase C_0 and increase the magnetic field, the constituent quark mass decreases, eventually becoming almost zero, this can be interpreted as a crossover to A_0. In the chiral limit the crossover becomes a second order transition. Finally, we would like to note that already at $B = 4m_\pi^2/e$ the phase C_0 exists as a metastable phase (we will discuss this in more detail later).

The qualitative behavior of the down quark is very similar, as the quarks only differ in charge, consequently Fig. 6.3 can be directly obtained from Fig. 6.2 by multiplying B by 2, for ease of comparison we show both figures. If one compares the two figures, one can immediately see that there are large regions where the constituent quark masses are considerably different. This is equivalent to a large nonzero $\langle\bar{\psi}\lambda_3\psi\rangle$ condensate, i.e., spontaneous isospin breaking. This will influence the behavior of the mesons accordingly, for example the masses.

Eventually, if one keeps increasing the magnetic field, the phase transitions of the quarks will take place at (almost) the same chemical potential and there will be no spontaneous isospin breaking.

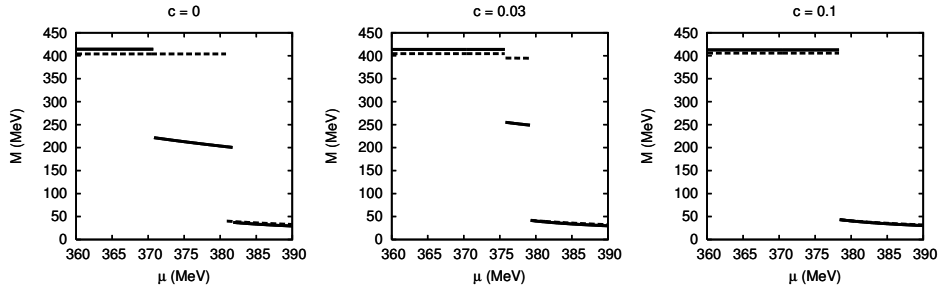

Figure 6.4: The dependence of the constituent quark masses on the quark chemical potential for $B = 5m_\pi^2/e$ and various c values. Solid lines denote the up quarks, the dashed lines the down quark.

The $c \neq 0$ case

In this section the consequences of the instanton interaction is studied, i.e., the parameter c is varied. Increasing c will cause mixing between the constituent quarks, which tends to bring the constituent quark masses together. Around the phase transition there is a competition between the effect of the magnetic field and the instanton interaction.

The competition is illustrated in Fig. 6.4, where the constituent quark masses are plotted as a function of the quark chemical potential for three characteristic values of c, $c = 0$, 0.03, and 0.1 with $B = 5m_\pi^2/e$. The qualitative behavior for different values of the magnetic field is similar. One can see that when $c \neq 0$, the phase transitions are indeed coupled. Furthermore, one observes that the two phase transitions merge into one when c is increased and that the phase C_0 disappears. Qualitatively the behavior is similar to the case of nonzero isospin chemical potential studied by Klein, Toublan, and Verbaarschot (2003), but in that case the phase C_0 does not exist.

When the coupling constant G_0 is lowered, it is possible to have C_k phases at $c = 1/2$, as in Ebert et al. (2000). Compared to the chiral limit studied there, the region of the phase diagram with C_k phases increases for $m \neq 0$.

More insight into the phase structure and phase transitions is obtained by looking at the behavior of local minima of the effective potential. Near the phase transition at these (strong) magnetic fields, metastable phases arise. These phases differ in the number of filled LL. Let us take as an example the $c = 1/2$ case, which is the easiest one to discuss, as the effective potential is then only a function of $M_u = M_d = M$. In Fig. 6.5 we show the effective potential as a function of M with $\mu = 378\,\mathrm{MeV}$ and $B = 5m_\pi^2/e$. At these values four minima can be seen, the global minimum is the phase in which the chiral symmetry breaking is largest, i.e. minimum 4. When μ is increased, minimum 1 will take over, which is A_1 for the up quark and A_2 for the down quark. The other two local minima never become the global one for our choice of G_0, but as they are almost degenerate with the other minima (also for other values of c), they are nevertheless important. These local minima correspond to C_k phases and can become the global minimum when G_0 is

lowered.

The various local minima have very different constituent quark masses, hence the amount of chiral symmetry breaking is also very different. Usually differences in the amount of symmetry breaking lead to distinct energies. However, the local minima start to appear near the "usual" phase transition, when the energy of the phase where chiral symmetry is broken is almost equal to the energy of the phase that exhibits chiral symmetry, therefore it may not be surprising that also the other phases will not much differ in energy despite their differences in symmetry breaking.

Similar results hold for $c \neq 1/2$; also then metastable phases exist with different fillings of LL. In Figs. 6.6 and 6.7 we show contourplots of the effective potential at $c = 0.03$ and $c = 0.1$ respectively. At small c ($c \lesssim 0.08$) the metastable phases differ in the values of M_u and M_d considerably, they again represent rather large broken isospin. In these cases some of the C_k phases can become the global minimum, as we have seen before. The number of such states depends on the choice of the other parameters. At larger c, the situation start to resemble the case $c = \frac{1}{2}$, i.e., the minima move to the diagonal and finally the effective potential depicted in Fig. 6.5 is obtained.

Whenever the system is going through the phase transition, it could be trapped in one of those metastable phases for some time and consequences from the changing meson masses can arise, for example, enhancing or suppressing certain decays.

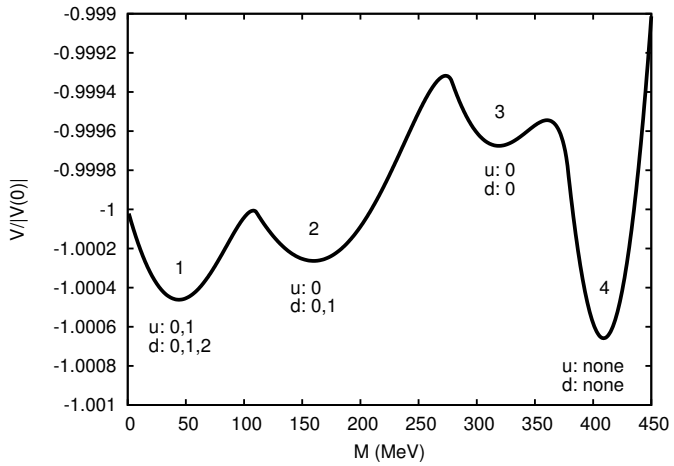

Figure 6.5: The normalized effective potential at the values $B = 5m_\pi^2/e$, $\mu = 378\,\mathrm{MeV}$ and $c = 1/2$. There are four minima. The numbers below the minima denote the LL occupied for each quark. Note that the minima are almost degenerate.

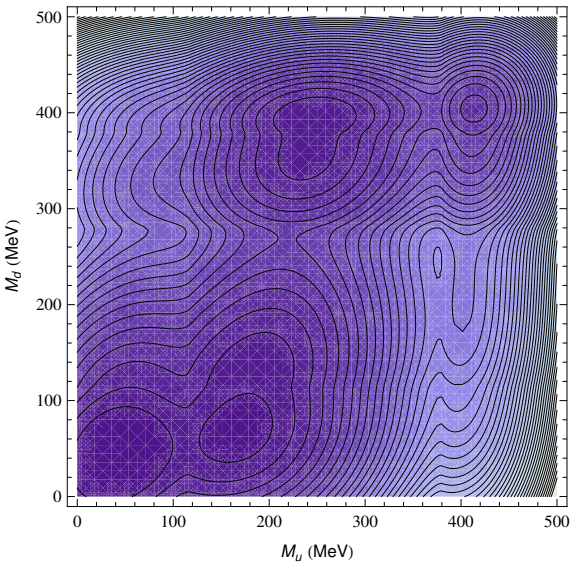

Figure 6.6: The effective potential as function of the constituent quark masses at $B = 5m_\pi^2/e$, $\mu = 378\,\text{MeV}$ and $c = 0.03$.

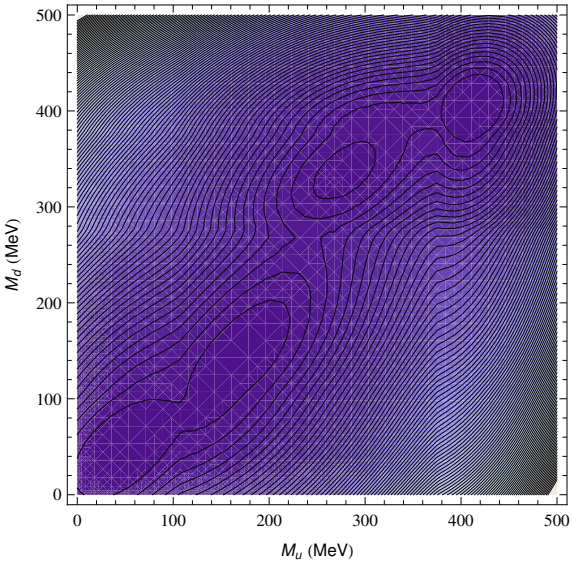

Figure 6.7: The effective potential as function of the constituent quark masses at $B = 5m_\pi^2/e$, $\mu = 378\,\text{MeV}$ and $c = 0.1$.

6.3.2 Nonzero temperature

In this section the temperature dependence of the ground state is investigated at zero chemical potential, but with a magnetic field. As the instanton interaction does not influence the temperature dependence much, we only consider $c = 1/2$ for simplicity. Fraga and Mizher (2008) found in the linear sigma model coupled to quarks, that the usual crossover becomes a first order transition at very high magnetic fields. However, we find that this is not the case in the NJL model.

In Fraga and Mizher (2008) only the lowest Landau level was taken into account. Here more Landau levels are included, so the effect of the higher Landau levels can be investigated in the NJL model. Since the levels with large k are exponentially suppressed, the summation can be truncated in Eq. (6.7), we will denote the largest k with k_{trunc}. The value of k_{trunc} depends on the temperature, constituent quark mass, chemical potential and magnetic field considered. If M and T are increased or if B is decreased, k_{trunc} has to be increased.

In Fig. 6.8 we show the temperature dependence of the constituent quark mass at $B = 15m_\pi^2/e$ for four different values of k_{trunc}. The 13 levels case is chosen such that the error is less than 1 percent at $M = 450\,\text{MeV}, T = 450\,\text{MeV}$. From the figure it can be inferred that taking more Landau levels into account, makes the crossover sharper. Also, there is a significant difference between including the zeroth and first Landau level. It is clear that including more Landau levels, influences the details of the transition. However, the qualitative aspects of the phase transition are not changed.

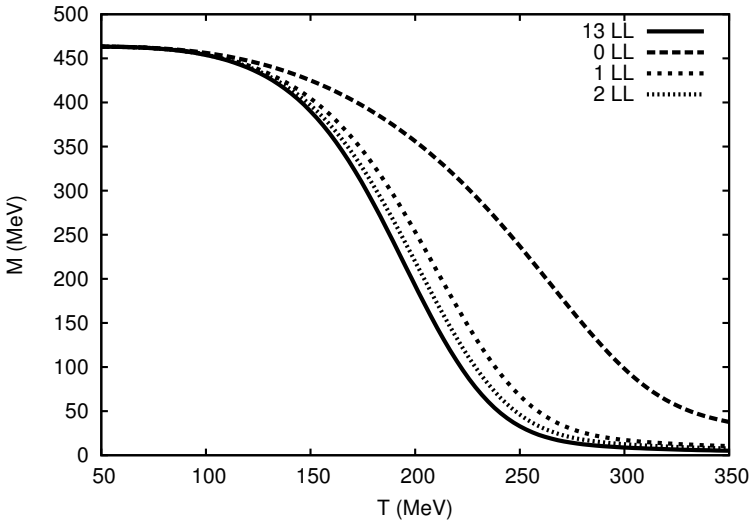

Figure 6.8: The temperature dependence of the constituent quark mass for strong magnetic field ($B = 15m_\pi^2/e$) and various k_{trunc} values.

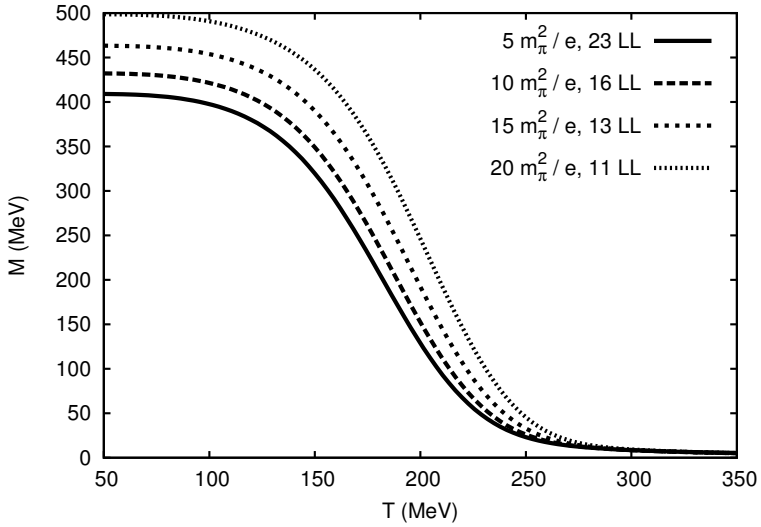

Figure 6.9: The temperature dependence of the constituent quark mass for various strong magnetic fields. We also indicate k_{trunc}.

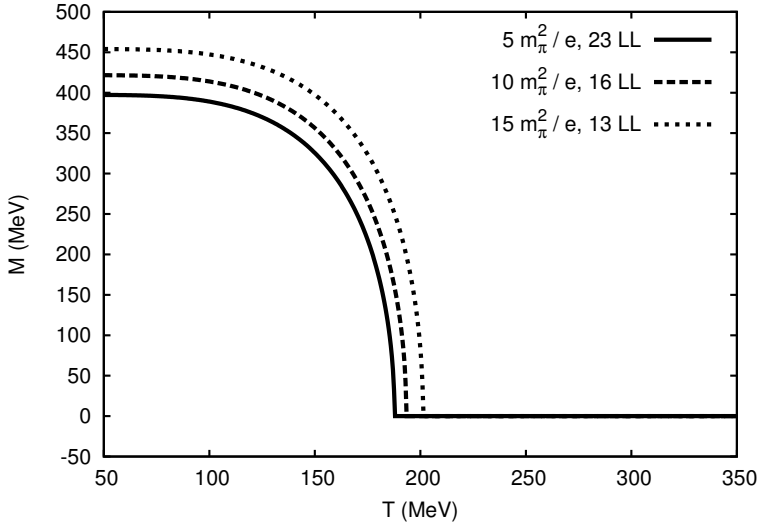

Figure 6.10: Same as Fig. 6.9, now in the chiral limit.

In Fig. 6.9 the temperature dependence of the constituent quark mass for different values of the external magnetic field is shown. The phase transition remains a crossover, in contrast to the results in the linear sigma model coupled to quarks. This difference is important, as a first order phase transition allows for meta-stable states, whereas a crossover does not. The situation is similar to the one discussed in the previous chapter, where the CP-restoring phase transition at $\theta = \pi$ and $B = 0$ was studied. In that chapter it was found that the way quarks are incorporated at zero temperature makes a difference between the models, which is likely also the reason for the discrepancy found here.

In Fig. 6.10 the results in the chiral limit are shown, where the transition remains a second order phase transition, like it is the case at zero magnetic field and confirms the results of Inagaki, Kimura, and Murata (2004) who calculated the phase diagram in a strong magnetic field in the chiral limit using the Fock-Schwinger proper time method. Note that the critical temperature increases slightly with increasing magnetic field.

6.4 Conclusions

The effect of a strong magnetic field on quark matter has been investigated in the NJL model in two regimes, zero temperature and finite chemical potential and vice versa. The first regime is of relevance for (the interior of) magnetars and the second for heavy-ion collisions.

At very high magnetic fields, when $M \approx 2|q|B \approx \mu$, the phase structure shows a variety of phases and phase transitions due to Landau quantization. In the phase with approximate chiral symmetry (the A_i-phases), the constituent quark masses show discontinuous oscillations as a function of B, similar to the de Haas-van Alphen effect. Moreover, as a function of chemical potential, more first order phase transitions occur, corresponding to Landau levels filling up successively. Due to the difference in charge, this pattern is different for the two quark flavors. When there is no mixing in the absence of the instanton interaction, the two patterns are not coupled. This generally leads to rather different constituent quark masses, or equivalently, spontaneous isospin breaking $\langle\bar{\psi}\lambda_3\psi\rangle \neq 0$. This affects the mesons inside the medium, for example their masses. It was found that for a realistic choice of parameters in the NJL model such a phase of broken chiral and isospin symmetry arises around $B = 4.5m_\pi^2/e$, but it is already present as a metastable phase for lower magnetic fields.

When the instanton interaction is included, a competition occurs between the strength c of this interaction and the magnetic field. This reduces the region in the phase diagram with large $\langle\bar{\psi}\lambda_3\psi\rangle$. For c sufficiently large it disappears entirely, leaving only one phase transition. However, around this transition the phase structure is still rather complex regarding metastable phases, which are characterized by different fillings of Landau levels and which differ only slightly in energy, but much in the amount of chiral symmetry breaking. For lower values of c some of these near-degenerate minima can also differ considerably in the amount of isospin breaking.

Finally the role of temperature was studied at zero chemical potential. In Fraga and Mizher (2008) it was found in the linear sigma model coupled to quarks that a strong

magnetic field changes the usual crossover as a function of temperature into a first order transition. In the NJL model it was found that the crossover remains a crossover. Also it was found that including higher Landau levels in the calculation of the effective potential changes the details of the crossover, it becomes sharper, although the qualitative aspects of the transition are not changed. The difference between the two models is important, as the first order transition allows for metastable phases, while a crossover does not. Probably the difference between the models comes from the treatment of the quarks at zero temperature, as discussed in Chapter 5.

Chapter 7

Summary

There are strong indications that in heavy-ion collisions a new phase of matter is created, quark matter, which is a state of matter with deconfined quarks. Besides being created in heavy-ion collisions, it is also believed to have existed in early universe. Today it might exist in the interior of very dense neutron stars. In this thesis we have studied how quark matter is influenced by instantons. These nonperturbative effects are closely related to the QCD vacuum angle θ. Because of the existence of instantons observables can become θ-dependent. In Nature θ appears to be very close zero, an additional argument for this was presented in Chapter 4 of this thesis. In heavy-ion collisions θ may effectively become nonzero, at least that conclusion is drawn from an effective low-energy theory of the strong interaction. When θ is different from $0 \pmod{\pi}$, the theory is not invariant under CP.

As effects of nonzero θ and instantons cannot be seen in perturbation theory and nonzero θ is also currently impossible to simulate on the lattice, effective theories and models have to be used. The most obvious one would be chiral perturbation theory, but unfortunately it is only valid at very low energies and for the ground state, not for the metastable states with effectively nonzero θ. Therefore, the investigations presented in this work were done using model calculations, the Nambu–Jona-Lasinio (NJL) model and the linear sigma model coupled to quarks. 't Hooft has shown that instantons induce an extra interaction in effective models, the 't Hooft determinant interaction. We studied the effects of this interaction on the phase structure of two-flavor quark matter. We studied, among others, the role that instantons play on phases of the strong interaction that spontaneously violate CP invariance.

We started the thesis with a short introduction to QCD, instantons and the consequences of a nonzero θ-angle in Chapter 1. Using chiral perturbation theory and experimental results we presented the arguments that $\theta < 10^{-10}$ in Nature. Furthermore, it was argued that for a certain range of parameters, metastable phases may become possible. These phases could be relevant in heavy-ion collisions and maybe for the early universe.

We continued our introduction with Chapter 2, where several facets of the QCD phase diagram were discussed. We first presented a short discussion about phase transitions

and a review about the best-known phase diagram of QCD, the $\mu_B - T$-phase diagram. Then we introduced the three physical systems where quark matter is thought to play a role, the early universe, heavy-ion collisions and dense neutron stars. Also we presented several ways of obtaining theoretical knowledge about the QCD phase diagram. Finally, we discussed some non-standard phase diagrams, the QCD phase diagram as a function of the current quark masses, the isospin chemical potential, and θ.

In Chapter 3 the NJL model was introduced, which is a quark model with four-quark interactions that is a good description of low-energy QCD. We started with some historical background. Then we discussed the vacuum structure, which induces a large effective mass of the quarks, usually referred to as the constituent quark mass. Also we introduced the bound states of the model, which can be interpreted as mesons. Finally some low-energy relations were derived that can be used to fit the parameters of the model to data.

In Chapter 4 we presented a detailed study of the chiral symmetry breaking aspects of the phase diagram of the two-flavor NJL model at $\theta = \pi$. We concentrated on the effects of instantons and the violation of CP invariance. This chapter is in essence an extension of Chapter 2. We started the chapter with discussing the full θ-dependence at zero temperature and chemical potential, and later we investigated the case $\theta = \pi$ in more detail. The latter case is special, as it allows for the spontaneous breaking of CP invariance. The occurrence of this spontaneous breaking depends, among others, on the strength of the determinant interaction. If this strength reaches a critical value, which depends on the values of the current quark masses, spontaneous breaking of CP invariance occurs.

When the phase diagram is considered as a function of the up and down current quark mass at $\theta = \pi$ and a large enough value for the determinant interaction strength, a region in the diagram exists that spontaneously breaks CP invariance. In the NJL model both a lower and an upper boundary are found, in contrast to Tytgat (2000), who studied two-flavor chiral perturbation theory and only found a lower boundary. If the temperature is increased, the region becomes smaller and eventually disappears. This behavior may indicate that the suggestions for metastable states with an effective nonzero θ may not hold in QCD. It remains to be seen if these conclusions persist beyond the mean-field approximation and for the three flavor case.

Apart from the current quark mass dependence, also the dependence on temperature, baryon chemical potential and isospin chemical potential were considered. We presented phase diagrams as a function of either one of these three variables on one axis together with the strength of the instanton interaction on the other. It was found that when baryon chemical potential and temperature is increased, the CP violation disappears as a second order phase transition. This disappearance indicates that the violation of CP invariance is inherently a low energy phenomenon.

Also the mesons are affected by a nonzero CP-violating condensate. The mass eigenstates of the mesons are no longer CP and parity eigenstates. The condensate induces mixing between the mesons, the pions mix with the a_0-mesons and the σ meson mixes with the η-meson.

In the phase diagram as a function of isospin chemical potential and strength of the determinant interaction at $\theta = \pi$, a novel phase with a nonzero $a_0^{\pm}$-condensate appears. Fur-

thermore, the usual condition for a charged pion condensate is altered when the strength of the instanton interaction is larger than its critical value.

As we said previously, the phase that violates CP invariance in the NJL model disappears as a second order transition as a function of temperature. This is in disagreement with the findings of Mizher and Fraga (2009), who calculated, among others, this transition in a related model, the linear sigma model coupled to quarks (LSMq). In the latter model a first order transition is found. In Chapter 5 we discussed the similarities and differences between the two models. It was shown how one obtains a linear sigma model when the NJL model is bosonized. The important difference between the two models is the way quarks are included in the model. In the case of the NJL model, the quarks are necessarily taken into account at all temperatures, as it is a quark model. However, in the case of the linear sigma model coupled to quarks, quarks are only taken into account at nonzero temperatures.

The analysis presented in Chapter 5 shows, using Landau-Ginzburg arguments, that the quarks at zero temperature introduce a logarithmic term, which is not included in the LSMq model. A similar logarithmic term is obtained from quarks at high temperatures, which exactly cancels the zero-temperature term. This cancellation takes place in the NJL model, but not in the LSMq model. We showed that it is exactly this term that causes the qualitative differences between the two models.

In Chapter 6 the competition between the instanton interaction and a strong magnetic field was studied at $\theta = 0$. This study could be relevant for describing non-central heavy-ion collisions and the interior of neutron stars. Charged particles in strong magnetic fields are subject to Landau quantization, the effect that the momentum perpendicular to the magnetic field becomes quantized. This quantization can affect the phase structure of the matter involved considerably.

Firstly, because the quarks do not have the same charge, they behave differently in a magnetic field. As a function of baryon chemical potential it becomes possible that the two quarks have rather different constituent quark masses, a form of spontaneous isospin violation. Such violation can for instance affect the masses and decay rates of the mesons. The magnetic field effect is opposed by the instanton interaction, which favors equal behavior for the quarks: the constituent masses of the quarks and their phase transitions become coupled. However, when the strength of the instanton interaction is not too large, it is still possible to have a relatively large difference in constituent mass for the two quarks. This possibility disappears as the strength of the interaction is increased.

In addition the phase structure includes metastable states for a range of chemical potentials and magnetic fields. These states differ in the number of filled Landau levels and the amount of chiral symmetry breaking, which will affect the mesons accordingly. Furthermore, they are almost degenerate with the ground state and can therefore not be discarded.

Finally, we showed how a strong magnetic field affects the high-temperature phase transition, relevant for heavy-ion collisions. In the linear sigma model coupled to quarks it has been found that a strong magnetic field turns the crossover at zero magnetic field into a (weak) first order transition. In the NJL model we found that the transition remains a crossover. This different is important, as a first order transition and a crossover have

very distinct experimental signatures, as in the case of a first order transition latent heat is absorbed or released, which does not happen in a crossover.

From the investigations reported in this thesis it is clear that instantons can play an important role in determining low-energy phenomena of the strong interaction and can affect the properties of quark matter. Hence, more detailed studies beyond the ones presented here would be valuable. The work we presented was performed using two-flavor effective models. It would be very interesting to extend our work by including the strange quark. In the chiral limit at $\theta = 0$, the order of the high-temperature phase transition is then different (Pisarski and Wilczek, 1984). It would be interesting to see whether this also holds for the CP restoring phase transition. Also, it would be interesting to see what happens beyond the mean-field approximation and when color superconductivity is included.

Another continuation of this work would be to calculate the equation-of-state and obtain mass-radius relations for stars obeying these relations, like for example Menezes et al. (2009a,b). From the mass-radius relation we would then see how the instantons and magnetic fields affect quark matter in compact stars.

Appendix A

Random-phase approximation

In this appendix the meson masses are calculated in the random-phase approximation (RPA), the first part of this appendix is mainly based on Klevansky (1992). First the case without a CP-violating condensate is considered, then we generalize the analysis by also including the CP-violating condensate $\langle\bar{\psi}i\gamma_5\psi\rangle$. The appendix ends with a discussion of the relation between the curvature at the minimum of the effective potential and the masses calculated in the RPA.

We start by discussing the quark-meson interaction. In case of the pions, we have the following interaction Lagrangian

$$\mathscr{L}_{\pi qq} = ig_{\pi qq}\bar{\psi}\gamma_5\lambda_i\pi_i\psi, \tag{A.1}$$

where ψ is the quark field, λ_i are the generators of $SU(2)$ and π_i is the pion-field. This interaction can be used to calculate the scattering of two quarks, for example the process $(ud) \to (u'd')$, shown in Fig. A.1, has the amplitude

$$[\bar{d}'i\gamma_5\lambda_1 u][ig^2_{\pi qq}]\frac{1}{k^2 - m^2_\pi}[\bar{u}'i\gamma_5\lambda_1 d], \tag{A.2}$$

From the amputated diagram one thus obtains an effective interaction

$$(i\gamma_5\lambda_1)\frac{-ig^2_{\pi qq}}{k^2 - m^2_\pi}(i\gamma_5\lambda_1). \tag{A.3}$$

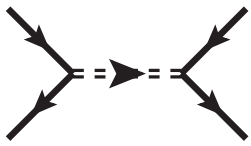

Figure A.1: The scattering of two quarks by the exchange of a pion.

Figure A.2: Lowest order contribution to the quark-antiquark polarization in the pseudoscalar channel.

for the exchange of a π_1. In the same way effective interactions can be derived for the exchange of the other mesons.

Also in the NJL model an effective interaction for the exchange of a meson can be obtained. The interaction parts of the interaction Lagrangian are responsible for exciting meson modes, for example, the term $(\bar{\psi} i\gamma_5 \lambda_i \psi)^2$ is responsible for exciting the isovector pseudoscalar $J^{PC} = 0^{-+}$ mode which will be identified as the pion. The effective interaction resulting from the exchange of a π-meson can be expressed to leading order in N_c as an infinite sum of terms in the RPA. Only the direct term, shown in Fig. A.2, is taken into account, which is the dominant term in the $1/N_c$-expansion. If we call the exchange diagram for the π_i iU_π, we have

$$\begin{aligned} iU_{\pi_i}(k^2) = (i\gamma_5\lambda_i)\Big[2i(G_1+G_2) + 2i(G_1+G_2)\left(\frac{1}{i}\Pi_{\pi_i}(k^2)\right)2i(G_1+G_2) \\ + 2i(G_1+G_2)\left(\frac{1}{i}\Pi_{\pi_i}(k^2)\right)2i(G_1+G_2)\left(\frac{1}{i}\Pi_{\pi_i}(k^2)\right)2i(G_1+G_2) + \cdots\Big](i\gamma_5\lambda_i) \\ = (i\gamma_5\lambda_i)\left[\frac{2i(G_1+G_2)}{1-2(G_1+G_2)\Pi_{\pi_i}(k^2)}\right](i\gamma_5\lambda_i), \quad \text{(A.4)} \end{aligned}$$

The exchange diagrams of the other channels have the same structure, only the $(i\gamma_5\lambda_i)$-terms have to be replaced with the appropriate ones for the different channels. Furthermore, for the η and a_0-channels $G_2 \to -G_2$.

The quark-antiquark polarization Π_{π_i} is given by the diagram of Fig. A.2, which is equal to the expression

$$\Pi_{\pi_i} = i\int \frac{\mathrm{d}^4 p}{(2\pi)^4} \mathrm{Tr}\,(i\gamma_5\lambda_i)\,S(p)\,(i\gamma_5\lambda_i)\,S(p+q), \quad \text{(A.5)}$$

where $S(p)$ is the dressed quark propagator,

$$S(p) = \frac{\not{p} + M}{p^2 - M^2}, \quad \text{(A.6)}$$

and M the constituent quark mass, related to the condensate α_0 and the bare quark mass m by $M = m + \alpha_0$. Note that degenerate current quark masses are used.

Comparing the results of Eq. (A.3) and Eq. (A.4) leads to the observation that the following equation has to be solved to obtain the mass of the pion

$$1 - 2(G_1+G_2)\Pi_{\pi_i}(k^2) = 0 \quad \text{(A.7)}$$

The result with $G_2 = 0$ was first derived by Nambu and Jona-Lasinio (1961a,b). The coupling constant can be related to the residue at the pole of Eq. (A.4) as explained in Chapter 4. Expanding Eq. (A.4) around its pole at $k^2 = m_\pi^2$ we find

$$iU_{\pi_i}(k^2) \simeq (i\gamma_5)\lambda_i \frac{-i\left(\partial\Pi_{\pi_i}/\partial k^2\right)^{-1}\Big|_{k^2=m_\pi}}{k^2 - m_\pi^2}(i\gamma_5)\lambda_i, \tag{A.8}$$

from which the value of the coupling constant can be deduced

$$g_{\pi qq}^2 = \left(\partial\Pi_{\pi_i}/\partial k^2\right)^{-1}\Big|_{k^2=m_\pi^2}. \tag{A.9}$$

A.1 Calculation of the quark-antiquark polarizations

As an example we will perform the calculation of the pion masses in some detail. Like in Chapter 4 it will be assumed that only the α_0-condensate is nonzero, which is the case when the quark masses are degenerate and when there is no CP violation. Performing the trace in Eq. (A.5) gives

$$\Pi_{\pi_i}(q^2) = iN_cN_f \int \frac{\mathrm{d}^4p}{(2\pi)^4} 2\Big[\frac{1}{p^2 - M^2} + \frac{1}{(p+q)^2 - M^2} - \frac{q^2}{[p^2 - M^2]\,[(p+q)^2 - M]}\Big], \tag{A.10}$$

for the quark-antiquark polarization. It will be convenient to introduce the following integrals

$$\begin{aligned} I_0(q^2) &= -4iN_c \int \frac{\mathrm{d}^4p}{(2\pi)^4} \frac{1}{[p^2 - M^2]\,[(p+q)^2 - M^2]}, \\ I_2 &= 4iN_c \int \frac{\mathrm{d}^4p}{(2\pi)^4} \frac{1}{p^2 - M^2} \\ &= \frac{M - m}{4MN_c(G_1 + G_2)}, \end{aligned} \tag{A.11}$$

where in the last step the gap equation has been used. Using these integrals, the polarization obtains the following form

$$\Pi_{\pi_i}(q^2) = N_f\left[I_2 + \frac{1}{2}q^2 I_0(q^2)\right]. \tag{A.12}$$

Inserting this expression in Eq. (A.7) and solving for the mass gives

$$m_\pi^2 = \frac{m}{M}\frac{1}{2(G_1 + G_2)I_0}. \tag{A.13}$$

The polarization in the η channel is equal to the one of the pions. For the σ and $\boldsymbol{a}_0$ channels the polarization yields

$$\Pi_\sigma = \Pi_{\boldsymbol{a}_0} = N_f \left[I_2 + \frac{1}{2}\left(q^2 + 4M^2\right) I_0(q^2) \right]. \tag{A.14}$$

Using these polarizations, expressions for the meson masses can be derived.

A.2 The masses of the mesons with a CP-violating condensate

At $\theta = \pi$ the expressions for the masses change. Apart from the usual α_0-condensate, also β_0 can become nonzero. A nonzero β_0-condensate causes the parity partners to mix with each other, i.e., the pions mix with the $\boldsymbol{a}_0$'s and the η with σ. The details of the mixing will be discussed in this section.

The mixing occurs because when $\beta_0 \neq 0$, the model is not invariant under CP anymore, consequently there is no reason for the mass eigenstates of the mesons to conserve CP invariance.

When the condensate β_0 becomes nonzero, the dressed quark propagator changes according to

$$S(p) = \frac{\not{p} + M - M_5\gamma_5}{p^2 - M^2 - M_5^2}, \tag{A.15}$$

where $M_5 = \beta_0$. This change of the quark propagator complicates the summation of the bubble diagrams, because it allows a coupling of the $i\gamma^5_{ij} i\gamma^5_{kl}$-type interaction to the $\delta_{ij}\delta_{kl}$-type interaction, using the structure given in Fig. A.3. We will concentrate on the mixing between σ and η for notational convenience. The calculation of the mixing between the pions and the $\boldsymbol{a}_0$ proceeds similarly with the vertices $i\gamma^5_{ij}$ and δ_{ij} replaced with $\gamma_5\lambda_i$ and λ_i.

The calculation of the massed of the mixed particles and their mixing angles is analogous to the calculation of the mixing between η and η' in the $SU(3)$-form of the NJL model. The latter mixing is discussed in detail by Klevansky (1992), which we will follow in order to describe the mixing between the CP and parity eigenstates of the mesons.

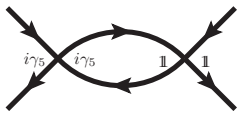

Figure A.3: A $\delta_{ij}\delta_{kl}$-interaction coupled to a $i\gamma^5_{ij} i\gamma^5_{kl}$-interaction, this interaction violates CP invariance and is only possible when $M_5 \neq 0$.

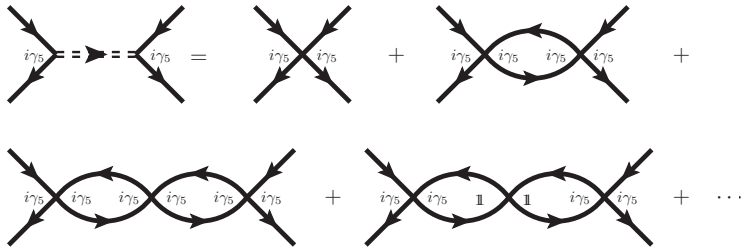

Figure A.4: Effective $\eta - \eta$ interaction in the random-phase approximation, with a CP-violating condensate. Only the direct term is considered.

A.2.1 The mass of σ and η

The effective interaction in the η-channel becomes the sum in Fig. A.4. Of course, a similar summation holds for the σ-particle. But Fig. A.3 also allows for an effective interaction in form of Fig. A.5. The existence of the β_0 condensate allows an interaction between the σ channel and the η channel, inducing mixing between particles.

In order to perform the summation, it is convenient to introduce the following notation

$$\begin{aligned}
c_{11}(q^2) &= N_c N_f \int \frac{\mathrm{d}^4 p}{(2\pi)^4} \mathrm{Tr}\, S(p) S(p+q)(G_1 + G_2 \cos\pi) \\
&= 4 N_c N_f \left[I_2 + \frac{1}{2}\left(q^2 - 4M_5^2\right) I_0(q^2) \right] (G_1 + G_2 \cos\pi), \\
c_{15}(q^2) &= N_c N_f \int \frac{\mathrm{d}^4 p}{(2\pi)^4} \mathrm{Tr}\, S(p) i\gamma_5 S(p+q)(G_1 - G_2 \cos\pi) \\
&= -8 N_c N_f I_0(q^2)(G_1 - G_2 \cos\pi), \\
c_{51}(q^2) &= N_c N_f \int \frac{\mathrm{d}^4 p}{(2\pi)^4} \mathrm{Tr}\, i\gamma_5 S(p) S(p+q)(G_1 + G_2 \cos\pi) \\
&= -8 N_c N_f I_0(q^2)(G_1 + G_2 \cos\pi),
\end{aligned}$$

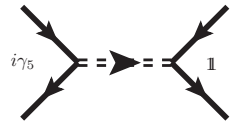

Figure A.5: Effective $\eta - \sigma$ interaction allowed due to the existence of a β_0-condensate.

$$c_{55}(q^2) = N_c N_f \int \frac{\mathrm{d}^4 p}{(2\pi)^4} \mathrm{Tr}\, i\gamma_5 S(p) i\gamma_5 S(p+q)(G_1 - G_2 \cos\pi)$$
$$= 4N_c N_f \left[I_2 + \frac{1}{2}\left(q^2 - 4M^2\right) I_0(q^2) \right] (G_1 - G_2 \cos\pi), \tag{A.16}$$

where have used generalized versions of the integrals $I_0(q^2)$ and I_2,

$$I_0(q^2) = -4iN_c \int \frac{\mathrm{d}^4 p}{(2\pi)^4} \frac{1}{\left[p^2 - M^2 - M_5^2\right]\left[(p+q)^2 - M^2 - M_5^2\right]},$$
$$I_2 = 4iN_c \int \frac{\mathrm{d}^4 p}{(2\pi)^4} \frac{1}{p^2 - M^2 - M_5^2}. \tag{A.17}$$

From now on, we will not write the q^2 dependence of the c's explicitly. Also, to avoid confusion, we keep all the factors $\cos\pi$ explicit. The sum of diagrams expressed in the c's yields

$$U_{55}(q^2) = (i\gamma_5)2(G_1 + G_2\cos\pi)[1 + 2c_{55} + 2c_{55}2c_{55} + 2c_{51}2c_{15} + 2c_{55}2c_{55}2c_{55}$$
$$+ 2c_{55}2c_{51}2c_{15} + 2c_{51}2c_{11}2c_{15} + 2c_{51}2c_{15}2c_{55} + \cdots]i\gamma_5. \tag{A.18}$$

Clearly, a c_{ij} is always followed by c_{jk}, with $i, j, k \in \{1, 5\}$. If we now introduce the matrices

$$\Gamma_{11} = \begin{pmatrix} 1 & 0 \\ 0 & 0 \end{pmatrix},$$
$$\Gamma_{15} = \begin{pmatrix} 0 & 1 \\ 0 & 0 \end{pmatrix},$$
$$\Gamma_{51} = \begin{pmatrix} 0 & 0 \\ 1 & 0 \end{pmatrix},$$
$$\Gamma_{55} = \begin{pmatrix} 0 & 0 \\ 0 & 1 \end{pmatrix}, \tag{A.19}$$

which satisfy

$$\Gamma_{ij}\Gamma_{kl} = \Gamma_{il} \qquad \text{when } j = k,$$
$$\Gamma_{ij}\Gamma_{kl} = 0 \qquad \text{when } j \neq k, \tag{A.20}$$

and if we furthermore introduce

$$\Sigma = \Gamma_{11}c_{11} + \Gamma_{15}c_{15} + \Gamma_{51}c_{51} + \Gamma_{55}c_{55}, \tag{A.21}$$

then the sum can be written as

$$U_{55}(q^2) = (i\gamma_5)2(G_1 - G_2\cos\pi)\mathrm{Tr}\,[\Gamma_{55} + \Gamma_{55}2\Sigma + \Gamma_{55}2\Sigma 2\Sigma$$
$$+ \Gamma_{55}2\Sigma 2\Sigma 2\Sigma + \cdots](i\gamma_5), \tag{A.22}$$

which equals

$$\begin{aligned} U_{55}(q^2) &= (i\gamma_5)2(G_1 + G_2\cos\pi)\mathrm{Tr}\left[\Gamma_{55}\left(\sum_{n=0}^{\infty}[2\Sigma]^n\right)\right](i\gamma_5) \\ &= (i\gamma_5)2(G_1 + G_2\cos\pi)\mathrm{Tr}\left[\Gamma_{55}\left(\mathbb{1} - 2\Sigma\right)^{-1}\right](i\gamma_5). \end{aligned} \tag{A.23}$$

If we now calculate the inverse of Σ we end up with

$$U_{55}(q^2) = (i\gamma_5)(G_1 + G_2\cos\pi)\frac{2 - 4c_{11}}{1 - 2c_{11} - 4c_{51}c_{15} - 2c_{55} + 4c_{11}c_{55}}(i\gamma_5). \tag{A.24}$$

In the same way we can calculate the effective interactions $U_{11}(q^2)$, $U_{15}(q^2)$, and $U_{51}(q^2)$. They are given by

$$\begin{aligned} U_{11}(q^2) &= 2(G_1 - G_2\cos\pi)\mathrm{Tr}\left[\Gamma_{11}\left(\mathbb{1} - 2\Sigma\right)^{-1}\right] \\ &= (G_1 - G_2\cos\pi)\frac{2 - 4c_{11}}{1 - 2c_{11} - 4c_{51}c_{15} - 2c_{55} + 4c_{11}c_{55}}, \\ U_{15}(q^2) &= 2(G_1 - G_2\cos\pi)\mathrm{Tr}\left[\Gamma_{51}\left(\mathbb{1} - 2\Sigma\right)^{-1}\right](i\gamma_5) \\ &= (G_1 + G_2\cos\pi)\frac{4c_{15}}{1 - 2c_{11} - 4c_{51}c_{15} - 2c_{55} + 4c_{11}c_{55}}, \\ U_{51}(q^2) &= (i\gamma_5)2(G_1 + G_2\cos\pi)\mathrm{Tr}\left[\Gamma_{51}\left(\mathbb{1} - 2\Sigma\right)^{-1}\right] \\ &= (G_1 + G_2\cos\pi)\frac{4c_{51}}{1 - 2c_{11} - 4c_{51}c_{15} - 2c_{55} + 4c_{11}c_{55}}. \end{aligned} \tag{A.25}$$

To again simplify notation we introduce an effective interaction $U(q^2)$ in the following way

$$\begin{aligned} U(q^2) &= \begin{pmatrix} U_{11}(q^2) & U_{15}(q^2) \\ U_{51}(q^2) & U_{55}(q^2) \end{pmatrix} \\ &= \frac{1}{D(q^2)}\begin{pmatrix} A(q^2)\mathbb{1}\otimes\mathbb{1} & B(q^2)\mathbb{1}\otimes(i\gamma_5), \\ B(q^2)(i\gamma_5)\otimes\mathbb{1} & C(q^2)(i\gamma_5)\otimes(i\gamma_5) \end{pmatrix}, \end{aligned} \tag{A.26}$$

where

$$\begin{aligned} A(q^2) &= 2(G_1 + G_2\cos\pi)(1 - 2c_{55}), \\ B(q^2) &= 2(G_1 + G_2\cos\pi)2c_{15} \\ &= 2(G_1 - G_2\cos\pi)2c_{51}, \\ C(q^2) &= 2(G_1 - G_2\cos\pi)(1 - 2c_{11}), \\ D(q^2) &= (1 - 2c_{11})(1 - 2c_{55}) - 4c_{15}c_{51}. \end{aligned} \tag{A.27}$$

The effective interaction has two poles, each can be associated with the meson masses. When only the chiral condensate is nonzero, the mass eigenstates are also CP eigenstates

and parity eigenstates in the case of the charged mesons, but now that changes. As we have seen, the parity partners mix and we can define mass-eigenstates, denoted with a tilde, as follows

$$\begin{aligned}
|\tilde{\sigma}\rangle &= \cos\theta_\eta\,|\sigma\rangle + \sin\theta_\eta\,|\eta\rangle\,,\\
|\tilde{\eta}\rangle &= \cos\theta_\eta\,|\eta\rangle - \sin\theta_\eta\,|\sigma\rangle\,,\\
|\tilde{\boldsymbol{a}}_0\rangle &= \cos\theta_{\boldsymbol{\pi}}\,|\boldsymbol{a}_0\rangle + \sin\theta_{\boldsymbol{\pi}}\,|\boldsymbol{\pi}\rangle\,,\\
|\tilde{\boldsymbol{\pi}}\rangle &= \cos\theta_{\boldsymbol{\pi}}\,|\boldsymbol{\pi}\rangle - \sin\theta_{\boldsymbol{\pi}}\,|\boldsymbol{a}_0\rangle\,,
\end{aligned} \tag{A.28}$$

where θ_η and $\theta_{\boldsymbol{\pi}}$ are the mixing angles. The states on the r.h.s. are the usual states of definite parity.

We calculate the masses as follows. First we expand $U(q^2)$ around the lowest pole. When the CP-violating condensate in zero, this would give the η mass, so we will denote these particles with $\tilde{\eta}$. The higher mass pole corresponds to the σ meson when we only have the chiral condensate, so we will call these particles the $\tilde{\sigma}$. Explicitly,

$$\begin{aligned}
U(q^2) \simeq\ & \frac{C}{(\mathrm{d}/\mathrm{d}q^2)\log D}\bigg|_{q^2\to m_{\tilde{\eta}}^2}\frac{1}{q^2-m_{\tilde{\eta}}^2}\\
& \left[(i\gamma_5)\otimes(i\gamma_5) + a_{\tilde{\eta}}(i\gamma_5)\otimes\mathbb{1} + a_{\tilde{\eta}}\mathbb{1}\otimes(i\gamma_5) + \frac{A}{C}\mathbb{1}\otimes\mathbb{1}\right],
\end{aligned} \tag{A.29}$$

where

$$a_{\tilde{\eta}}(q^2) = \frac{U_{15}(q^2)}{U_{55}(q^2)}\bigg|_{q^2\to m_{\tilde{\eta}}^2} = \frac{B(q^2)}{C(q^2)}\bigg|_{q^2\to m_{\tilde{\eta}}^2}. \tag{A.30}$$

Furthermore, $A(q^2)C(q^2) - B^2(q^2) = 4(G_1^2 - G_2^2\cos^2\pi)D(q^2)$, which means that at a root of $D(q^2)$ the relation $A(q^2)C(q^2) = B^2(q^2)$ holds. Therefore,

$$\frac{U_{11}(q^2)}{U_{55}(q^2)} = \frac{A(q^2)}{C(q^2)} = \frac{B^2(q^2)}{C^2(q^2)} = a_{\tilde{\eta}}^2(q^2). \tag{A.31}$$

which makes it possible to factor $U(q^2)$ in the following way

$$U(q^2) = \frac{g_{\tilde{\eta}qq}^2}{q^2-m_{\tilde{\eta}}^2}\left(\cos\theta_\eta(i\gamma_5) + \sin\theta_\eta\mathbb{1}\right)\otimes\left(\cos\theta_\eta(i\gamma_5) + \sin\theta_\eta\mathbb{1}\right), \tag{A.32}$$

where

$$\begin{aligned}
\frac{g_{\tilde{\eta}qq}^2}{1+a_{\tilde{\eta}}^2} &= \frac{U_{55}}{(\mathrm{d}/\mathrm{d}q^2)\log D}\bigg|_{q^2\to m_{\tilde{\eta}}^2},\\
\tan\theta_\eta &= a_{\tilde{\eta}}.
\end{aligned} \tag{A.33}$$

Similar relations hold for the pions and $\boldsymbol{a}_0$ mesons. The results obtained in this appendix are used in the calculation of the c dependence of the mesons masses and their mixing angles, which are shown in Fig. 4.13 and 4.14 of Chapter 4.

A.3 The curvature of the effective potential

The masses calculated in the random-phase approximation are related, but in general not equal to the curvature of the effective potential at the minimum. In this section we make this relation explicit. First of all, in this section we will for ease of notation only discuss the CP-conserving case at zero temperature and chemical potentials, with degenerate current quark masses. This analysis can be extended straightforwardly.

The main problem when calculating the curvature of the effective potential is the $\log\det K$-term in Eq. (4.8), let us therefore focus on this term

$$\frac{\partial^2}{\partial x_i^2}\log\det K, \tag{A.34}$$

where

$$\begin{aligned} K &= \lambda_0 \otimes (i\gamma_0 p_0 + \gamma_i p_i) - \mathscr{M}, \\ \mathscr{M} &= m\lambda_0 \otimes \mathbb{1}_{\mathrm{d}} + \alpha_a \lambda_a \otimes \mathbb{1}_{\mathrm{d}} + \beta\lambda_a \otimes i\gamma_5, \end{aligned} \tag{A.35}$$

and $x_i = \{\alpha_0, \alpha_1, \alpha_2, \alpha_3, \beta_0, \beta_1, \beta_2, \beta_3\}$. We can now proceed with calculating the curvature

$$\begin{aligned} \frac{\partial^2}{\partial x_i^2}\log\det K &= \frac{\partial}{\partial x_i}\frac{1}{\det K}\frac{\partial \det K}{\partial x_i} \\ &= -\frac{1}{(\det K)^2}\left(\frac{\partial \det K}{\partial x_i}\right)^2 + \frac{1}{\det K}\frac{\partial^2 \det K}{\partial x_i^2} \\ &= \mathrm{Tr}\left[K^{-1}\frac{\partial^2 K}{\partial x_i^2}\right] - \mathrm{Tr}\left[\left(K^{-1}\frac{\partial K}{\partial x_i}\right)^2\right] \\ &= -\mathrm{Tr}\left[\left(K^{-1}\frac{\partial K}{\partial x_i}\right)^2\right], \end{aligned} \tag{A.36}$$

as K is linear in x_i. We are interested in the curvature at the minimum, assuming that then only $\alpha_0 \neq 0$ the matrices K and K^{-1} reduce to

$$\begin{aligned} K_{\mathrm{min}} &= \lambda_0 \otimes \left[(i\gamma_0 p_0 + \gamma_i p_i) - (m + \alpha_0)\right], \\ K_{\mathrm{min}}^{-1} &= -\frac{\lambda_0 \otimes \left[(i\gamma_0 p_0 + \gamma_i p_i) - (m + \alpha_0)\right]}{p_0^2 + \mathbf{p}^2 + (m + \alpha_0)^2}. \end{aligned} \tag{A.37}$$

Using all these expressions, we obtain the following results for the curvatures

$$\begin{aligned} \frac{\partial^2}{\partial \alpha_a^2}\log\det K\bigg|_{\mathrm{min}} &= -\frac{8\left[(\alpha_0^2 + m)^2 - p_0^2 - \mathbf{p}^2\right]}{(\alpha_0 + m)^2 + p_0^2 + \mathbf{p}^2}, \\ \frac{\partial^2}{\partial \beta_a^2}\log\det K\bigg|_{\mathrm{min}} &= \frac{8}{(\alpha_0 + m)^2 + p_0^2 + \mathbf{p}^2}. \end{aligned}$$

Integrating over p_0 (as we work at $T = 0$) yields

$$\int \frac{\mathrm{d}p_0}{2\pi} \frac{\partial^2}{\partial \alpha_a^2} \log\det K = \frac{4\mathbf{p}^2}{\sqrt{(\alpha_0 + m)^2 + \mathbf{p}^2}},$$
$$\int \frac{\mathrm{d}p_0}{2\pi} \frac{\partial^2}{\partial \beta_a^2} \log\det K = \frac{4}{\sqrt{(\alpha_0 + m)^2 + \mathbf{p}^2}}. \tag{A.38}$$

Putting everything together we obtain the following final results for the curvature of the effective potential at the minimum

$$\frac{\partial^2 \mathcal{V}}{\partial \alpha_0} = \frac{1}{G_1 + G_2} - 4N_c \int \frac{\mathrm{d}^3 p}{(2\pi)^3} \frac{\mathbf{p}^2}{\sqrt{(\alpha_0 + m)^2 + \mathbf{p}^2}} = I_0 m_\sigma^2,$$
$$\frac{\partial^2 \mathcal{V}}{\partial \alpha_i} = \frac{1}{G_1 - G_2} - 4N_c \int \frac{\mathrm{d}^3 p}{(2\pi)^3} \frac{\mathbf{p}^2}{\sqrt{(\alpha_0 + m)^2 + \mathbf{p}^2}} = I_0 m_{a_0}^2,$$
$$\frac{\partial^2 \mathcal{V}}{\partial \beta_0} = \frac{1}{G_1 - G_2} - 4N_c \int \frac{\mathrm{d}^3 p}{(2\pi)^3} \frac{1}{\sqrt{(\alpha_0 + m)^2 + \mathbf{p}^2}} = I_0 m_\eta^2,$$
$$\frac{\partial^2 \mathcal{V}}{\partial \beta_i} = \frac{1}{G_1 + G_2} - 4N_c \int \frac{\mathrm{d}^3 p}{(2\pi)^3} \frac{1}{\sqrt{(\alpha_0 + m)^2 + \mathbf{p}^2}} = I_0 m_\pi^2. \tag{A.39}$$

To conclude, the curvature of the effective potential with respect to the different fields gives up to a factor I_0 the masses of the corresponding mesons.

Appendix B

The magnetic field dependence of the effective potential

In this appendix the magnetic field dependent effective potential in the mean-field approximation is derived using the method developed by Ritus (1972, 1978). This method of implementing the magnetic field has been applied to the magnetic catalysis of chiral symmetry by Leung, Ng, and Ackley (1996), Lee, Leung, and Ng (1997), Ferrer and de la Incera (1998, 2000), Elizalde, Ferrer, and de la Incera (2003) and Ayala et al. (2006). Furthermore, Ferrer, de la Incera, and Manuel (2005, 2006) have used this method in order to describe the effects of strong magnetic fields on color superconductivity. The effective potential derived in this way is equal to the one of Ebert et al. (2000), Ebert and Klimenko (2003), and Klimenko and Zhukovsky (2008) using the Fock-Schwinger proper time method. The present discussion is based on Leung, Ng, and Ackley (1996) and Ferrer, de la Incera, and Manuel (2006).

When a constant magnetic field is present, the asymptotic states of the quarks are given by (see e.g. Ritus, 1972, 1978; Leung, Ng, and Ackley, 1996; Ferrer and de la Incera, 1998)

$$\psi_p(x) = E_{p\sigma}(x)\omega_{\sigma\chi}, \tag{B.1}$$

which are eigenvectors of the operator $(i\gamma^\mu\partial_\mu + q_f\lambda_f B\gamma^2 x_1)^2$ with eigenvalues $-p^2$. The $\omega_{\sigma\chi}$ are bispinors which are eigenvectors of the spin operator $i\gamma^1\gamma^2$ and γ^5 with eigenvalues σ and χ. Note that we are working in the chiral representation. The eigenfunctions $E_{p\sigma}(x)$ equal

$$E_{p\sigma}(x) = N(k)e^{ip_0x^0+p_2x^2p_3x^3}D_k(\rho) \tag{B.2}$$

with $D_k(\rho)$ the parabolic cylinder functions with argument $\rho = \sqrt{2|q_fB|}x_1 - p_2/q_fB$. The integer k equals

$$k = k(n,\sigma) \equiv n + \frac{q_fB\sigma}{2|q_fB|} - \frac{1}{2}. \tag{B.3}$$

Finally $N(k) = (4\pi|q_f B|)^{1/4}/\sqrt{k!}$ denotes a normalization factor. The functions $D_k(\rho)$ satisfy the following orthogonality property

$$\int_{-\infty}^{\infty} \mathrm{d}\rho D_{k'}(\rho) D_k(\rho) = \sqrt{2\pi} k! \delta_{kk'}. \tag{B.4}$$

As discussed by Ritus (1972, 1978), these eigenfunctions $E_{p\sigma}(x)$ can be used for the transformation to momentum space. It will be convenient to introduce the following matrices

$$E_p(x) = \sum_{\sigma} E_{p\sigma}(x)\Delta(\sigma), \tag{B.5}$$

with $\Delta(\sigma) = \mathrm{diag}(\delta_{\sigma 1}, \delta_{\sigma -1}, \delta_{\sigma 1}, \delta_{\sigma -1})$ the spin projector. The matrices $E_p(x)$ satisfy the following completeness relation

$$\sum_{k=0}^{\infty} \int \frac{\mathrm{d}p_0 \mathrm{d}p_2 \mathrm{d}p_3}{(2\pi)^4} E_p(x)\bar{E}_p(y) = \delta^{(4)}(x-y), \tag{B.6}$$

and are orthogonal

$$\int \mathrm{d}^4 x \bar{E}_{p'}(x) E_p(x) = (2\pi)^4 \delta_{nn'} \delta(p_0 - p_0') \delta(p_2 - p_2') \delta(p_3 - p_3'). \tag{B.7}$$

These orthogonal matrices $E_p(x)$ are the transformation matrices to momentum space when an external constant magnetic field is present, similar to the usual $e^{ip\cdot x}$ at zero field, i.e. (Ferrer, de la Incera, and Manuel, 2006)

$$\psi(x) = \sum_{k=0}^{\infty} \int \frac{\mathrm{d}p_0 \mathrm{d}p_2 \mathrm{d}p_3}{(2\pi)^4} E_p(x)\psi(p). \tag{B.8}$$

Furthermore, the $E_p(x)$ obey the following important property

$$(-i\gamma^\mu \partial_\mu - q_f \lambda_f B \gamma^2 x_1) E_p(x) = E_p(x) \gamma^\mu \bar{p}_\mu \tag{B.9}$$

with $\bar{p}_\mu = (p_0, 0, -\mathrm{sgn}(q_f B)\sqrt{2|q_f B|n}, p_3)$.

Using these $E_p(x)$ and their properties cited above, one can show, using a similar analysis as in Sect. 4.3, that the effective potential becomes equal to

$$\begin{aligned}
\mathcal{V} &= \frac{(M_0 - m)^2}{4G_0} + \frac{M_3^2}{4(1-2c)G_0} + \sum_{f=u}^{d} \log \mathrm{Det}\left(i\gamma^\mu \partial_\mu - q_f B \gamma^2 x_1 - M_f - \mu\gamma_0\right) \\
&= \frac{(M_0 - m)^2}{4G_0} + \frac{M_3^2}{4(1-2c)G_0} - \frac{N_c}{2\pi} \sum_{\sigma,n,f} |q_f| B \int \frac{\mathrm{d}p_3}{2\pi} \Big\{ E_{p,f}(B) \\
&\quad + T \ln\left[1 + e^{-\left[E_{p,f}(B)+\mu\right]/T}\right] + T \ln\left[1 + e^{-\left[E_{p,f}(B)-\mu\right]/T}\right] \Big\},
\end{aligned} \tag{B.10}$$

where $E_{p,f}(B) = \sqrt{p_3^2 + (2n + 1 - \sigma)|q_f|B + M_f^2}$ and Det denotes a functional determinant. This expression for the effective potential has been obtained using different methods by Ebert et al. (2000), Ebert and Klimenko (2003), Klimenko and Zhukovsky (2008), Menezes et al. (2009a,b).

Following the analysis of Menezes et al. (2009a), Eq. (B.10) can be split in three pieces, a part that is independent of external parameters, a part that only depends on the magnetic field and a part that depends on the magnetic field, chemical potential and temperature. First we split Eq. (B.10) according to

$$\mathcal{V} = \frac{(M_0 - m)^2}{4G_0} + \frac{M_3^2}{4(1-2c)G_0} + \mathcal{V}_q^{T=0}(B) + \mathcal{V}_2(B,\mu,T), \tag{B.11}$$

where

$$\begin{aligned}
\mathcal{V}_q^{T=0} &= -\frac{N_c}{2\pi}\sum_{\sigma,n,f}|q_f|B\int\frac{\mathrm{d}p_3}{2\pi}E_{p,f}(B),\\
\mathcal{V}_2(B,\mu,T) &= -\frac{N_c}{2\pi}\sum_{\sigma,n,f}|q_f|B\int\frac{\mathrm{d}p_3}{2\pi}\Big\{T\ln\Big[1+e^{-\left[E_{p,f}(B)+\mu\right]/T}\Big]\\
&\quad + T\ln\Big[1+e^{-\left[E_{p,f}(B)-\mu\right]/T}\Big]\Big\},
\end{aligned} \tag{B.12}$$

and start with evaluating $\mathcal{V}_q^{T=0}$. The summation over n and σ can be rearranged as

$$\mathcal{V}_q^{T=0} = -\frac{N_c}{\pi}\sum_{f=u}^{d}\sum_{k=0}^{\infty}|q_f|B\int\frac{\mathrm{d}p_3}{2\pi}\left[E_{p,k}(B) - \frac{E_{p,0}(B)}{2}\right]. \tag{B.13}$$

where $E_{p,k}(B) = \sqrt{p_3^2 + M_f^2 + 2k|q_f|B}$ and k denotes the Landau levels.

The integrals are now performed using dimensional regularisation

$$\int\frac{\mathrm{d}^d p}{(2\pi)^d}\frac{1}{(p^2+M^2)^n} = \frac{4\pi}{d/2}\frac{\Gamma(n-\frac{d}{2})}{\Gamma(n)}\left(\frac{1}{M^2}\right)^{n-\frac{d}{2}}, \tag{B.14}$$

yielding, with $d = 1 - \epsilon$ and $x_f = M_f^2/(2|q_f|B)$

$$\mathcal{V}_q^{T=0} = -\frac{2N_c}{\pi}\sum_{f=u}^{d}\left(|q_f|B\right)^2\frac{1}{(4\pi)^{\frac{1}{2}-\frac{\epsilon}{2}}}\frac{\Gamma(-1+\frac{\epsilon}{2})}{\Gamma(\frac{1}{2})}\left[\sum_{k=0}^{\infty}\left(\frac{1}{x+k}\right)^{-1+\frac{\epsilon}{2}} - \frac{1}{2}\left(\frac{1}{x}\right)^{-1+\frac{\epsilon}{2}}\right]. \tag{B.15}$$

Using the definition of the Hurwitz zeta function we obtain

$$\mathcal{V}_q^{T=0} = \frac{N_c}{2\pi^2}\sum_{f=u}^{d}\left(|q_f|B\right)^2(4\pi)^{\frac{\epsilon}{2}}\,\Gamma\left(-1+\frac{\epsilon}{2}\right)\left[\zeta\left(-1+\frac{\epsilon}{2},x\right) - \frac{1}{2}x^{-1+\frac{\epsilon}{2}}\right]. \tag{B.16}$$

Expanding around $\epsilon = 0$ and neglecting x_f-independent terms (including a UV-divergent one) yields

$$\mathcal{V}_q^{T=0} = \frac{N_c}{2\pi^2} \sum_{f=u}^{d} \left(|q_f|B\right)^2 \left[\frac{x^2}{\epsilon} + \frac{x_f^2}{2}(1-\gamma_E) - \frac{x_f}{2} \ln x_f - \zeta'(-1,x) \right], \tag{B.17}$$

which is still UV-divergent. This divergence can be removed by adding and subtracting the 1-loop contribution when no magnetic field is present,

$$\mathcal{V}_q^{T=0}(B=0) = -2N_c \sum_{f=u}^{d} \int \frac{\mathrm{d}^3 p}{(2\pi)^3} \sqrt{\mathbf{p}^2 + M_f}. \tag{B.18}$$

The subtracted term is calculated using dimensional regularization, after we change variables according to $\mathbf{p}^2 \to \mathbf{p}^2/(2|q_f|B)$ and $M_f^2 \to x_f = M_f^2/(2|q_f|B)$ we obtain

$$-\mathcal{V}_q^{T=0}(B=0) = -\frac{N_c}{2\pi^2} \sum_{f=u}^{d} (|q_f|B)^2 \left[\frac{x_f^2}{\epsilon} + \frac{x_f^2}{2}(1-\gamma_E) - \frac{x_f^2}{2} \ln x_f + \frac{x_f^2}{4} \right]. \tag{B.19}$$

The added term is calculated using the conventional three-momentum UV cut-off used in this thesis. Rearranging terms gives

$$\mathcal{V}_q^{T=0} = -2N_c \sum_{f=u}^{d} \int \frac{\mathrm{d}^3 p}{(2\pi)^3} \sqrt{\mathbf{p}^2 + M_f^2} + \mathcal{V}_1(B), \tag{B.20}$$

where

$$\mathcal{V}_1(B) = -\frac{N_c}{2\pi^2} \sum_{f=u}^{d} (|q_f|B)^2 \left[\zeta'(-1,x_f) - \frac{1}{2}(x_f^2 - x_f) \ln x_f + \frac{x_f^2}{4} \right]. \tag{B.21}$$

Putting all terms together gives the following final expression for the effective potential

$$\mathcal{V} = \mathcal{V}_0 + \mathcal{V}_1(B) + \mathcal{V}_2(B,\mu,T), \tag{B.22}$$

with

$$\mathcal{V}_0 = \frac{(M_0 - m)^2}{4G_0} + \frac{M_3^2}{4(1-2c)G_0} - 2N_c \sum_{f=u}^{d} \int \frac{\mathrm{d}^3 p}{(2\pi)^3} \sqrt{\mathbf{p}^2 + M_f^2}. \tag{B.23}$$

The term $\mathcal{V}_0$ is divergent and needs to be regularized. Here a conventional three-momentum UV cut-off is used, yielding the expression

$$\mathcal{V}_0 = \frac{(M_0 - m)^2}{4G_0} + \frac{M_3^2}{4(1-2c)G_0} - \frac{N_c}{8\pi^2} \sum_{f=u}^{d} |M_f| \Bigg(M_f^3 \ln \left(\frac{\Lambda}{M_f} + \sqrt{1 + \frac{\Lambda^2}{M_f^2}} \right) - \Lambda \left(M_f^2 + 2\Lambda^2 \right) \sqrt{1 + \frac{\Lambda^2}{M_f^2}} \Bigg). \tag{B.24}$$

As discussed previously, the summation over σ and n in $\mathcal{V}_2(B,\mu,T)$ can be rewritten as

$$\mathcal{V}_2(B,\mu,T) = -\frac{N_c}{2\pi}\sum_{k,f}(2-\delta_{k0})|q_f|B\int\frac{\mathrm{d}p_3}{2\pi}\Big\{T\ln\Big[1+e^{-\left[E_{p,k}(T)+\mu\right]/T}\Big] + T\ln\Big[1+e^{-\left[E_{p,k}(T)-\mu\right]/T}\Big]\Big\}, \quad \text{(B.25)}$$

The effective potential is evaluated further in Chapter 6.

Samenvatting

Uit het dagelijks leven weten we dat materialen in verschillende fases kunnen voorkomen. Water komt bijvoorbeeld voor als vloeibaar water, waterdamp en ijs. Behalve deze bekende drie zijn er nog meer fases mogelijk; zo zijn er minstens 15 verschillende soorten ijs, allemaal met een andere kristalstructuur. Externe parameters, zoals druk en temperatuur, bepalen de toestand waarin het water zich bevindt. Bij andere materialen kunnen ook andere parameters een rol spelen, zoals bijvoorbeeld de sterkte van een magneetveld bij een magnetisch materiaal.

In dit proefschrift, getiteld "*Effecten van instantoninteracties op de fases van quarkmaterie*", wordt materie onderzocht bij extreme dichtheden, ongeveer een triljoen (1 met 18 nullen) kilogram per kubieke meter, en extreme temperaturen, rond de twee biljoen (2 met 12 nullen) graden Celsius. Deze extreme omstandigheden komen (of kwamen) voor in de oerknal, hoog-energetische botsingen van zware ionen en in de kern van neutronensterren. Om te begrijpen wat er gebeurt met materie in deze gevallen zullen we eerst in de volgende paragraaf kort bespreken hoe men tegenwoordig denkt dat materie opgebouwd is.

Bouwstenen van de natuur

Alle materie rondom ons heen is opgebouwd uit atomen, die weer bestaan uit positief geladen atoomkernen en negatief geladen elektronen. Een elektron is een elementair deeltje. Dit betekent dat het niet meer opgedeeld kan worden. Atoomkernen zijn wel opgebouwd uit andere deeltjes, namelijk protonen en neutronen. Protonen zijn positief geladen, neutronen hebben geen lading. Protonen en neutronen zijn geen elementaire deeltjes, zij bestaan weer uit quarks. In totaal zijn er zes "smaken" quarks, maar in de materie om ons heen komen maar twee smaken voor: up en down. Het proton bestaat uit twee up-quarks en een down-quark, bij het neutron is het omgekeerd. Een up-quark heeft een lading van $+2/3e$ en het down-quark heeft een lading van $-1/3e$, waarbij e de lading is van het elektron. Voor zover bekend hebben quarks geen interne structuur, het zijn dus elementaire deeltjes. Onder normale omstandigheden komen quarks in de natuur niet vrij voor. Ze kunnen alleen voorkomen als gebonden toestanden, zoals in protonen en neutronen.

Behalve deze "gewone" materie, bestaat er ook materie die je in het dagelijkse leven nooit tegenkomt. Materie bestaande uit de andere smaken quarks is een voorbeeld, maar

er bestaan nog meer soorten elementaire deeltjes. In de twintigste eeuw is er een model ontwikkeld dat al deze deeltjes en hun onderlinge krachten beschrijft; het Standaard Model. Dit model beschrijft drie van de vier fundamentele krachten: de zwakke kernkracht, de sterke kernkracht en de elektromagnetische kracht. Hoe ook de zwaartekracht opgenomen kan worden is nog steeds onbekend. Dit proefschrift beperkt zich tot de sterke kernkracht, de kracht die de quarks in protonen en neutronen bij elkaar houdt.

Maar de natuur zit nog complexer in elkaar. Er bestaan namelijk ook antideeltjes. Dit zijn deeltjes met dezelfde massa als hun corresponderende deeltje, maar met een tegengestelde lading. Het antideeltje van het elektron is bijvoorbeeld het positief geladen positron. Het antideeltje van het up-quark is het anti-up-quark enzovoorts. In de natuur komen ook gebonden toestanden van een quark met een antiquark voor, zogenaamde mesonen. De gebonden toestanden van drie quarks, zoals protonen en neutronen, heten baryonen.

De theorie die de sterke kernkracht beschrijft is de quantumchromodynamica (QCD). De theorie bevat twee typen deeltjes: quarks en gluonen. De quarks zijn hierboven al besproken, de gluonen zijn de krachtoverbrengende deeltjes van de theorie. Op hoge energieën kunnen allerlei verschijnselen binnen QCD beschreven worden door middel van storingstheorie, waarbij grootheden worden geëxpandeerd in de koppelingsconstante[1] van de theorie. Om technische redenen werkt bij (relatief) lage energieën deze methode niet meer. Daarom worden in dit proefschrift effectieve theorieën en modellen voor QCD gebruikt.

Symmetrieën

Als alle deeltjes in antideeltjes zouden worden omgezet en vice versa, zouden de sterke kernkracht en de elektromagnetische kracht daar niets van merken. De hypothetische transformatie van alle deeltjes in hun corresponderende antideeltjes wordt ladingsconjugatie (afgekort C) genoemd. Daarom wordt gezegd dat de sterke kernkracht en de elektromagnetische kracht invariant of symmetrisch zijn onder C. De zwakke kernkracht is niet invariant onder C en gedraagt dus anders in de “normale” wereld dan in de getransformeerde wereld.

Afgezien van de hierboven besproken ladingsconjugatie zijn er nog andere transformaties belangrijk voor elementaire deeltjes, zoals bijvoorbeeld de pariteitstransformatie (afgekort P). In het geval van P wordt alles in de theorie gespiegeld; van een rechtshandig assenstelsel wordt overgegaan naar een linkshandig assenstelsel. Wederom zijn de sterke en elektromagnetische kracht invariant onder P en de zwakke kracht niet. De transformatie die van belang is voor dit proefschrift is de combinatie van C en P, kortweg CP. Net als C en P afzonderlijk is alleen de zwakke kracht niet invariant onder CP.

Het is echter onbegrepen waarom de sterke kernkracht invariant is onder CP. In principe is het voor deze kracht wel mogelijk om CP-invariantie te schenden. De theorie bevat een CP-schendende parameter θ, de vacuümhoek van QCD. Dankzij het bestaan van ob-

[1] De koppelingsconstante geeft de sterkte van de interactie aan.

jecten binnen QCD genaamd instantonen[2] worden meetbare grootheden afhankelijk van de hoek θ. Als θ ongelijk is aan $0 \pmod{\pi}$ schendt de theorie CP-invariantie. Experimenten geven aan dat θ kleiner is dan 10^{-10}. Dit theoretisch onbegrepen feit wordt het sterke CP-probleem genoemd. Het is echter interessant om θ effecten te bestuderen, aangezien er theoretische aanwijzingen zijn dat CP misschien geschonden wordt in QCD onder hoge temperaturen in botsingen van zware ionen. Zulke schendingen van CP zijn te beschrijven door aan te nemen dat θ effectief een waarde krijgt ongelijk aan 0.

Effecten van eindige θ en instantonen kunnen niet waargenomen worden in storingstheorie, zodat ze moeilijk theoretisch te onderzoeken zijn. Ook computersimulaties met eindige θ zijn op dit moment niet mogelijk, maar de effecten kunnen wel in effectieve theorieën en modellen onderzocht worden. Vooral chirale storingstheorie is in de literatuur veel gebruikt. Helaas kan chirale storingstheorie alleen bij hele lage energieën gebruikt worden. In dit proefschrift worden daarom modelberekeningen gebruikt, met name het Nambu–Jona-Lasinio-model (NJL-model). In zulke modellen worden de effecten van instantonen nagebootst door een extra interactie, de 't Hooft determinantinteractie.

Materie onder extreme omstandigheden

Zoals hierboven al besproken komen quarks in normale materie altijd per twee of drie voor. Dit verandert echter bij extreem hoge temperaturen en dichtheden. De protonen en neutronen beginnen dan als het ware te overlappen. In die situatie kunnen de quarks relatief vrij bewegen. Daarom wordt deze materie quarkmaterie genoemd.

Vlak na de oerknal waren de temperatuur en de dichtheid van het universum zo hoog dat de quarks zich nog vrij konden bewegen en dus bestond het universum uit quarkmaterie. Na ongeveer 10 microsecondes vond er een faseovergang plaats naar de huidige toestand van materie, zonder vrije quarks. De situatie van de oerknal wordt experimenteel onderzocht door middel van botsingen van zware ionen. Bij deze experimenten wordt de oerknal als het ware gesimuleerd door zware ionen, zoals goud, koper en lood, te versnellen tot bijna de lichtsnelheid en dan op elkaar te laten botsen. Er zijn zeer sterke aanwijzingen dat in zulke botsingen quarkmaterie wordt geproduceerd. Dergelijke experimenten worden tegenwoordig uitgevoerd in de Relativistic Heavy Ion Collider (RHIC) in Brookhaven en in de toekomst in de Large Hadron Collider (LHC) van CERN in Genève. Ten slotte is in neutronensterren de dichtheid van de kern zo hoog dat er waarschijnlijk quarkmaterie voorkomt.

In het geval van botsingen van zware ionen en neutronensterren kunnen ook nog enorm sterke magneetvelden worden gecreëerd, zodat het ook van belang is te begrijpen hoe quarkmaterie zich gedraagt in reusachtig sterke magneetvelden.

[2] Het QCD-vacuüm is topologisch niet-triviaal. QCD heeft namelijk oneindig veel vacua, elk gekarakteriseerd door een windingsgetal. Instantonen zijn objecten die tunnelen tussen deze vacua. Het "echte" QCD-vacuüm is een superpositie van al deze windingsgetal-vacua en kan worden gekarakteriseerd met behulp van de hoek θ. Voor een meer gedetailleerde discussie zie paragraaf 1.1.

Overzicht en resultaten van dit proefschrift

Het proefschrift begint met een motivatie en een algemene inleiding op QCD, instantonen en de hoek θ. Daarna volgt een korte inleiding op chirale storingstheorie (χPT), de effectieve theorie voor QCD bij lage energieën. Ook wordt besproken hoe instantoneffecten kunnen worden meegenomen in χPT. Deze uitbreiding is in de literatuur veel gebruikt om te bestuderen wat er gebeurt bij eindige θ, zo kan gebruikmakend van χPT en experimentele resultaten afgeleid worden dat $\theta \approx 0$. Ten slotte wordt de mogelijkheid besproken dat in botsingen van zware ionen toestanden worden gecreëerd die CP-invariantie schenden. Zulke toestanden kunnen worden beschreven met een effectieve θ ongelijk aan 0 en zijn de aanleiding om de effecten van eindige θ te onderzoeken.

De introductie gaat verder in hoofdstuk 2, waarin de verschillende fases van de sterke kernkracht worden besproken. Allereerst worden een aantal algemene aspecten van fasediagrammen en de drie mogelijke typen faseovergangen besproken: eerste-orde, tweede-orde en gladde overgangen. Bij een eerste-orde-overgang komt warmte vrij of wordt er warmte geabsorbeerd tijdens de overgang, waardoor hij experimenteel relatief makkelijk waar te nemen is. Bovendien divergeren een aantal thermodynamische grootheden op het punt van de overgang. In het geval van een tweede-orde-overgang is er geen sprake van het absorberen of vrijkomen van warmte, maar nog steeds divergeren bepaalde thermodynamische grootheden. Bij gladde overgangen treden helemaal geen divergenties op, waardoor ze relatief moeilijk experimenteel te bepalen zijn.

Na deze korte inleiding op faseovergangen wordt het fasediagram van de sterke interactie als functie van temperatuur en baryon-chemische potentiaal (een maat voor de baryondichtheid) besproken. Bij hoge dichtheden en temperaturen is de fase een quark-gluonplasma, maar er zijn nog meer exotische fases mogelijk, zoals bijvoorbeeld kleursupergeleiding bij lage temperaturen en hoge baryon-chemische potentiaal.

In dit hoofdstuk worden ook de drie fysische systemen waarbij quarkmaterie een rol speelt geïntroduceerd: de oerknal, botsingen van zware ionen en de kern van neutronensterren. Vervolgens worden een aantal theoretische methodes besproken die men gebruikt om het fasediagram te bestuderen. Tot slot worden een aantal minder bekende fasediagrammen besproken, zoals het fasediagram als functie van de quarkmassa's en de isospinchemische potentiaal (een maat voor het verschil in up- en down-quarkdichtheid), waarbij ook weer nieuwe fases voorkomen. Sommige van deze diagrammen zijn alleen van belang voor theoretische studies, terwijl andere ook relevant zijn voor het begrip van de drie hierboven genoemde systemen. Een voorbeeld is het gedrag als functie van de isospinchemische potentiaal, waarbij de mogelijkheid van pioncondensatie ontstaat. In de rest van dit proefschrift worden waar mogelijk de resultaten met deze diagrammen vergeleken.

In hoofdstuk 3 wordt het model dat het meest in dit proefschrift gebruikt wordt geïntroduceerd, het NJL-model. Het NJL-model bevat enkel quarks. Dit proefschrift beperkt zich tot de twee quarksmaken met de kleinste massa, het up- en het down-quark. Effecten van de gluonen worden meegenomen door middel van effectieve vierpuntsinteracties. Dit geldt ook voor de effecten van instantonen, die leiden tot de hierboven genoemde 't Hooft determinantinteractie. De sterkte van deze interactie kan ruw geschat worden, maar is niet precies bekend. De fysische gevolgen hangen wel sterk van deze interactiesterkte af.

Na een korte bespreking van de historische ontwikkeling van het NJL-model wordt de vacuümstructuur van het model besproken. Deze structuur zorgt voor een grote effectieve massa van de quarks in vacuüm. Verder worden de gebonden toestanden van het model behandeld, die te interpreteren zijn als mesonen. Het hoofdstuk eindigt met een discussie van een aantal lage-energie relaties, die kunnen worden gebruikt om de parameters van het model vast te leggen.

Hoofdstuk 4 bevat een gedetailleerde studie over het spontaan schenden van CP-invariantie binnen het NJL-model op $\theta = \pi$. Dit hoofdstuk is te zien als een uitbreiding op hoofdstuk 2. Eerst wordt de volledige θ-afhankelijkheid van het vacuüm bekeken. In het bijzondere geval $\theta = \pi$ is spontane schending van CP-invariantie mogelijk, maar deze mogelijkheid is afhankelijk van de sterkte van de instantoninteractie. Uit de gepresenteerde analyse kan geconcludeerd worden dat als deze sterkte groter wordt dan een kritische waarde, het model CP-invariantie schendt. Verder blijkt dat de kritische sterkte afhangt van de waardes van de quarkmassa's. Ook blijken mesonen zich kwalitatief anders te gedragen als CP-schending optreedt. Dit levert een extra argument op waarmee aangetoond kan worden dat θ in de natuur gelijk is aan 0 en niet aan π.

Vervolgens wordt het fasediagram bestudeerd als functie van de quarkmassa's, waarbij de sterkte van de instantoninteractie constant wordt gehouden. Er wordt een gebied van quarkmassa's gevonden waarin spontane schending van CP-invariantie optreedt. In het onderzochte NJL-model wordt zowel een onder- als bovengrens gevonden. In tegenstelling tot twee-smaken-χPT, onderzocht door Tytgat (2000), waarin alleen een ondergrens is gevonden. De NJL-analyse toont aan dat bij hogere temperatuur het gebied met spontane CP-schending kleiner wordt, totdat het uiteindelijk helemaal verdwijnt. Dit betekent dat de metastabiele CP-schendende toestanden op hoge temperatuur, gesuggereerd door Kharzeev, Pisarski, and Tytgat (1998), misschien niet voorkomen in de natuur.

Behalve de massa-afhankelijkheid wordt ook de temperatuurafhankelijkheid en de afhankelijkheid van de baryon-chemische potentiaal van de spontane CP-schending onderzocht. In paragraaf 4.6 worden fasediagrammen gepresenteerd als functie van deze parameters op één as en de sterkte van de instantoninteractie op de andere. Het blijkt dat de spontane CP-schending verdwijnt in de vorm van een twee-orde-overgang als de temperatuur of baryon-chemische potentiaal groter worden dan een kritische waarde. Hieruit kan de conclusie getrokken worden dat de spontane CP-schending een laag-energetisch verschijnsel is.

Het hoofdstuk wordt afgesloten met het bestuderen van het fasediagram als functie van de isospin-chemische potentiaal en de sterkte van de instantoninteractie. In dit diagram blijkt een nieuwe fase voor te komen met $a_0^{\pm}$-condensatie.

Zoals hierboven al gezegd, is de CP-herstellende faseovergang in het NJL-model tweede-orde. Dit in tegenstelling tot de resultaten van Mizher and Fraga (2009), die het vergelijkbare lineaire sigma-model gekoppeld aan quarks (LSMq) hebben onderzocht. Zij hebben een eerste-orde-faseovergang gevonden. Hoofdstuk 5 gaat over de overeenkomsten en de verschillen van deze twee modellen. Gebruikmakend van de methode van Eguchi (1976) wordt aangetoond dat als het NJL-model "gebosoniseerd" wordt, een lineair sigma-model wordt verkregen.

Het belangrijkste verschil tussen de twee modellen is de behandeling van quarks. In

het NJL-model worden quarks altijd meegenomen, het is immers een quarkmodel. In het LSMq-model worden de quarks alleen meegenomen bij eindige temperatuur. De analyse van hoofdstuk 5 laat zien dat de quarks voor een logaritmische term zorgen op $T = 0$, die niet meegenomen wordt in het LSMq-model. Een vergelijkbare logaritmische term komt van de temperatuursafhankelijkheid van de quarks. Deze valt weg tegen de term op $T = 0$. Het blijkt dat het precies deze term is die het verschil tussen de twee modellen bepaalt. Als het NJL-model wordt gezien als onderliggende theorie voor het lineaire sigma-model gekoppeld aan quarks, is er geen goede reden om deze term te verwaarlozen.

In het afsluitende hoofdstuk 6 wordt de gecombineerde invloed van magneetvelden en de instantoninteractie bij $\theta = 0$ onderzocht. Deze studie is relevant voor het beschrijven van botsingen van zware ionen en kernen van neutronensterren, waar zeer grote magneetvelden kunnen optreden.

Sterke magneetvelden kunnen een grote invloed hebben op de structuur van quarkmaterie. Als namelijk een geladen deeltje, zoals een quark, zich in een heel sterk magneetveld bevindt, raakt de impuls loodrecht op het magneetveld gequantiseerd. Dit wordt Landau-quantisatie genoemd. De twee quarks hebben echter verschillende ladingen, waardoor hun gedrag in een magneetveld verschilt. Uit de gepresenteerde resultaten blijkt dat hierdoor op hoge baryon-chemische potentiaal de mogelijkheid ontstaat dat de quarks sterk verschillende effectieve massa's hebben. Dit verschil beïnvloedt de massa's en vervaltijden van mesonen.

Het effect van de instantoninteractie is tegengesteld aan het effect van het magneetveld. De instantoninteractie zorgt ervoor dat de effectieve massa's aan elkaar gekoppeld raken, wat leidt tot gelijk gedrag voor de quarks. Bij een kleine waarde voor de sterkte van deze interactie is er nog steeds een fase aanwezig waarbij de massa's flink verschillen, die verdwijnt bij verhoging van de sterkte. Bovendien blijkt dat binnen een gebied van baryon-chemische potentialen en magneetvelden metastabiele fases mogelijk zijn. Deze fases verschillen in het aantal gevulde Landau niveaus en de mate van symmetriebreking. Aangezien de energieën van deze toestanden bijna gelijk zijn aan de energie van de grondtoestand, kunnen ze niet verwaarloosd worden en zijn dus fysisch relevant.

Ten slotte wordt onderzocht hoe een sterk magneetveld de faseovergang op hoge temperatuur beïnvloedt. Dit is relevant in de studie van botsingen van zware ionen. In LSMq wordt een zwakke eerste-orde-overgang gevonden (Fraga and Mizher, 2008). In het NJL-model wordt een gladde overgang gevonden. De oorzaak van dit verschil is waarschijnlijk dezelfde als die besproken is in hoofdstuk 5.

De studies gepresenteerd in dit proefschrift maken duidelijk dat instantonen een grote rol kunnen spelen bij verschijnselen van de sterke interactie bij lage energieën, waarbij ze de eigenschappen van quarkmaterie kwalitatief kunnen beïnvloeden. Om deze redenen is het nuttig om meer gedetailleerde studies dan die in dit werk beschreven staan uit te voeren. Allereerst zou het nuttig zijn om een methode te vinden om de instantoninteractiesterkte te bepalen. Verder is in dit werk alleen het geval van twee quarksmaken onderzocht, het zou interessant zijn om te kijken wat er gebeurt als een derde quark, het strange-quark, wordt toegevoegd. In de limiet dat alle quarks massaloos zijn, is er namelijk een kwalitatief verschil tussen twee of drie quarksmaken (Pisarski and Wilczek, 1984); er is sprake van een tweede- respectievelijk eerste-orde-overgang. Het zou inte-

ressant zijn om te onderzoeken of dit ook geldt voor de faseovergang die CP-invariantie herstelt. Ook zouden meer fases bestudeerd kunnen worden, zoals kleursupergeleidende fases en er zou gekeken kunnen worden in hoeverre onze resultaten van de gebruikte benaderingen afhangen. Een andere richting van vervolgonderzoek is uitzoeken of de resultaten van dit proefschrift waarneembare gevolgen zouden kunnen hebben voor de structuur van neutronensterren.

Dankwoord

Hoewel alleen mijn naam op dit proefschrift staat, heb ik het werk niet alleen gedaan. Allereerst wil ik mijn copromotor Daniël Boer bedanken. Ik heb prettig met je samengewerkt en ik heb je begeleiding als erg inspirerend ervaren. Je enthousiasme en je altijd aanwezige vertrouwen in een goede afloop waren erg motiverend.

Mijn promotor Piet Mulders wil ik bedanken voor de prettige werksfeer binnen de vakgroep, voor de ondersteuning en voor de goede samenwerking bij het college quantummechanica. Iemand anders die zorgde voor de fijne werksfeer is Ben Bakker. De koffie/thee-pauzes waren altijd erg gezellig. We hebben de afgelopen viereneenhalf jaar vele interessante discussies gehad. Ook Harmen Warringa wil ik graag bedanken voor de leuke discussies in de afgelopen jaren en voor het beschikbaar stellen van het computerprogramma dat aan de basis van hoofdstuk 4 ligt.

I would like to thank all the members of the reading committee, consisting of Jens Andersen, Ben Bakker, Eduardo Fraga, Rob Timmermans and Harmen Warringa for taking the time and effort to read the manuscript. All your suggestions were very welcome. I would like to thank Eduardo Fraga for the useful comments on our last two papers and for the nice discussions. Furthermore, I would like to thank Wilco den Dunnen, Thomas van Dijk, Ana Mizher and Jordy de Vries for their suggestions on my thesis

Thomas, jou wil ik verder bedanken voor de fijne studie- en promotietijd. Gesprekken met jou heb ik altijd als erg nuttig, gezellig en inspirerend ervaren. Ook de pauzes waren altijd leuk, ik zal je gaan missen!

Ana, I would like to thank you for our very nice year together. It was great working with you.

Verder wil ik Mathieu Blom, Felina Brethouwer, Wilco den Dunnen en Thijs Stegeman bedanken voor de gezelligheid op en buiten de VU. De invloed van Raymond van het Groenewoud en André Hazes op dit proefschrift is niet te verwaarlozen. Erik, jij mag zeker niet ontbreken in dit rijtje, hoewel jouw muzieksmaak wel wat te wensen over laat. Misschien dat Ashley daar nu wat verbetering in aanbrengt. Dankzij jou weet ik nu wel de TT te waarderen.

Ik heb al een aantal collega's bedankt, maar er zijn nog veel meer mensen die zorgden voor een goede werksfeer: Klaas Allaard, Federica Bazzocchi, Elmar Biernat, Chase Broederz, Cedran Bomhof, Kirk Green, Marja Herronen, Fred MacKintosh, Christiaan Mantz, Paul McCullough, Cristian Pisano, Ted Rogers, Andre Utermann en Taco Visser.

Afgezien van de Amsterdamse groep, ben ik ook nog een beetje geïntegreerd geraakt

in de groep op het KVI. Jordy, Lotje en Rob wil ik graag bedanken voor hun immer vriendelijke Groningse gastvrijheid en natuurlijk niet te vergeten voor het klaverjassen. Lotje, wij waren toch echt onverslaanbaar.

Mijn voormalige huisgenoten, Ashley, Guit-Jan, Jennie en Lydia, wil ik graag bedanken voor de fijne tijd samen. Ik mis onze gesprekken 's avonds nog steeds.

Graag wil ik ook mijn andere vrienden bedanken, die altijd voor de broodnodige ontspanning zorgen. In het bijzonder Kirsten, ik vond onze vakanties heel erg leuk. En Petra, jou wil ik graag bedanken voor het schaatsen en de gezelligheid, dankzij jou ben ik toch nog een beetje sportief.

Mijn ouders wil ik graag bedanken voor hun onvoorwaardelijke steun. Roel, jou wil ik bedanken voor je altijd aanwezige vrolijkheid en enthousiasme, op naar jouw promotie!

Lieve Irene, ook jou wil ik bedanken voor je steun en voor je relativeringsvermogen, maar eigenlijk vooral voor hoe fijn we het samen hebben.

Amsterdam, 13 april 2010

Bibliography

Abelev, B. I. et al. *Azimuthal charged-particle correlations and possible local strong parity violation*. Phys. Rev. Lett. **103** (2009a) 251601.

Abelev, B. I. et al. *Observation of charge-dependent azimuthal correlations and possible local strong parity violation in heavy ion collisions*. arXiv:0909.1717 [nucl-ex].

Abuki, H., Anglani, R., Gatto, R., Nardulli, G., and Ruggieri, M. *Chiral crossover, deconfinement and quarkyonic matter within a Nambu–Jona-Lasinio model with the Polyakov loop*. Phys. Rev. D **78** (2008) 034034.

Akemann, G., Lenaghan, J. T., and Splittorff, K. *Dashen's phenomenon in gauge theories with spontaneously broken chiral symmetries*. Phys. Rev. D **65** (2002) 085015.

Alford, M. G., Rajagopal, K., and Wilczek, F. *QCD at finite baryon density: Nucleon droplets and color superconductivity*. Phys. Lett. B **422** (1998) 247.

Alford, M. G., Schmitt, A., Rajagopal, K., and Schafer, T. *Color superconductivity in dense quark matter*. Rev. Mod. Phys. **80** (2008) 1455.

Allton, C. R., Döring, M., Ejiri, S., Hands, S. J., Kaczmarek, O., Karsch, F., Laermann, E., and Redlich, K. *Thermodynamics of two flavor QCD to sixth order in quark chemical potential*. Phys. Rev. D **71** (2005) 054508.

Andersen, J. O., Braaten, E., Petitgirard, E., and Strickland, M. *HTL perturbation theory to two loops*. Phys. Rev. D **66** (2002) 085016.

Aoki, Y., Borsanyi, S., Durr, S., Fodor, Z., Katz, S. D., Krieg, S., and Szabo, K. *The QCD transition temperature: Results with physical masses in the continuum limit II*. JHEP **06** (2009) 088.

Aoki, Y., Fodor, Z., Katz, S. D., and Szabo, K. K. *The QCD transition temperature: Results with physical masses in the continuum limit*. Phys. Lett. B **643** (2006) 46.

Asorey, M. *Vacuum energy and θ-vacuum*. Nucl. Phys. Proc. Suppl. **127** (2004) 15.

Ayala, A., Bashir, A., Raya, A., and Rojas, E. *Dynamical mass generation in strong coupling quantum electrodynamics with weak magnetic fields*. Phys. Rev. D **73** (2006) 105009.

Bailin, D. and Love, A. *Superfluidity and superconductivity in relativistic fermion systems*. Phys. Rept. **107** (1984) 325.

Baker, C. A., Doyle, D. D., Geltenbort, P., Green, K., van der Grinten, M. G. D., Harris, P. G., Iaydjiev, P., Ivanov, S. N., May, D. J. R., Pendlebury, J. M., Richardson, J. D., Shiers, D., and Smith, K. F. *An improved experimental limit on the electric dipole moment of the neutron*. Phys. Rev. Lett. **97** (2006) 131801.

Baluni, V. *CP-nonconserving effects in quantum chromodynamics*. Phys. Rev. D **19** (1979) 2227.

Barducci, A., Casalbuoni, R., Pettini, G., and Ravagli, L. *A calculation of the QCD phase diagram at finite temperature, and baryon and isospin chemical potentials*. Phys. Rev. D **69** (2004) 096004.

Barducci, A., Casalbuoni, R., Pettini, G., and Ravagli, L. *Pion and kaon condensation in a 3-flavor NJL model*. Phys. Rev. D **71** (2005) 016011.

Barducci, A., Pettini, G., Ravagli, L., and Casalbuoni, R. *Ladder-QCD at finite isospin chemical potential*. Phys. Lett. B **564** (2003) 217.

Barrois, B. C. *Superconducting quark matter*. Nucl. Phys. B **129** (1977) 390.

Bég, M. A. B. *Question of spontaneous genesis of CP violation*. Phys. Rev. D **4** (1971) 3810.

Belavin, A. A., Polyakov, A. M., Shvarts, A. S., and Tyupkin, Y. S. *Pseudoparticle solutions of the Yang-Mills equations*. Phys. Lett. B **59** (1975) 85.

Bernard, V., Jaffe, R. L., and Meissner, U. G. *Flavor mixing via dynamical chiral symmetry breaking*. Phys. Lett. B **198** (1987) 92.

Bernardini, C. C. and Bonolis, L., editors. *Enrico Fermi: his work and legacy*. Springer, Società Italiana di Fisica, Bologna, Italy, 2004.

Boer, D. and Boomsma, J. K. *Spontaneous CP violation in the strong interaction at $\theta = \pi$*. Phys. Rev. D **78** (2008) 054027.

Boomsma, J. K. and Boer, D. *The high temperature CP-restoring phase transition at $\theta = \pi$*. Phys. Rev. D **80** (2009) 034019.

Boomsma, J. K. and Boer, D. *Influence of strong magnetic fields and instantons on the phase structure of the two-flavor Nambu–Jona-Lasinio model*. Phys. Rev. D **81** (2010) 074005.

Braun-Munzinger, P. and Stachel, J. *The quest for the quark-gluon plasma*. Nature **448** (2007) 302.

Braun-Munzinger, P. and Wambach, J. *Colloqium: The phase diagram of strongly-interacting matter*. Rev. Mod. Phys. **81** (2009) 1031.

Brown, F. R., Butler, F. P., Chen, H., Christ, N. H., Dong, Z., Schaffer, W., Unger, L. I., and Vaccarino, A. *On the existence of a phase transition for QCD with three light quarks*. Phys. Rev. Lett. **65** (1990) 2491.

Buballa, M. *NJL model analysis of quark matter at large density*. Phys. Rept. **407** (2005) 205.

Buckley, K., Fugleberg, T., and Zhitnitsky, A. *Can θ vacua be created in heavy ion collisions?* Phys. Rev. Lett. **84** (2000) 4814.

Cabibbo, N. and Parisi, G. *Exponential hadronic spectrum and quark liberation*. Phys. Lett. B **59** (1975) 67.

Cheng, M., Christ, N. H., Datta, S., van der Heide, J., Jung, C., Karsch, F., Kaczmarek, O., Laermann, E., Mawhinney, R. D., Miao, C., Petreczky, P., Petrov, K., Schmidt, C., Soeldner, W., and Umeda, T. *QCD equation of state with almost physical quark masses*. Phys. Rev. D **77** (2008) 014511.

Cheng, M., Christ, N. H., Datta, S., van der Heide, J., Jung, C., Karsch, F., Kaczmarek, O., Laermann, E., Mawhinney, R. D., Miao, C., Petreczky, P., Petrov, K., Schmidt, C., and Umeda, T. *The transition temperature in QCD*. Phys. Rev. D **74** (2006) 054507.

Cheng, T.-P. and Li, L.-F. *Gauge theory of elementary particle physics*. University Press, Oxford, UK, 1984.

Christenson, J. H., Cronin, J. W., Fitch, V. L., and Turlay, R. *Evidence for the 2π decay of the K_2^0 meson*. Phys. Rev. Lett. **13** (1964) 138.

Cohen, T. D. *Spontaneous parity violation in QCD at finite temperature: On the inapplicability of the Vafa-Witten theorem*. Phys. Rev. D **64** (2001) 047704.

Collins, J. C. and Perry, M. J. *Superdense matter: Neutrons or asymptotically free quarks?* Phys. Rev. Lett. **34** (1975) 1353.

Creutz, M. *Monte Carlo study of quantized SU(2) gauge theory*. Phys. Rev. D **21** (1980) 2308.

Creutz, M. *Spontaneous violation of CP symmetry in the strong interactions*. Phys. Rev. Lett. **92** (2004) 201601.

Crewther, R. J., di Vecchia, P., Veneziano, G., and Witten, E. *Chiral estimate of the electric dipole moment of the neutron in Quantum Chromodynamics*. Phys. Lett. B **88** (1979) 123.

Dashen, R. *Some features of chiral symmetry breaking*. Phys. Rev. D **3** (1971) 1879.

Detmold, W., Orginos, K., Savage, M. J., and Walker-Loud, A. *Kaon condensation with lattice QCD*. Phys. Rev. D **78** (2008) 054514.

Dine, M. and Kusenko, A. *The origin of the matter-antimatter asymmetry*. Rev. Mod. Phys. **76** (2004) 1.

Dmitrasinovic, V. *$U_A(1)$ breaking and scalar mesons in the Nambu-Jona- Lasinio model*. Phys. Rev. C **53** (1996) 1383.

Dosch, H. G. and Narison, S. *Direct extraction of the chiral quark condensate and bounds on the light quark masses*. Phys. Lett. B **417** (1998) 173.

Duncan, R. C. and Thompson, C. *Formation of very strongly magnetized neutron stars - implications for gamma-ray bursts*. Astrophys. J. **392** (1992) L9.

Ebert, D. and Klimenko, K. G. *Quark droplets stability induced by external magnetic field*. Nucl. Phys. A **728** (2003) 203.

Ebert, D., Klimenko, K. G., Vdovichenko, M. A., and Vshivtsev, A. S. *Magnetic oscillations in dense cold quark matter with four-fermion interactions*. Phys. Rev. D **61** (2000) 025005.

Ebert, D. and Reinhardt, H. *Effective chiral hadron Lagrangian with anomalies and skyrme terms from Quark Flavor Dynamics*. Nucl. Phys. B **271** (1986) 188.

Ebert, D. and Volkov, M. K. *Composite meson model with vector dominance based on U(2) invariant four quark interactions*. Z. Phys. C **16** (1983) 205.

Eguchi, T. *A new approach to collective phenomena in superconductivity models*. Phys. Rev. D **14** (1976) 2755.

Einhorn, M. B. and Wudka, J. *On the Vafa-Witten theorem on spontaneous breaking of parity*. Phys. Rev. D **67** (2003) 045004.

Elizalde, E., Ferrer, E. J., and de la Incera, V. *Beyond-constant-mass-approximation magnetic catalysis in the gauge Higgs-Yukawa model*. Phys. Rev. D **68** (2003) 096004.

Engels, J., Karsch, F., Satz, H., and Montvay, I. *High temperature SU(2) gluon matter on the lattice*. Phys. Lett. B **101** (1981) 89.

Erlich, J., Katz, E., Son, D. T., and Stephanov, M. A. *QCD and a holographic model of hadrons*. Phys. Rev. Lett. **95** (2005) 261602.

Ferrer, E. J. and de la Incera, V. *Ward-Takahashi identity with external field in ladder QED*. Phys. Rev. D **58** (1998) 065008.

Ferrer, E. J. and de la Incera, V. *Magnetic catalysis in the presence of scalar fields*. Phys. Lett. B **481** (2000) 287.

Ferrer, E. J. and de la Incera, V. *Magnetic fields boosted by gluon vortices in color superconductivity*. Phys. Rev. Lett. **97** (2006) 122301.

Ferrer, E. J. and de la Incera, V. *Chromomagnetic instability and induced magnetic field in neutral two-flavor color superconductivity*. Phys. Rev. D **76** (2007a) 114012.

Ferrer, E. J. and de la Incera, V. *Magnetic phases in three-flavor color superconductivity*. Phys. Rev. D **76** (2007b) 045011.

Ferrer, E. J. and de la Incera, V. *Dynamically induced Zeeman effect in massless QED*. Phys. Rev. Lett. **102** (2009) 050402.

Ferrer, E. J. and de la Incera, V. *Dynamically generated anomalous magnetic moment in massless QED*. Nucl. Phys. B **824** (2010) 217.

Ferrer, E. J., de la Incera, V., and Manuel, C. *Magnetic color flavor locking phase in high density QCD*. Phys. Rev. Lett. **95** (2005) 152002.

Ferrer, E. J., de la Incera, V., and Manuel, C. *Color-superconducting gap in the presence of a magnetic field*. Nucl. Phys. B **747** (2006) 88.

de Forcrand, P. and Philipsen, O. *The chiral critical line of $N_f = 2 + 1$ QCD at zero and non- zero baryon density*. JHEP **01** (2007) 077.

de Forcrand, P., Stephanov, M. A., and Wenger, U. *On the phase diagram of QCD at finite isospin density*. PoS **LAT2007** (2007) 237.

Fraga, E. S. and Mizher, A. J. *Chiral transition in a strong magnetic background*. Phys. Rev. D **78** (2008) 025016.

Frank, M., Buballa, M., and Oertel, M. *Flavor-mixing effects on the QCD phase diagram at non-vanishing isospin chemical potential: one or two phase transitions?* Phys. Lett. B **562** (2003) 221.

Frautschi, S. C. *Asymptotic freedom and color superconductivity in dense quark matter*. Presented at Workshop on Hadronic Matter at Extreme Energy Density, Erice, Italy, Oct 13-21, 1978.

Fujihara, T., Inagaki, T., and Kimura, D. *Influence of QED corrections on the orientation of chiral symmetry breaking in the NJL Model*. Prog. Theor. Phys. **117** (2007) 139.

Fujikawa, K. *Path integral measure for gauge invariant fermion theories*. Phys. Rev. Lett. **42** (1979) 1195.

Fukushima, K. *Chiral effective model with the Polyakov loop*. Phys. Lett. B **591** (2004) 277.

Fukushima, K. *Phase diagrams in the three-flavor Nambu–Jona-Lasinio model with the Polyakov loop*. Phys. Rev. D **77** (2008) 114028.

Fukushima, K. and Warringa, H. J. *Color superconducting matter in a magnetic field*. Phys. Rev. Lett. **100** (2008) 032007.

Gasser, J. and Leutwyler, H. *Light quarks at low temperatures*. Phys. Lett. B **184** (1987a) 83.

Gasser, J. and Leutwyler, H. *Thermodynamics of chiral symmetry*. Phys. Lett. B **188** (1987b) 477.

Gell-Mann, M. and Lévy, M. *The axial vector current in beta decay*. Nuovo Cim. **16** (1960) 705.

Gell-Mann, M., Oakes, R. J., and Renner, B. *Behavior of current divergences under SU_3 x SU_3*. Phys. Rev. **175** (1968) 2195.

Gerber, P. and Leutwyler, H. *Hadrons below the chiral phase transition*. Nucl. Phys. B **321** (1989) 387.

Giusti, L., Rapuano, F., Talevi, M., and Vladikas, A. *The QCD chiral condensate from the lattice*. Nucl. Phys. B **538** (1999) 249.

Goldberger, M. L. and Treiman, S. B. *Decay of the π meson*. Phys. Rev. **110** (1958) 1178.

Gross, D. J., Pisarski, R. D., and Yaffe, L. G. *QCD and instantons at finite temperature*. Rev. Mod. Phys. **53** (1981) 43.

Gubser, S. S., Klebanov, I. R., and Tseytlin, A. A. *Coupling constant dependence in the thermodynamics of N = 4 supersymmetric Yang-Mills theory*. Nucl. Phys. B **534** (1998) 202.

Gusynin, V. P., Miransky, V. A., and Shovkovy, I. A. *Catalysis of dynamical flavor symmetry breaking by a magnetic field in (2+1)-dimensions*. Phys. Rev. Lett. **73** (1994) 3499.

Gusynin, V. P., Miransky, V. A., and Shovkovy, I. A. *Dimensional reduction and dynamical chiral symmetry breaking by a magnetic field in (3+1)-dimensions*. Phys. Lett. B **349** (1995a) 477.

Gusynin, V. P., Miransky, V. A., and Shovkovy, I. A. *Dynamical chiral symmetry breaking by a magnetic field in QED*. Phys. Rev. D **52** (1995b) 4747.

Gusynin, V. P., Miransky, V. A., and Shovkovy, I. A. *Dynamical flavor symmetry breaking by a magnetic field in (2+1)-dimensions*. Phys. Rev. D **52** (1995c) 4718.

Gusynin, V. P., Miransky, V. A., and Shovkovy, I. A. *Dimensional reduction and catalysis of dynamical symmetry breaking by a magnetic field*. Nucl. Phys. B **462** (1996) 249.

Gyulassy, M. and McLerran, L. *New forms of QCD matter discovered at RHIC*. Nucl. Phys. A **750** (2005) 30.

Hatsuda, T. and Kunihiro, T. *Possible critical phenomena associated with the chiral symmetry breaking*. Phys. Lett. B **145** (1984) 7.

Hatsuda, T. and Kunihiro, T. *Effects of explicit $SU_f(3)$ breaking on the quark condensates*. Phys. Lett. B **198** (1987) 126.

He, L. and Zhuang, P. *Phase structure of Nambu–Jona-Lasinio model at finite isospin density*. Phys. Lett. B **615** (2005) 93.

't Hooft, G. *Computation of the quantum effects due to a four-dimensional pseudoparticle*. Phys. Rev. D **14** (1976) 3423.

't Hooft, G. *How instantons solve the U(1) problem*. Phys. Rep. **142** (1986) 357.

Inagaki, T., Kimura, D., and Murata, T. *Four-fermion interaction model in a constant magnetic field at finite temperature and chemical potential*. Prog. Theor. Phys. **111** (2004) 371.

Kapusta, J. I. and Gale, C. *Finite-temperature field theory: Principles and applications*. University Press, Cambridge, UK, 2006.

Karsch, F. *Lattice QCD at high temperature and density*. Lect. Notes Phys. **583** (2002) 209.

Karsch, F., Laermann, E., and Peikert, A. *Quark mass and flavor dependence of the QCD phase transition*. Nucl. Phys. B **605** (2001) 579.

Kawarabayashi, K. and Ohta, N. *On the partial conservation of the U(1) current*. Prog. Theor. Phys. **66** (1981) 1789.

Kharzeev, D. *Parity violation in hot QCD: Why it can happen, and how to look for it*. Phys. Lett. B **633** (2006) 260.

Kharzeev, D. and Pisarski, R. D. *Pionic measures of parity and CP violation in high energy nuclear collisions*. Phys. Rev. D **61** (2000) 111901.

Kharzeev, D., Pisarski, R. D., and Tytgat, M. H. G. *Possibility of spontaneous parity violation in hot QCD*. Phys. Rev. Lett. **81** (1998) 512.

Kharzeev, D. and Zhitnitsky, A. *Charge separation induced by P-odd bubbles in QCD matter*. Nucl. Phys. A **797** (2007) 67.

Kharzeev, D. E., McLerran, L. D., and Warringa, H. J. *The effects of topological charge change in heavy ion collisions: 'Event by event P and CP violation'*. Nucl. Phys. A **803** (2008) 227.

Klein, B., Toublan, D., and Verbaarschot, J. J. M. *The QCD phase diagram at nonzero temperature, baryon and isospin chemical potentials in random matrix theory*. Phys. Rev. D **68** (2003) 014009.

Kleinert, H. *On the hadronization of quark theories*. Lectures presented at Erice Summer School of Subnuclear Physics, Erice, Italy, Jul 23 - Aug 8, 1976.

Klevansky, S. *The Nambu–Jona-Lasinio model of quantum chromodynamics*. Rev. Mod. Phys. **64** (1992) 649.

Klimenko, K. G. *Three-dimensional Gross-Neveu model in an external magnetic field*. Theor. Math. Phys. **89** (1991) 1161.

Klimenko, K. G. *Three-dimensional Gross-Neveu model at nonzero temperature and in an external magnetic field*. Theor. Math. Phys. **90** (1992a) 1.

Klimenko, K. G. *Three-dimensional Gross-Neveu model at nonzero temperature and in an external magnetic field*. Z. Phys. C **54** (1992b) 323.

Klimenko, K. G. and Zhukovsky, V. C. *Does there arise a significant enhancement of the dynamical quark mass in a strong magnetic field?* Phys. Lett. B **665** (2008) 352.

Kobayashi, M. and Maskawa, T. *CP Violation in the renormalizable theory of weak interaction*. Prog. Theor. Phys. **49** (1973) 652.

Kogut, J. B. and Sinclair, D. K. *Lattice QCD at finite isospin density at zero and finite temperature*. Phys. Rev. D **66** (2002) 034505.

Kogut, J. B. and Sinclair, D. K. *The finite temperature transition for 2-flavor lattice QCD at finite isospin density*. Phys. Rev. D **70** (2004) 094501.

Kogut, J. B. and Stephanov, M. A. *The phases of quantum chromodynamics: From confinement to extreme environments*. Camb. Monogr. Part. Phys. Nucl. Phys. Cosmol. **21** (2004) 1.

Kuti, J., Polonyi, J., and Szlachanyi, K. *Monte Carlo study of SU(2) gauge theory at finite temperature*. Phys. Lett. B **98** (1981) 199.

Lai, D. and Shapiro, S. L. *Cold equation of state in a strong magnetic field - Effects of inverse β-decay*. Astrophys. J. **383** (1991) 745.

Landau, L. D. and Lifshitz, E. M. *Quantum Mechanics: Non-Relativistic Theory; 3rd ed.* Course Theor. Phys. Butterworth, Oxford, 1977. Trans. from Russian.

Lattimer, J. M. and Prakash, M. *Neutron star observations: Prognosis for equation of state constraints*. Phys. Rept. **442** (2007) 109.

Lee, D. S., Leung, C. N., and Ng, Y. J. *Chiral symmetry breaking in a uniform external magnetic field*. Phys. Rev. D **55** (1997) 6504.

Lee, D. S., Leung, C. N., and Ng, Y. J. *Chiral symmetry breaking in a uniform external magnetic field. II: Symmetry restoration at high temperatures and chemical potentials*. Phys. Rev. D **57** (1998) 5224.

Lee, T. D. *A theory of spontaneous T violation*. Phys. Rev. D **8** (1973) 1226.

Leung, C. N., Ng, Y. J., and Ackley, A. W. *Schwinger-Dyson equation approach to chiral symmetry breaking in an external magnetic field*. Phys. Rev. D **54** (1996) 4181.

Maldacena, J. M. *The large N limit of superconformal field theories and supergravity*. Adv. Theor. Math. Phys. **2** (1998) 231.

Manchester, R. N., Hobbs, G. B., Teoh, A., , and Hobbs, M. *The Australia Telescope National Facility Pulsar Catalogue*. The Astronomical Journal **129** (2005) 1993.

McLerran, L. and Pisarski, R. D. *Phases of cold, dense quarks at large N_c*. Nucl. Phys. A **796** (2007) 83.

McLerran, L., Redlich, K., and Sasaki, C. *Quarkyonic matter and chiral symmetry breaking*. Nucl. Phys. A **824** (2009) 86.

McLerran, L. D. *The quark - gluon plasma and the little bang*. Invited talk given at Physics in Collisions: High Energy ee/ep/pp Interactions, Blacksburg, Va., May 28-31, 1981.

McLerran, L. D. and Svetitsky, B. *A Monte Carlo study of SU(2) Yang-Mills theory at finite temperature*. Phys. Lett. B **98** (1981a) 195.

McLerran, L. D. and Svetitsky, B. *Quark liberation at high temperature: A Monte Carlo study of SU(2) gauge theory*. Phys. Rev. D **24** (1981b) 450.

Menezes, D. P., Benghi Pinto, M., Avancini, S. S., Perez Martinez, A., and Providencia, C. *Quark matter under strong magnetic fields in the Nambu–Jona-Lasinio model*. Phys. Rev. C **79** (2009a) 035807.

Menezes, D. P., Benghi Pinto, M., Avancini, S. S., and Providencia, C. *Quark matter under strong magnetic fields in the su(3) Nambu–Jona-Lasinio model*. Phys. Rev. C **80** (2009b) 065805.

Metlitski, M. A. and Zhitnitsky, A. R. *θ-parameter in 2 color QCD at finite baryon and isospin density*. Nucl. Phys. B **731** (2005) 309.

Metlitski, M. A. and Zhitnitsky, A. R. *θ dependence of QCD at finite isospin density*. Phys. Lett. B **633** (2006) 721.

Meyer-Ortmanns, H. and Reisz, T. *Principles of phase structures in particle physics*, volume 77 of *World Scientific Lecture Notes in Physics*. World Scientific, Hackensack, USA, 2007.

Mizher, A. J. and Fraga, E. S. *CP violation and chiral symmetry restoration in the hot linear sigma model in a strong magnetic background*. Nucl. Phys. A **831** (2009) 91 .

Morley, P. D. and Schmidt, I. A. *Strong P, CP, T violations in heavy-ion collisions*. Z. Phys. C **26** (1985) 627.

Muta, T. *Foundations of quantum chromodynamics. Second edition*. World Sci. Lect. Notes Phys. **57** (1998) 1.

Nambu, Y. and Jona-Lasinio, G. *Dynamical model of elementary particles based on an analogy with superconductivity I*. Phys Rev. **122** (1961a) 345.

Nambu, Y. and Jona-Lasinio, G. *Dynamical model of elementary particles based on an analogy with superconductivity II*. Phys. Rev. **124** (1961b) 246.

Nishida, Y. *Phase structures of strong coupling lattice QCD with finite baryon and isospin density*. Phys. Rev. D **69** (2004) 094501.

Noronha, J. L. and Shovkovy, I. A. *Color-flavor locked superconductor in a magnetic field*. Phys. Rev. D **76** (2007) 105030.

Nuyts, J. *Is CP-invariance violation caused by an SU(3) singlet?* Phys. Rev. Lett. **26** (1971) 1604.

Olesen, P. *On the possible creation of a background W condensate in the electroweak phase transition*. Phys. Lett. B **281** (1992) 300.

Oppenheimer, J. R. and Volkoff, G. M. *On massive neutron cores*. Phys. Rev. **55** (1939) 374.

Osipov, A. A., Hiller, B., Blin, A. H., and da Providencia, J. *Dynamical chiral symmetry breaking by a magnetic field and multi-quark interactions*. Phys. Lett. B **650** (2007) 262.

Paech, K., Stoecker, H., and Dumitru, A. *Hydrodynamics near a chiral critical point*. Phys. Rev. C **68** (2003) 044907.

Panero, M. *Thermodynamics of the QCD plasma and the large-N limit*. Phys. Rev. Lett. **103** (2009) 232001.

Peccei, R. D. and Quinn, H. R. *Constraints imposed by CP conservation in the presence of instantons*. Phys. Rev. D **16** (1977a) 1791.

Peccei, R. D. and Quinn, H. R. *CP conservation in the presence of instantons*. Phys. Rev. Lett. **38** (1977b) 1440.

Peikert, A., Karsch, F., and Laermann, E. *The flavour and quark mass dependence of thermodynamic quantities in lattice QCD*. Nucl. Phys. Proc. Suppl. **83** (2000) 390.

Peskin, M. and Schroeder, D. *An Introduction to quantum field theory*. Addison-Wesley, Reading, USA, 1995.

Pisarski, R. D. *Anomalous mesonic interactions near a chiral phase transition*. Phys. Rev. Lett. **76** (1996) 3084.

Pisarski, R. D. and Wilczek, F. *Remarks on the chiral phase transition in chromodynamics*. Phys. Rev. D **29** (1984) 338.

Rapp, R., Schafer, T., Shuryak, E. V., and Velkovsky, M. *Diquark Bose condensates in high density matter and instantons*. Phys. Rev. Lett. **81** (1998) 53.

Ritus, V. I. *Radiative corrections in quantum electrodynamics with intense field and their analytical properties*. Ann. Phys. **69** (1972) 555.

Ritus, V. I. *Eigenfunction method and mass operator in the quantum electrodynamics of a constant field*. Sov. Phys. JETP **48** (1978) 788.

Sakharov, A. D. *Violation of CP invariance, C asymmetry, and baryon asymmetry of the Universe*. Pisma Zh. Eksp. Teor. Fiz. **5** (1967) 32.

Sano, T., Fujii, H., and Ohtani, M. *$U_A(1)$ breaking and phase transition in chiral random matrix model*. Phys. Rev. **D80** (2009) 034007. 0904.1860.

Scavenius, O., Mocsy, A., Mishustin, I. N., and Rischke, D. H. *Chiral phase transition within effective models with constituent quarks*. Phys. Rev. C **64** (2001) 045202.

Schaefer, B.-J. and Wambach, J. *Susceptibilities near the QCD (tri)critical point*. Phys. Rev. D **75** (2007) 085015.

Schierholz, G. *θ vacua, confinement and the continuum limit*. Nucl. Phys. Proc. Suppl. **42** (1995) 270.

Selyuzhenkov, I. V. *Global polarization and parity violation study in Au + Au collisions*. Rom. Rep. Phys. **58** (2006) 049.

Selyuzhenkov, I. V. *Azimuthal charged particle correlations as a probe for local strong parity violation in heavy-ion collisions*. arXiv:0910.0464 [nucl-ex].

Shuryak, E. V. *Theory of hadronic plasma*. Sov. Phys. JETP **47** (1978) 212.

Shuryak, E. V. *The QCD vacuum, hadrons and the superdense matter*. World Sci. Lect. Notes Phys. **71** (2004) 1.

Skokov, V., Illarionov, A. Y., and Toneev, V. *Estimate of the magnetic field strength in heavy-ion collisions*. Int. J. Mod. Phys. A **24** (2009) 5925.

Smilga, A. V. *QCD at $\theta \sim \pi$*. Phys. Rev. D **59** (1999) 114021.

Smilga, A. V. *Lectures on quantum chromodynamics*. World Scientific, Singapore, Singapore, 2001.

Son, D. T. and Stephanov, M. A. *QCD at finite isospin density*. Phys. Rev. Lett. **86** (2001) 592.

Son, D. T. and Stephanov, M. A. *QCD and dimensional deconstruction*. Phys. Rev. D **69** (2004) 065020.

Svetitsky, B. and Yaffe, L. G. *Critical behavior at finite temperature confinement transitions*. Nucl. Phys. B **210** (1982a) 423.

Svetitsky, B. and Yaffe, L. G. *First order phase transition in the SU(3) gauge theory at finite temperature*. Phys. Rev. D **26** (1982b) 963.

Thompson, C. and Duncan, R. C. *Neutron star dynamos and the origins of pulsar magnetism*. Astrophys. J. **408** (1993) 194.

Thompson, C. and Duncan, R. C. *The soft gamma repeaters as very strongly magnetized neutron stars. 2. Quiescent neutrino, x-ray, and Alfven wave emission*. Astrophys. J. **473** (1996) 322.

Tolman, R. C. *Static solutions of Einstein's field equations for spheres of fluid*. Phys. Rev. **55** (1939) 364.

Toublan, D. and Kogut, J. B. *Isospin chemical potential and the QCD phase diagram at nonzero temperature and baryon chemical potential*. Phys. Lett. B **564** (2003) 212.

Tytgat, M. H. G. *QCD at $\theta \sim \pi$ reexamined: Domain walls and spontaneous CP violation*. Phys. Rev. D **61** (2000) 114009.

Vachaspati, T. *Magnetic fields from cosmological phase transitions*. Phys. Lett. B **265** (1991) 258.

Vafa, C. and Witten, E. *Parity Conservation in Quantum Chromodynamics*. Phys. Rev. Lett. **53** (1984) 535.

di Vecchia, P. and Veneziano, G. *Chiral dynamics in the large N limit*. Nucl. Phys. B **171** (1980) 253.

Veneziano, G. *U(1) without instantons*. Nucl. Phys. B **159** (1979) 213.

Vicari, E. and Panagopoulos, H. *θ dependence of SU(N) gauge theories in the presence of a topological term*. Phys. Rept. **470** (2009) 93.

Volkov, M. K. *Meson Lagrangians in a superconductor quark model*. Ann. Phys. **157** (1984) 282.

Voloshin, S. A. *Parity violation in hot QCD: How to detect it*. Phys. Rev. C **70** (2004) 057901.

Voloshin, S. A. *Experimental study of local strong parity violation in relativistic nuclear collisions*. Nucl. Phys. A **830** (2009) 377c.

Warringa, H. J. *The phase diagram of neutral quark matter with pseudoscalar condensates in the color-flavor locked phase*. arXiv:hep-ph/0606063.

Warringa, H. J., Boer, D., and Andersen, J. O. *Color superconductivity vs. pseudoscalar condensation in a three-flavor NJL model*. Phys. Rev. D **72** (2005) 014015.

Weinberg, S. *Phenomenological Lagrangians*. Physica A **96** (1979) 327.

Weinberg, S. *The quantum theory of fields. Vol. 2: Modern applications*. University Press, Cambridge, UK, 1996.

Weiss, N. *Introduction to Z_N symmetry in SU_N gauge theories at finite temperatures*. Talk given at 3rd Workshop on Thermal Field Theories and their Applications, Banff, Canada, 15-27 Aug 1993, hep-ph/9311233.

Wilczek, F. *Problem of strong P and T invariance in the presence of instantons*. Phys. Rev. Lett. **40** (1978) 279.

Witten, E. *Current algebra theorems for the U(1) Goldstone boson*. Nucl. Phys. B **156** (1979) 269.

Witten, E. *Large N chiral dynamics*. Ann. Phys. **128** (1980) 363.